

Stefan Velikogne, BSc

Characterization of Novel Imine Reductases for the Stereoselective Synthesis of Chiral Amines

MASTER'S THESIS

to achieve the university degree of

Master of Science

Master's degree programme: Biochemistry and Molecular Biomedical Sciences

submitted to

Graz University of Technology

Supervisor

Univ.-Prof. Dipl.-Ing. Dr.techn. Wolfgang Kroutil

Institute for Organic and Bioorganic Chemistry

Department of Chemistry
University of Graz

AFFIDAVIT

I declare that I have authored this thesis independently, that I have not used other than the declared sources/resources, and that I have explicitly indicated all material which has been quoted either literally or by content from the sources used. The text document uploaded to TUGRAZonline is identical to the present master's thesis dissertation.

28.05.2015

Date

Stefan Velić

Signature

Acknowledgements

This page is dedicated to all the people that directly or indirectly participated in the creation of this unique master thesis.

First and foremost I want to thank Wolfgang Kroutil and Jörg Schrittwieser. Wolfgang for accepting me in the working group “biocatalysis“ and therefore giving me the possibility to create such an interesting, multifaceted and fascinating master thesis.

Very special thanks go to my supervisor Jörg for being such a great supporter during this master thesis, for answering all the questions that occurred, for his widespread knowledge and therefore the immense input he gave me throughout the six months in the working group, for his enormous patience with me, for the discussions we had and of course for creating this wonderful working experience. I am really glad that I had such a great and kind "go-to guy"!

Babsi, thank you very much for all the times you had to show me where to find things and for being this good-humored person all the time!

Desi, I want to say thank you, for being one of the most cheerful and pleasant lab buddies I have ever had. I really enjoyed the talks we had, the good music and the chocolate goodies every now and then.

And of course I want to say thank you to the whole elk crew, for making my stay in this working group not only a pleasant but also a funny and unforgettable one.

Last but not least I want to thank my parents and siblings for their invaluable support, for their encouragement not to give up, for believing in me and for always being there.

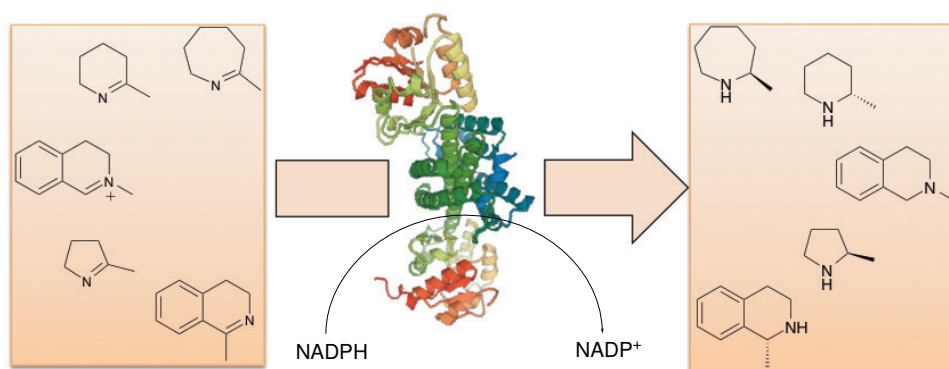
My friends and colleagues for helping me with any kind of problem and most importantly for making my student hood one of the most beautiful times I can imagine.

Zusammenfassung

Mehrere neue Iminreduktasen, welche der Literatur noch unbekannt sind, konnten erfolgreich in *E. coli* heterolog überexprimiert und mittels HisTrap Ni²⁺ Affinitätschromatographie gereinigt werden. Zehn dieser neu entdeckten Enzyme waren stabil in Lösung und zeigten, in einem ersten Versuch, Iminreduktase-Aktivität gegenüber dem 5-gliedrigen Modellssubstrat 2-Methyl-1-pyrrolin.

Ihre Charakterisierung offenbarte ein Temperaturstabilitätsmaximum von unter 40 °C, wobei die höchste gemessene Reduktionsaktivität bei neutralem bis leicht saurem pH, für den Großteil der Proteine, festgestellt wurde.

Desweiteren wurde keine oder nur eine sehr stark reduzierte Aktivität festgestellt, wenn an Stelle des NADPH NADH als Cofaktor zu Verfügung gestellt wurde.



Für viele der hier beschriebenen Reduktasen konnte gezeigt werden, dass sie über ein breites Substratspektrum verfügen, welches vor allem für die Darstellung von zyklischen sekundären Aminen als auch eines tertiären Amins geeignet ist.

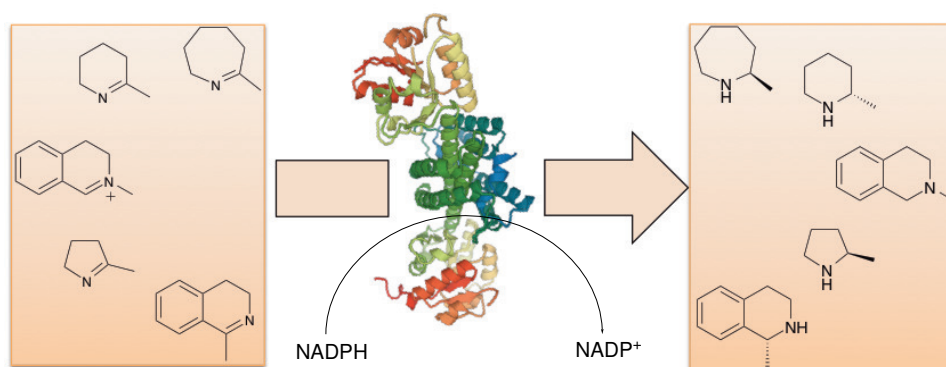
In den Biotransformationsreaktionen konnten die chiralen Amine in guten bis sehr guten Ausbeuten, bereits nach 2 h, umgesetzt werden, wobei die Enantioselektivitäten zwischen 94 - >99% *e.e.*, für das entsprechende (*R*)- oder (*S*)-Enantiomer lagen.

Summary

Several new imine reductases, not known to literature yet, were successfully heterologously overexpressed in *E. coli* and purified *via* HisTrap Ni²⁺ affinity chromatography. Ten of these newly discovered enzymes were found to be stable proteins in solution and, in a first attempt, showed imine reductase activity towards 5-membered model substrate 2-methyl-1-pyrroline.

Their characterization revealed a temperature stability optimum of below 40 °C, with the highest reduction activity measured at a neutral to a slight acidic pH for the greater part of these enzymes.

Furthermore no or only sharply reduced activities were observed, when providing NADH instead of NADPH as reducing cofactor.



Many of the described reductases were proven to possess a broad substrate scope, suitable for the preparation of cyclic chiral secondary amines as well as one tertiary amine also demonstrated.

When applied in biotransformational reactions, the chiral amine products were obtained in good to excellent yields, even after 2 h incubation, with enantioselectivities ranging from 94 - >99% *e.e.* for the corresponding (*R*)- or (*S*)-enantiomer, in most of the cases.

Table of Contents

1	Introduction	1
1.1	Background	2
1.2	Imine Reduction in Nature	4
1.3	Reduction of Cyclic Imines and Imino Acids	5
1.3.1	Biosynthesis of Pterin Cofactors and Siderophores	5
1.3.2	Alkaloid Biosynthesis	6
1.3.3	Bioreduction of Cyclic Imino Acids	8
1.4	Reductive Amination of α -Keto Acids	13
1.4.1	Amino Acid Dehydrogenases	13
1.4.2	Opine Dehydrogenases	14
1.5	Imine Reduction Employing Wild-Type Microbial Cells	17
1.6	Imine Reduction Using Defined Enzymes	21
1.6.1	Artificial Metalloenzymes	21
1.7	Imine Reductases and Imino Acid Reductases	25
1.7.1	Imino Acid Reductases	25
1.7.2	Imine Reductases	26
1.8	Amino Acid Dehydrogenases and Amine Dehydrogenases	34
1.8.1	Amino Acid Dehydrogenases	34
1.8.2	Amine Dehydrogenases	35
1.9	Opine Dehydrogenases and 'Reductive Aminases'	38
1.9.1	Opine Dehydrogenases	38
1.9.2	Engineering of a 'Reductive Aminase's	39
1.10	Structural and Mechanistic Aspects	40
2	Results and Discussion	48
2.1	Characterization of Novel Imine Reductases	49
2.2	Gene Subcloning and Plasmid Transformation	50
2.3	Heterologous Protein Expression and Protein Purification	51
2.4	Temperature Stability of Selected Enzymes	54
2.5	pH Dependence of Imine Reduction	57
2.6	Substrate Scope Determination & Cofactor Dependence of R- and S-IREDs	60
2.7	Biotransformations and Enantioselectivity	67
2.8	Summary	71
2.9	Outlook	71
3	Experimental	72
3.1	Materials	73
3.1.1	Compounds Used for Buffer Solutions	73
3.1.2	Compounds Used for Cell Cultivation	73
3.1.3	Chemicals Used for Activity Assay, Substrate Screening & Biotransformations	74
3.1.4	Materials Used for DNA Isolation and Ligation	75
3.1.5	Materials Used for Restriction Digest and Colony PCR	75
3.2	Procedures	76
3.2.1	Gene Subcloning & Plasmid Transformation	76

3.2.2	Colony Polymerase Chain Reaction (Colony PCR)	76
3.2.3	Protein Expression, Protein Purification & Desalting	77
3.2.4	SDS-PAGE analysis & Bradford assay	79
3.2.5	Activity Assay	79
3.2.6	Biotransformations	80
3.2.7	Buffer Recipes and Media Preparation	81
3.2.8	GC-FID Methods	82
3.2.9	HPLC Methods	84
3.2.10	Determination of Absolute Configurations	85
4	Appendix	86
4.1	Protein and DNA Sequences of Characterized IREDs	86
4.2	GC & HPLC Chromatograms	99
	References	112

1 Introduction

“Hence, enantioselective, NAD(P) -
dependent amine dehydrogenases remain a
holy grail in biocatalysis.”

Roger Sheldon in “Multi-Step Enzyme Catalysis”, 2008, Wiley-VCH

This part of the masters' thesis has been published as a review article in *Advanced Synthesis & Catalysis*, doi: 10.1002/adsc.201500213.

1.1 Background

Chiral amines represent the core structure of a myriad of natural products as well as man-made compounds of public demand, such as pharmaceuticals and agrochemicals (Figure 1). According to recent estimates, chiral amine moieties are present in about 40% of active pharmaceutical ingredients (APIs) and 20% of agrochemicals.^[1] Moreover, optically pure amines, amino acids, and amino alcohols are frequently employed in chemical synthesis as chiral auxiliaries or resolving agents.

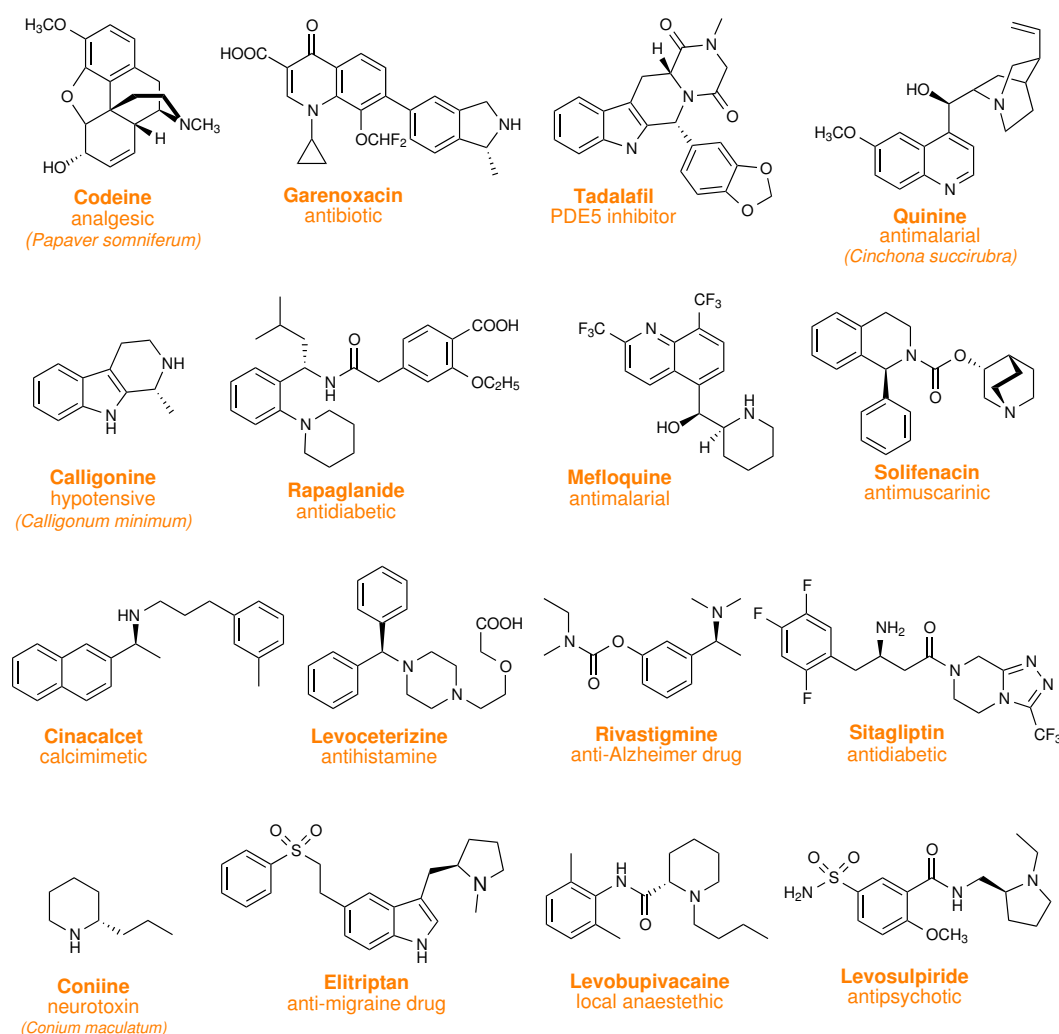


Figure 1. Examples of natural products and pharmaceutical drugs containing a chiral amine moiety. Biological activities and natural sources (in parentheses) are specified below the compound names.

Their paramount importance across several chemical disciplines and industrial sectors has made chiral amines and amino acids attractive targets for asymme-

tric synthesis. Established approaches for their preparation are the stereoselective addition of nucleophiles to imines (including the famous Mannich and Strecker reactions), asymmetric C–H amination and hydroamination, and the asymmetric reduction of enamines and imines, which may either be pre-formed or may occur as intermediates in an asymmetric reductive amination process.^[2–5] Metallo- or organocatalytic methods for asymmetric imine and enamine reduction are broadly applied and intense research efforts are devoted to the improvement of the scope and stereoselectivity of these processes.^[2–11]

In cases where established asymmetric synthesis methods are inapplicable or fail to provide the desired optical purity, diastereomeric salt crystallisation is still widely used for the classical resolution of racemic amines or for upgrading the enantiomeric excess of an optically enriched product.^[5]

Biocatalytic transformations are increasingly being recognised as an attractive option for the asymmetric synthesis of chiral molecules.^[12–14] Particularly in the pharmaceutical industry, biocatalysis has become a key technology for the development of cleaner and more efficient production processes, offering high chemo-, regio-, and stereoselectivity, high catalytic activity under near-ambient conditions, and ample possibilities for the tailoring of biocatalyst properties to match the demands of the desired process.^[15–19] In the context of chiral amine and amino acid synthesis, the first important contribution from biocatalysis has come in the form of amino acid dehydrogenases and α -transaminases, two enzyme classes that have found broad industrial application in the preparation of L- and D-amino acids *via* (true or formal) reductive amination of the corresponding α -keto acids.^[20] Moreover, hydrolytic enzymes such as amidases, hydantoinases, and carbamoylases are established biocatalysts for the preparation of α -amino acids and have been applied on industrial scale since the 1980s.^[21, 22] More recently, these biocatalytic methods for amino acid synthesis have been complemented by enzymatic hydroamination reactions catalysed by ammonia lyases and aminomutases.^[23–28]

The available methods for asymmetric synthesis of amines that are not amino acids are more limited. For many years, the only generally relevant option has been the kinetic resolution of racemic amines *via* enantioselective acylation using lipases,^[29, 30] a reaction that has also been implemented on industrial scale.^[31] An alternative, which is also applicable to tertiary amines, is deracemisation using a combination of monoamine oxidases and borane reducing agents.^[1, 32–38] Recently, ω -transaminases have emerged as a powerful tool for the asymmetric synthesis of α -chiral primary amines.^[32, 33, 39–41]

An impressive and much-cited example illustrating the potential of ω -transaminase catalysis is the biocatalytic process for the manufacture of sitagliptin, an antidia-

betic drug, which replaced a transition metalbased hydrogenation process.^[42] The asymmetric reduction of imines using NAD(P)H dependent enzymes represents a particularly attractive option for biocatalytic amine synthesis. This reaction can, in theory, give access to almost any primary, secondary, or tertiary amine, and the substrate imine or iminium ion can either be pre-formed or generated *in situ* by the condensation of amines and carbonyl compounds. Moreover, the regeneration of the required nicotinamide cofactors is nowadays practically and economically feasible even on a large scale. However, compared to the established biocatalytic methods for chiral amine synthesis, the enzymatic reduction of imines is still in its infancy. Until half a decade ago, biocatalytic methods for the reduction of imines that do not bear a carboxylic acid group in vicinal position were limited to few isolated reports using whole microbial cells (cf. Section 3). The enzymes catalysing the described reactions have never been identified, nor have the reported biotransformations found broader application.

From 2011 onwards, however, significant advances in biocatalytic asymmetric imine reduction and asymmetric reductive amination of ketones have been achieved following three main strategies: (i) the design of artificial metalloenzymes, in which a transition metalbased hydrogen transfer catalyst capable of reducing imines is anchored in a protein scaffold, (ii) structurebased semi-rational engineering of amino acid dehydrogenases or opine dehydrogenases to provide biocatalysts which accept non-functionalised ketones as substrates for reductive amination, and (iii) classical activity screening of microbial culture collections, which has led to the discovery of the novel enzyme family of imine reductases. Through these ongoing efforts, a growing number of imine-reducing enzymes is being made available for biocatalytic application, and some of the recent developments in the field have already been summarised in review articles or book chapters.^[1, 32, 43–45]

1.2 Imine Reduction in Nature

As stated in every organic chemistry textbook, imines – and even more so iminium ions – are rather reactive compounds. Their electrophilic character and the comparably low bond energy of the C=N double bond make them susceptible to attack by a wide range of nucleophiles, including water. As a consequence, most imines are hydrolytically labile in aqueous media, and hence also in biological systems. Nevertheless, the reduction of imines is a common reaction in both primary and secondary metabolism, and some of the involved enzymes, *e.g.*, dihydrofolate reductase and L-amino acid dehydrogenases, are even ubiquitous in living beings. The inherent instability of C=N bonds towards hydrolysis poses limitations on the possible structure of naturally occurring imines: they are either cyclic, whereby five- and six-membered rings are most common, or be-

ar a carboxylic acid substituent on the imine carbon atom. The latter structural feature might help to stabilize iminium ions via an internal hydrogen bond, although experimental evidence for such an interaction has only been obtained for the analogous case of aromatic iminium ions in ortho-position to a phenolate oxygen (Figure ??).^[46] Both cyclic and openchain α -imino acids may be formed in situ as an intermediate in the reductive amination of the corresponding α -keto acid.

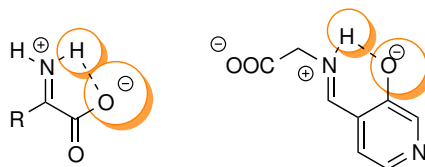


Figure 2. Stabilization of iminium ions by intramolecular hydrogen bonds.

Natural imine-reducing enzymes can hence be classified into two groups according to the structure of their substrate and the overall reaction they catalyse: Some enzymes are capable of performing a reductive amination and require a α -keto acid as substrate, while others reduce pre-formed, cyclic imines, which need not bear a carboxylic acid functionality.

1.3 Reduction of Cyclic Imines and Imino Acids

1.3.1 Biosynthesis of Pterin Cofactors and Siderophores

Among the most well-characterised of all imine-reducing enzymes are dihydrofolate reductase (EC 1.5.1.3) and 6,7-dihydropteridine reductase (EC 1.5.1.34), whose physiological roles are the formation of the cofactors 5,6,7,8-tetrahydrofolate and 5,6,7,8-tetrahydrobiopterin, respectively (Figure 3).^[47–51] Both are highly efficient, NAD(P)H-dependent enzymes showing specific activities of several hundred units per milligram and K_m values in the micromolar range for their natural substrates.^[52, 53] Their substrate scope, on the other hand, is rather narrow, and hence the great scientific interest in these enzymes is due to their physiological significance rather than their potential for biocatalytic application. The same is true for thiazoline reductases, which are NADPH-dependent enzymes responsible for the reduction of a 2-thiazoline ring in the biosynthesis of bacterial siderophores (iron-binding molecules; *e.g.*, pyochelin and yersiniabactin; Figure 3). Two enzymes of this type have been described in the literature, one originating from *Pseudomonas aeruginosa* and the other from *Yersinia enterocolitica*.^[54–57] Their natural substrates are immature siderophores linked to a non-ribosomal peptide synthase, and little is known about their substrate scope and their kinetic properties.

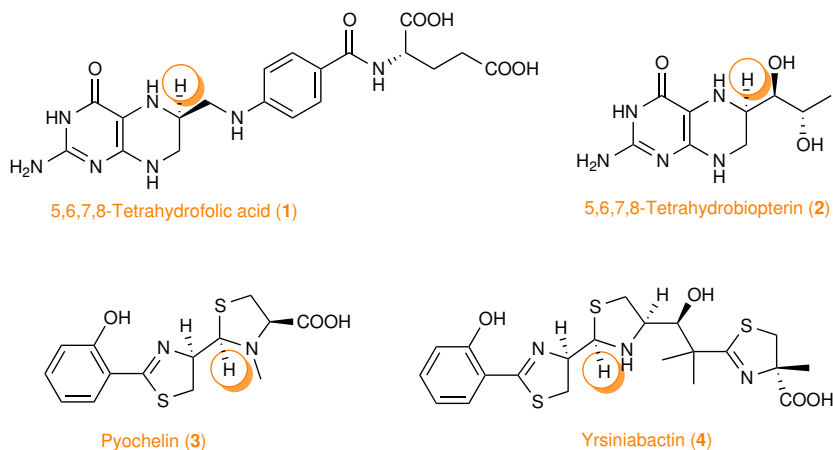
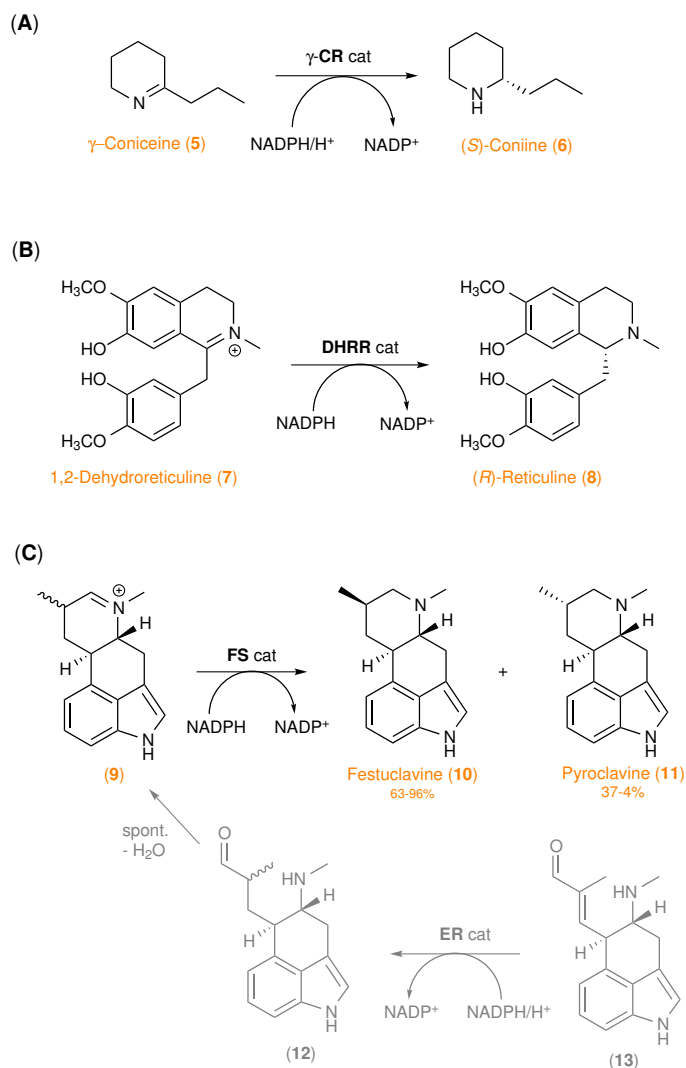


Figure 3. Molecular structures of the cofactors 5,6,7,8-tetrahydrofolate and 5,6,7,8-tetrahydrobiopterin and the siderophores pyochelin and yersiniabactin. Hydrogen atoms originating from NAD(P)H *via* enzymatic imine reduction are highlighted.

1.3.2 Alkaloid Biosynthesis

One of the first imine reductases to be purified and characterized was γ -coniceine reductase, the enzyme that catalyzes the last step in the biosynthesis of the poisonous hemlock alkaloid coniine (6; Scheme 1, A). The enzyme was extracted from leaves and fruits of *Conium maculatum* already in 1975, and its activity was studied using radioactively labelled substrate.^[58] NADPH was shown to be the preferred cofactor, but neither substrate scope nor enantioselectivity were investigated, and the enzyme has not been studied since. It is hence unclear whether the fact that both enantiomers of coniine are found in poison hemlock, with (*S*)-coniine being the major isomer,^[59] reflects the stereoselectivity of γ -coniceine reductase. Similar bioreductions have also been proposed to take place in the biosynthesis of the structurally related *Pinaceae* alkaloids pinidine and dihydropinidine, although in these cases the responsible enzymes have not been identified yet.^[60, 61]



Scheme 1. Reduction of imines and iminium ions in alkaloid biosynthesis: **(A)** Reduction of γ -coniceine (**5**) by γ -coniceine reductase (γ -CR), **(B)** reduction of the 1,2-dehydroreticulinium ion by 1,2-dehydroreticuline reductase (DHRR), and **(C)** reduction of iminium **9** to festuclavine **10** and pyroclavine **11** by festuclavine synthase (FS).

Like coniine, the benzylisoquinoline alkaloid reticuline (**8**; Scheme 1, B) is among the few natural products that occur in both enantiomeric forms.^[62] Its *de novo* biosynthesis affords exclusively the (*S*)-enantiomer, which can undergo stereoinversion *via* oxidation to the dihydroreticulinium ion (**7**) by an oxidase and reduction to the (*R*)-enantiomer an imine reductase called 1,2-dehydroreticuline reductase (EC 1.5.1.27). This NADPH-dependent monomeric enzyme has been purified from opium poppy and characterized in the early 1990s.^[63, 64] Dehydroreticuline reductase has a high affinity for its natural substrate ($K_m = 10 \mu\text{M}$) and does not show activity with closely related benzylisoquinolines like 1,2-dehydronorreticuline and 1,2-dehydrococlaurine. Unfortunately, neither the protein sequence nor the gene sequence of dehydroreticuline reductase are known, and so this enzyme is currently inaccessible for detailed biocatalytic studies.

Recently, another enzyme with an iminium ion as physiological substrate has be-

en identified: Festuclavine synthase (EC 1.5.1.44) catalyses the reduction of iminium compound **9** to the ergot alkaloids festuclavine (**10**, major product) and pyruclavine (**11**, minor product; Scheme 1, C). Festuclavine synthases from *Aspergillus fumigatus* and *Penicillium commune* have been cloned and heterologously expressed in *E. coli*.^[65, 66] Both enzymes can use NADH and NADPH, but prefer the phosphorylated form of the cofactor. The diastereomeric excess of the reduction product, *i.e.* the ratio of **10** to **11**, varied depending on the enzyme used and the reaction conditions (63:37 to 96:4).

1.3.3 Bioreduction of Cyclic Imino Acids

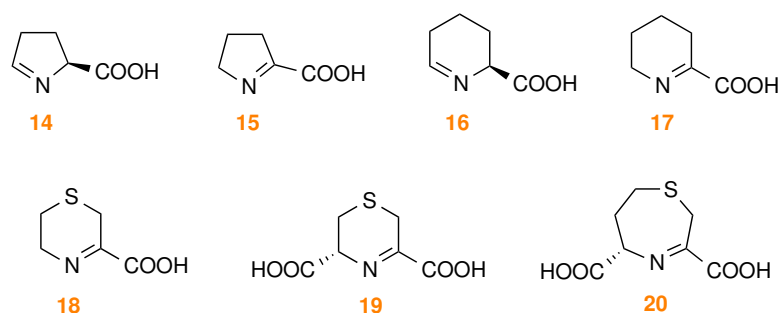
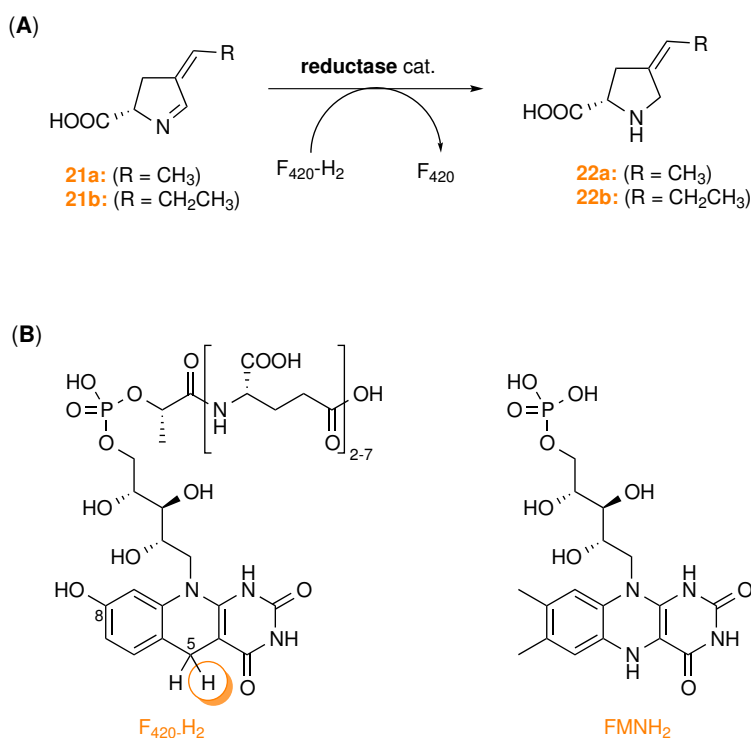


Figure 4. Examples of naturally occurring cyclic imino acids: L- Δ^1 -pyrroline-5-carboxylic acid (**14**), Δ^1 -pyrroline-2-carboxylic acid (**15**), L- Δ^1 -piperideine-6-carboxylic acid (**16**), Δ^1 -piperideine-2-carboxylic acid (**17**), S-aminoethylcysteine ketimine (**18**), lanthionine ketimine (**19**) and cystathionine ketimine (**20**).

Cyclic imino acids like Δ^1 -pyrroline-5-carboxylic acid (**14**), Δ^1 -pyrroline-2-carboxylic acid (**15**), and Δ^1 -piperideine-2-carboxylic acid (**17**; Figure 4) are intermediates in L-proline and L-lysine metabolism. The stereoselective reduction of these compounds to the corresponding cyclic amino acids by NAD(P)H dependent reductases is well documented, whereby a strict substrate specificity is observed: Compounds bearing the carboxylic acid group on the imine carbon atom are transformed by different enzymes than the non-conjugated derivatives, while in both cases rings of different size are accepted. As yet, the only known NAD(P)H-dependent enzyme acting on non-conjugated imino acids is Δ^1 -pyrroline-5-carboxylate reductase (Pyr5CR; EC 1.5.1.2). It catalyses the last step in L-proline biosynthesis and is thought to be ubiquitous.^[67] Pyr5CR was first isolated in the 1950s from *Neurospora crassa* (a red bread mould)^[68] and from human liver,^[69] and has since been identified in many organisms from all kingdoms of life. Basic functional and kinetic data are hence amply available, and these indicate that Pyr5CRs are highly efficient biocatalysts that can often use both NADH and NADPH as cofactor at comparable rates. The reductase from *Mycobacterium tuberculosis*, for instance, reduces its natural substrate with a k_{cat} of 451.7 s^{-1} in the presence of

NADPH (0.4 mM), and with a k_{cat} of 387.3 s^{-1} when supplied with NADH at the same concentration.^[70] The substrate scope of Pyr5CR has been investigated much less thoroughly, perhaps because non-natural substrate analogues are not readily available. The *Pseudomonas aeruginosa* enzyme has been shown to reduce Δ^1 -piperidine-6-carboxylate at about 10% of the activity shown with the natural substrate.^[71] In the reverse reaction – the oxidation of saturated cyclic amino acids at the expense of NAD(P)^+ , which is only detectable at pH values above 8.5 – proline esters and thioproline are accepted.^[72,73] The enzymatic reduction of the dihydropyrrole-2-carboxylic acid derivatives **21a** and **21b** (Scheme 2, A) represents a common step in the biosynthesis of various pyrrolobenzodiazepine antibiotics.



Scheme 2. (A) Reduction of alkylidene-3,4-dihydropyrrole-2-carboxylic acids **21** by F_{420} -dependent reductases. (B) Structure of reduced F_{420} ($\text{F}_{420}\text{-H}_2$) and reduced flavin mononucleotide (FMNH_2) for comparison. The hydrogen atom transferred as hydride from $\text{F}_{420}\text{-H}_2$ is highlighted.

These natural products are produced by actinomycetes and marine fungi and exert potent antitumour activities.^[74] The conversion of the α,β -unsaturated imines **21** into the corresponding amines **22** is catalysed by F_{420} -dependent oxidoreductases. To date, four of these enzymes have been identified on the DNA level *via* gene cluster analysis.^[75–78] Studies on the proteins themselves have not been reported yet, so there is no direct evidence for their proposed catalytic activity. Consequently, it is also unclear whether these enzymes show any chiral recognition of the stereogenic centre at C2 of the substrate or whether prochi-

ral substrate analogues can be reduced stereoselectively. The F_{420} cofactor used by these imine reductases is an uncommon deazaflavin derivative featuring a hydroxyl moiety at C8 and a methylene group instead of N5 of the isoalloxazin ring (Scheme 2, B). These modifications result in a remarkably low redox potential of -360 mV, which places F_{420} much closer to the nicotinamide cofactors NAD^+ and $NADP^+$ (-320 mV) than the common flavins FAD and FMN (-180 mV).^[79] F_{420} is therefore well suited for hydride transfer reactions, but since it has a more negative redox potential than $NAD(P)^+$ it cannot be regenerated by the latter as other flavins can. Moreover, widely used hosts for heterologous expression of recombinant enzymes, such as *E. coli*, *P. pastoris*, and *S. cerevisiae*, are unable to produce the F_{420} cofactor. Its unavailability is hence a major hurdle on the way to preparative application of F_{420} -dependent oxidoreductases.^[80] NAD(P)H-dependent enzymes that reduce the C=N bond of cyclic α -imino acids have been categorized into different classes, namely Δ^1 -pyrroline-2-carboxylate reductase (Pyr2CR; EC 1.5.1.1), Δ^1 -piperidine-2-carboxylate reductase (Pip2CR; EC 1.5.1.21), and ketimine reductase (EC 1.5.1.25). However, their substrate spectrum does not provide a clear basis for this categorisation, since enzymes from all three classes transform various α -imino acids of different ring size. Perhaps more helpful is a categorisation according to phylogenetic and functional criteria, which allows to distinguish two main groups: (i) the eukaryotic ketimine reductases, whose physiological role is thought to be the reduction of sulfur-containing ketimines that function as neurotransmitters or neuromodulators,^[81] and (ii) Δ^1 -piperidine-2-carboxylate/ Δ^1 -pyrroline-2-carboxylate reductases of bacterial origin (most importantly from *Pseudomonas* spp.), which are essential for the catabolism of D-lysine and D-proline.^[82] Ketimine reductases have first been discovered in mammalian tissues (*e.g.*, rat and rabbit liver; rat kidney, brain, liver, testis, heart, and skeletal muscle).^[82, 83] Early studies on the liver enzymes have established that the cofactors NADH and NADPH as well as the substrates Δ^1 -piperidine-2-carboxylic acid (**17**) and Δ^1 -pyrroline-2-carboxylic acid (**15**) are accepted about equally well, and that the corresponding amino acids are formed as optically pure L-enantiomers.^[82, 83] Besides **17** and **15**, sulfur-containing imino acids *S*-aminoethylcysteine ketimine (**18**), lanthionine ketimine (**19**), and cystathionine ketimine (**20**; Figure 4) have been identified as substrates, and the specific activities towards these compounds range from 1 to 52 units per milligram (Table 10).

Table 1. Kinetic parameters of various α -imino acid reductases.

Substrate	Cofactor	K_m [mM]	V_{max} [U/mg]
<i>Ketimine reductases from pig kidney</i> ^(a)			
18	NADH	0.14	20.3
19	NADH	0.47	1
20	NADH	3.0	16
<i>Ketimine reductases from bovine brain</i> ^(b)			
17	NADPH	0.33	32.7
18	NADH	0.24	21.4
19	NADPH	1.17	2.2
20	NADPH	10	52
<i>Recombinant human μ-crystallin</i> ^[84]			
18	NADH	0.047	9.6
<i>Pip2CR/Pyr2CR from <i>P. putida</i></i> ^[82]			
15	NADPH	0.043	168
17	NADPH	0.015	220
<i>Pip2CR/Pyr2CR from <i>P. syringae</i></i> ^[85]			
15	NADPH	<i>nd</i>	390
17	NADPH	<i>nd</i>	150

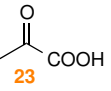
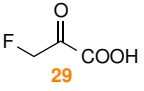
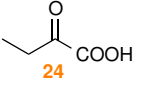
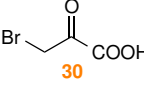
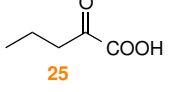
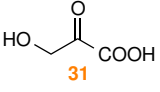
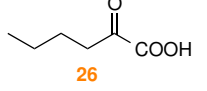
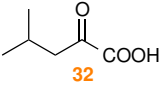
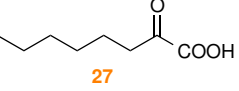
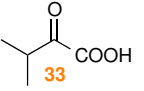
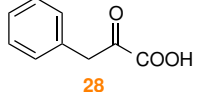
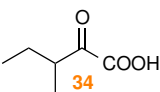
^(a) Data from ref. [86]; native enzyme purified from source tissue, approx. 80% purity (estimated by native PAGE).

^(b) Data from ref [87]; native enzyme purified from source tissue, approx. 70% purity (estimated by native PAGE).
nd, not determined

Ketimine reductases from various mammalian tissues have been isolated and studied over the years, but only recently researchers have identified the ketimine reductase from mammalian forebrain as μ -crystallin (CRYM), a protein previously known for binding the thyroid hormone 3,5,3'-L-triiodothyronine (T3).^[84] CRYM shows catalytic properties similar to those of ketimine reductases from other sources, as it can use both NADH and NADPH and readily accepts the ketimines **17**, **18**, and **20** as substrates. Human CRYM has been cloned and heterologously expressed in *E. coli*, but unfortunately the recombinant protein has proven rather unstable,^[84] a property it shares with native mammalian ketimine reductases.^[86, 87] These enzymes therefore hold little promise for biocatalytic application. Bacterial Δ^1 -piperidine-2-carboxylate/ Δ^1 -pyrroline-2-carboxylate reductases have a substrate scope similar to ketimine reductases, but are structurally unrelated to them and show different catalytic properties: The reductase from *Pseudomonas putida* exhibits specific activities (with **15** and **17**) one order of magnitude higher than the mammalian enzymes (Table 10), and shows a strong preference for NADPH over NADH as cofactor. Like ketimine reductases, bacterial α -imino acid reductases afford L-configured products.^[82] The *P. putida* enzyme shows only limited thermal stability, undergoing rapid deactivation at 35 °C, the temperature at which it reaches its maximum activity. However, a homologous

reductase from *Pseudomonas syringae*, showing 71% sequence identity with the enzyme from *P. putida*, was found to retain full activity for at least 30 min at 35 °C.

Table 2. Specific activities (U/mg) of Δ^1 -piperideine-2-carboxylate/ Δ^1 -pyrroline-2-carboxylate reductases from *P. putida* and *P. syringae* in the reductive methylation of α -keto acids.

Substrate	<i>Pp</i> DpkA ^(a)	<i>Ps</i> DpkA ^(b)	Substrate	<i>Pp</i> DpkA	<i>Ps</i> DpkA
	42	140		11	20
	13	14		<i>nd</i>	14
	6.7	13		2.4	<i>nd</i>
	22	32		3.8	18
	3.2	<i>nd</i>		0	0
	13	8.8		0	<i>nd</i>

^(a) Δ^1 -Piperideine-2-carboxylate/ Δ^1 -pyrroline-2-carboxylate reductase from *P. putida*, recombinantly expressed in *E. coli*; 10 mM α -keto acid, 60 mM methylamine (pH=10), 0.2 mM NADPH, 30 °C; data from ref. [88].

^(b) Δ^1 -Piperideine-2-carboxylate/ Δ^1 -pyrroline-2-carboxylate reductase from *P. syringae*, recombinantly expressed in *E. coli*; 10 mM α -keto acid, 60 mM methylamine (pH=10), 0.2 mM NADPH, 30 °C; data from ref. [85]. *nd*, not determined

An intriguing feature of the bacterial Δ^1 -Piperideine-2-carboxylate/ Δ^1 -pyrroline-2-carboxylate reductases is the fact that their imine-reducing activity is not restricted to cyclic compounds. Both the *P. putida* and the *P. syringae* enzyme have been shown to catalyze the reductive amination of α -keto acids with methylamine at rates in the same order of magnitude as their natural activity (>100 U/mg). In fact, the reductase from *P. putida* has originally been characterized as N-methyl-L-amino acid dehydrogenase before its true metabolic role has been unravelled.^[89] The products of this 'side activity', N-methyl α -amino acids, are components of bacterial pilins^[90] and of several biologically interesting nonribosomal peptides; for example, cyclosporins,^[91] enniatins,^[92] and vancomycin.^[93] In medicinal chemistry, N-methyl amino acids are used to modify the properties of peptides,^[94, 95] and their synthesis has hence attracted considerable interest.^[96]

The two *Pseudomonas* enzymes are able to reductively methylamine a fairly wi-

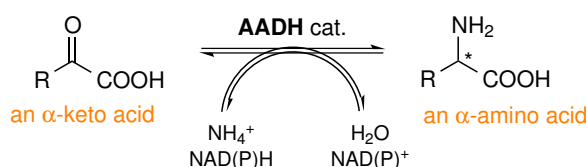
de range of α -keto acids: in addition to pyruvate, which is the preferred substrate for both enzymes, linear aliphatic and arylaliphatic keto acids are accepted well, including those carrying halogen or hydroxyl substituents (Table 2). β -Branched compounds like α -ketoisovaleric acid (**33**) and α -keto- β -methylvaleric acid (**34**), on the other hand, are inert.^[85, 88] The amine scope is much more restricted, as the second-best amine substrate of the enzyme from *P. putida*, ethylamine, is turned over at only 4.4% of the rate observed with methylamine.^[88] The activities observed with other amines, including 2-chloroethylamine, n-propylamine, dimethylamine, hydroxylamine, and isopropylamine, are below 1% relative to methylamine. Interestingly, ammonia is not accepted at all by the *Pseudomonas* reductases, a characteristic that renders them complementary to the well-known amino acid dehydrogenases. Biocatalytic applications of bacterial Δ^1 -piperidine-2-carboxylate/ Δ^1 -pyrroline-2-carboxylate reductases are discussed in Section 4.2.

1.4 Reductive Amination of α -Keto Acids

The last enzyme discussed in the previous section, Δ^1 -piperidine-2-carboxylate/ Δ^1 -pyrroline-2-carboxylate reductase, is an example of a biocatalyst that can not only reduce cyclic imines but can also catalyze the reductive amination of α -keto acids. Two additional classes of enzymes that perform this type of reaction, amino acid dehydrogenases and opine dehydrogenases, are discussed in this section.

1.4.1 Amino Acid Dehydrogenases

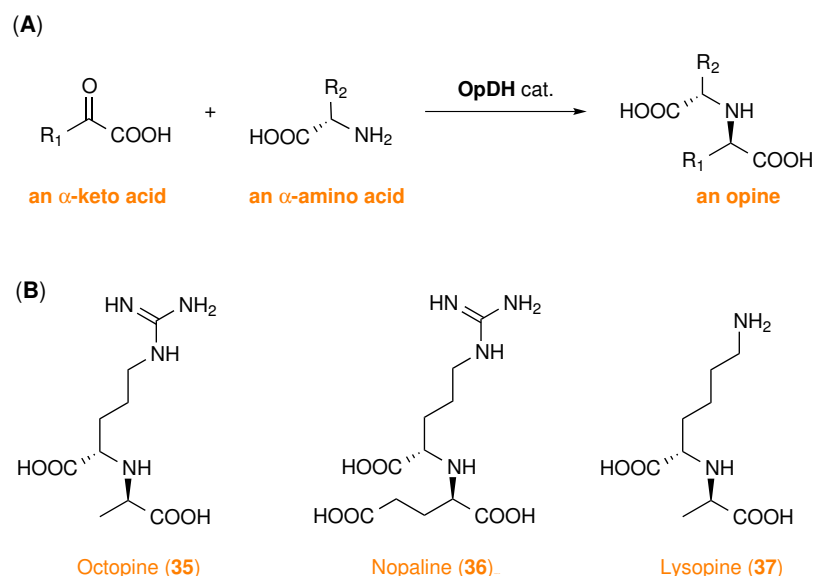
Amino acid dehydrogenases (AADHs; EC 1.4.1.–) catalyze the reductive amination of α -keto acids with ammonia as well as the reverse reaction, the oxidative deamination of α -amino acids (Scheme 3). L-selective AADHs are ubiquitous enzymes with central roles in amino acid metabolism, and are the most intensively studied ‘reductive aminases’. Both the general characteristics and the numerous industrial applications of L-AADHs have been extensively reviewed,^[97–104] so I will only provide a brief account here.



Scheme 3. General reaction catalyzed by amino acid dehydrogenases (AADHs).

L-Amino acid dehydrogenases require a nicotinamide cofactor and the majority show a strong preference for NADH over NADPH, although NADP-specific AADHs from microbial sources are known.^[105] The substrate scope of L-AADHs is strictly limited to α -amino acids and α -keto acids; hence, amines and ketones lacking a vicinal carboxyl group are not converted. Moreover, in reductive amination, these enzymes are restricted to ammonia as substrate amine. D-selective AADHs are also found in nature, but are far less abundant than their L-selective counterparts. They are membrane-bound enzymes dependent on flavin and non-heme iron, whose oxidative action on D-amino acids is coupled to the respiratory chain.^[106, 107] When used in solubilized form, they require inconvenient cofactors such as coenzyme Q, methylene blue, or 2,6-dichlorophenolindophenol as terminal electron acceptors.^[106, 108] Since these molecules are not easily regenerated and hence have to be supplied in stoichiometric amounts, natural D-AADHs are of little interest for biocatalytic application. However, nicotinamide cofactor-dependent, D-selective AADHs have recently been developed *via* protein engineering, and their use in amino acid synthesis is discussed in Section 4.3.

1.4.2 Opine Dehydrogenases



Scheme 4. (A) General reaction catalyzed by opine dehydrogenases (OpDHs). (B) Examples of opines found in invertebrate muscle or crown gall tumors.

Opines (Scheme 4, B) are amino acid conjugates found in marine invertebrates and in crown gall tumors of plants,^[109] with very different physiological roles in these two environments: In invertebrates, opines are formed by the enzyme opine dehydrogenase in muscle tissue upon anaerobic exercise (Scheme 4, A). Through this process, the end products of glycolysis – pyruvate and NADH – are

consumed, which ensures a favorable redox balance and keeps glycolysis running under oxygen-limited conditions, much in the same way as the formation of lactate by lactate dehydrogenase does in mammals.^[110-114] Opines in crown gall tumors, on the other hand, serve as a nutrient for the parasitic *Agrobacteria* that are the cause for crown gall disease. These bacteria insert a small region of DNA (the so-called transfer DNA or T-DNA), which encodes for an opine dehydrogenase, into the genome of their host, thus forcing the plant to produce the opines on which they thrive.^[115-117]

Table 3. Kinetic parameters of opine dehydrogenase from *Arthrobacter* sp. 1C and *Pecten maximus* in the reductive amination of pyruvate with various amino acids and amines.

Substrate	V_{max} [U/mg]	k_{cat} [s ⁻¹]	K_m [mM]	k_{cat}/K_m [mM ⁻¹ s ⁻¹]
<i>OpDH from Pecten maximus</i> ^(a)				
	886 (634)	640	0.5	1,330
	<i>nd</i> (154.6)	<i>nd</i>	<i>nd</i>	<i>nd</i>
<i>OpDH from Arthrobacter sp. 1C</i> ^(b)				
	607	364	2.17	168
	519	311	20.0	16
	523	314	3.72	84
	362	217	3.19	68
	294	176	5.94	30
	222	133	8.70	15
	153	92	8.69	11
	105	63	11.9	5.3
	82.2	49	28.3	1.7
	18.2	11	46.0	0.2

(a) Kinetic parameters from ref. [118], determined at pH 7.0, 25 °C and varied concentrations of pyruvate, L-arginine and NADH; V_{max} values in parenthesis are specific activities taken from ref. [119], determined at pH 7.0, 25 °C, 3 mM pyruvate, 0.16 mM NADH.

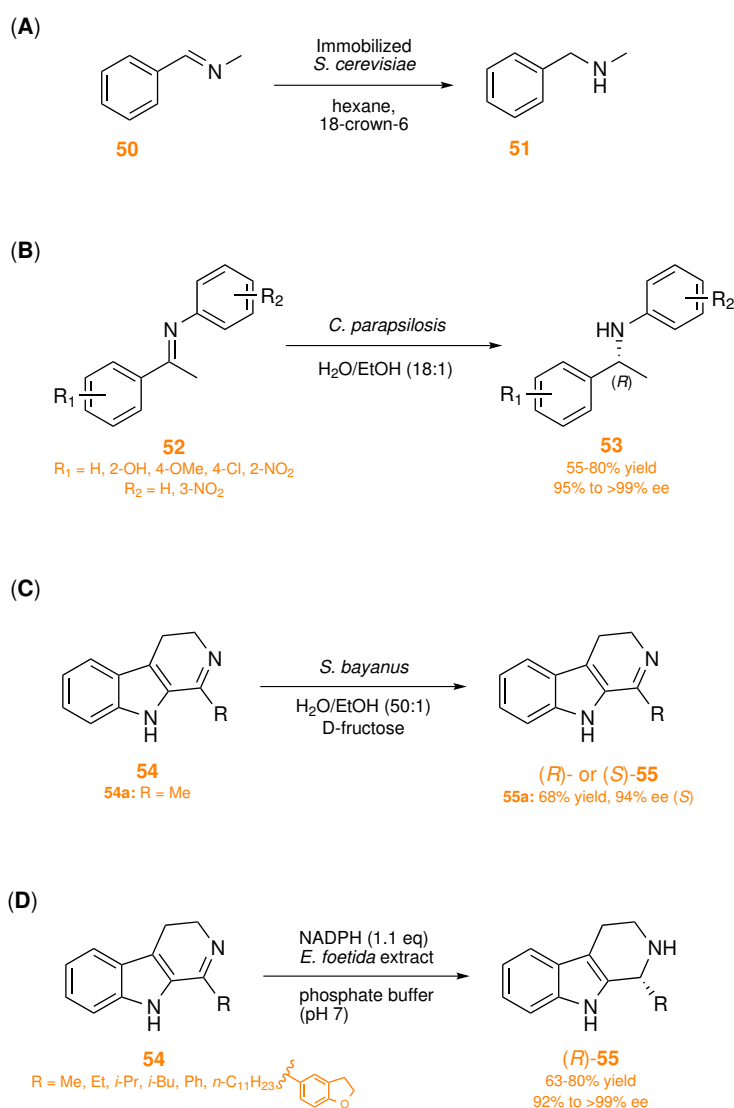
(b) V_{max} and K_m values from ref. [120], determined at pH 8.0, 25 °C 10 mM pyruvate, 0.1 mM NADH; k_{cat} values calculated from V_{max} values based on an enzyme molecular weight of 36 kDa.^[121]
nd, not determined

Opine dehydrogenases (OpDHs) of either origin are highly efficient catalysts, reaching specific activities of several hundred units per milligram with their physiological substrates (Table 3).^[118–121] The well-characterised enzymes from *Arthrobacter* sp. 1C and *Pecten maximus* (king scallop) show a strong preference for pyruvate as electrophile, but a number of other small α -keto acids (e.g., α -ketobutyric acid, α -ketovaleric acid) are also accepted. The scope of amino acids as coupling partners is broad for the bacterial enzyme, which converts several apolar L-amino acids at comparable rates and even accepts (S)-phenylalaninol as an example of an amine lacking a carboxylic acid group.^[120, 121] Michaelis constants (K_m) in the mM range (Table 3) indicate a generally weak binding interaction of the enzyme with its amino acid substrates. OpDH from *P. maximus*, on the other hand, shows a comparably strong affinity for L-arginine, which is bound in the active site *via* electrostatic interactions between its guanidinium group and a negatively charged pocket of the protein. This binding event triggers a conformational change of the enzyme, thereby generating the binding site for the second substrate, pyruvate.^[119, 122] As a consequence, the scallop enzyme shows high catalytic activity only with L-arginine (**38**) and the closely related L-canavanine (**39**), while other L-amino acids are poor substrates. Both the *Arthrobacter* and the *P. maximus* opine dehydrogenase strictly require NADH as cofactor (no activity is observed with NADPH) and form products with (R)-configuration at the newly generated stereogenic centre.

1.5 Imine Reduction Employing Wild-Type Microbial Cells

Many of the imine-reducing enzymes discussed in the previous section have been known for decades, yet only few of them have been applied in biocatalysis. Most natural imine reductases require complex substrates or are highly substrate-specific, which diminishes their applicability as biocatalysts, while others – with gene and protein sequences unknown – are not accessible. Researchers have therefore long resorted to whole microbial cells when trying to establish a general biocatalytic method for the reduction of imines and their derivatives. *Saccharomyces cerevisiae* and other yeasts – which have proven useful in the asymmetric reduction of ketones – were often the biocatalysts of choice, and indeed some biotransformations offering a broad scope and good enantioselectivity are reported in the literature. Unfortunately, none of these proof-of-principle studies have been investigated further and the responsible enzyme(s) have not been identified. Nevertheless, a brief overview will be provided here.

The first report on the biocatalytic reduction of an open-chain imine dates back to 1997, when baker's yeast immobilised in calcium alginate beads was used to reduce *N*-benzylidenemethylamine (**50**) to *N*-methylbenzylamine (**51**) in THF or hexane as solvent and in the presence of 18-crown-6 as additive (Scheme 5, A).^[123]



Scheme 5. Examples of imine reduction processes catalyzed by whole cells or cell-free extracts of wild-type organisms: **(A)** Reduction of benzylidenemethylamine (**50**) by immobilized baker's yeast in organic medium, **(B)** asymmetric reduction of aryl imines **52** by *Candida parapsilosis* ATCC 7330, **(C)** asymmetric reduction of 3,4-dihydro- β -carboline **54** by *Saccharomyces bayanus*, affording (*R*)- or (*S*)-amines depending on the substituent at C1, and **(D)** reduction of 3,4-dihydro- β -carboline **54** by a cell-free extract of *Eisenia foetida* (Californian earthworm).

In the absence of the crown ether, **50** was recovered unchanged, while neither the imine nor the amine could be isolated from reactions in aqueous media. Unfortunately, no yields are reported in the publication and the reduction of prochiral imines was not investigated.

Cell preparations of the strict anaerobe *Acetobacterium woodii* were also found to

be active for imine reduction.^[124] Instead of a single substrate, the authors chose to use a dynamic combinatorial library of imines generated by the spontaneous condensation of amines (*n*-butylamine, aniline) with aldehydes (*n*-butyraldehyde, benzylaldehyde). The assays were performed in a 4:1 mixture of phosphate buffer (pH 7.0) and tetradecane under hydrogen atmosphere, and the phases were separately analysed by GC–MS. The formation of the *sec*-amine products *N*-butylaniline and *N*-benzylaniline was detected as minute peaks in the gas chromatograms. The main products formed during the 24 h incubation of the assay mixtures were benzyl alcohol and benzoic acid, which were found in 200–20,000 times higher concentration than the desired amines.

In 2008, the reduction of six prochiral aromatic imines **52** by resting cells of the yeast *Candida parapsilosis* ATCC 7330 was reported to provide the (*R*)-configured *sec*-amines **53** in 55–80% isolated yield and enantiomeric excesses between 95% and >99% (Scheme 5, B).^[125] However, these interesting results come at the cost of using an exceptionally high biocatalyst loading of >1 g/mL, corresponding to a biocatalyst/substrate mass ratio of 500. Other research groups have been unsuccessful in reproducing the reduction of aryl imines with whole cells of *C. parapsilosis* or known reductases from this organism, detecting substrate hydrolysis instead.^[126–128] As mentioned before, cyclic imines are stable towards hydrolysis and hence are viable substrates for biocatalytic reduction in aqueous medium. The asymmetric bioreduction of 3,4-dihydro- β -carboline **54** (Scheme 5, C) using whole-cell catalysts has been the subject of two recent studies. In the first paper, strains of *Saccharomyces cerevisiae* and *Saccharomyces bayanus* that are usually used in wine production were investigated as biocatalysts.^[129] The reactions were carried out in non-buffered water, employing 260 mg/mL of lyophilized cells and 160 mg/mL of fructose as ‘electron donor’. The *S. bayanus* strains were found to generally afford products of higher enantiomeric purity than the *S. cerevisiae* strains under these conditions (ee = 91–94% vs. 74–80%, using substrate **54a**), and *S. bayanus* U2642 (from Danster Ferment AG) was chosen for detailed investigation. Dihydro- β -carboline carrying a wide range of substituents at C1 were tested as substrates, whereby an interesting switch in stereoselectivity was observed: Aliphatic substituents with up to 11 carbon atoms gave rise to the (*S*)-configured products in 74–94% ee, while longer aliphatic chains or aromatic groups resulted in the formation of (*R*)-amines (62–97% ee). Yields of the isolated products varied between 45% and 68%.

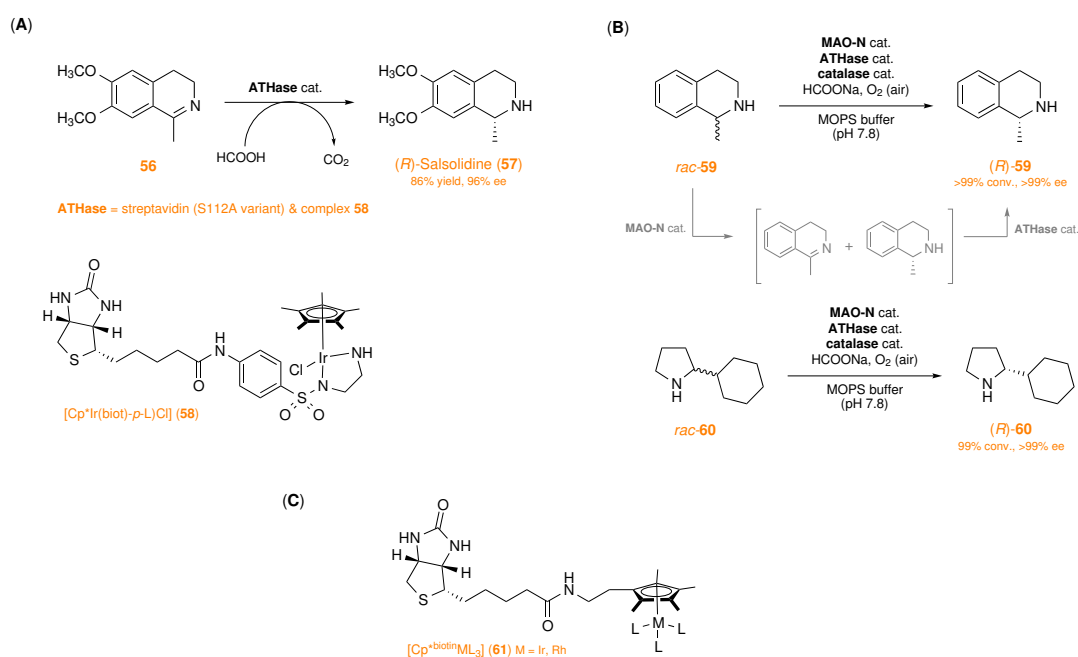
In a follow-up study, the same research group has investigated the reduction of dihydro- β -carboline **54** by a rather extraordinary biocatalyst – a crude cell-free extract of the Californian earthworm, *Eisenia foetida* (Scheme 5, D).^[130] *E. foetida* extracts formed the desired tetrahydro- β -carboline **55** in decent yields (63–80%)

and with excellent enantioselectivities (ee between 92% and >99%). In contrast to the bioreduction using *S. bayanus*, reactions with *E. foetida* extract furnished (*R*)-amines in all cases, independent of the substituent size. While these are promising results, the method suffers from scalability issues: NADPH was supplied in stoichiometric amounts, and according to the published procedure around 1000 earthworms would need to be sacrificed to enable the production of 1 g of tetrahydro- β -carboline.

1.6 Imine Reduction Using Defined Enzymes

1.6.1 Artificial Metalloenzymes

Artificial metalloenzymes are hybrid catalysts created by anchoring a catalytically active metal complex into a biological macromolecule like a protein or DNA. The chiral environment of the host macromolecule provides a second coordination sphere for the organometallic moiety and can thus influence the selectivity and the rate of the catalyzed chemical transformation. Since first reports in the late 1970s, various strategies for designing artificial metalloenzymes have been developed, and the resulting catalysts have been used in a wide variety of reactions, including hydrogenation, transfer hydrogenation, hydration of C=C bonds, conjugate addition, Diels–Alder reactions, olefin metathesis, and C–H activation reactions.^[131–133]



Scheme 6. (A) Preparation of (*R*)-salsolidine **57** via asymmetric transfer hydrogenation catalysed by an artificial transfer hydrogenase (ATHase) composed of the biotinylated iridium(III) piano-stool complex **58** non-covalently bound to the bacterial protein streptavidin. (B) Examples of deracemisation reactions realised by combining (*R*)-selective ATHases with (*S*)-selective variants of monoamine oxidase from *Aspergillus niger* (MAO-N). (C) General structure of alternative piano-stool complexes **61** in which the Cp* ring is directly tethered to biotin.

Recently, the scope of reactions has been expanded with an asymmetric transfer hydrogenation of imines.^[134] In an initial screening, the authors combined several d⁵ and d⁶ piano-stool complexes bearing the biotinylated aminosulfonamide

ligand biot-*p*-L with wild-type streptavidin (Sav; a bacterial protein with high binding affinity for biotin) and tested the resulting metalloenzymes for their activity and selectivity in the transfer hydrogenation of imine **56** (Scheme 6, A). The iridium(III) complex **58** was identified as the most promising candidate, affording (*R*)-salsolidine (**57**) in quantitative yield and 57% *ee* under non-optimised conditions.

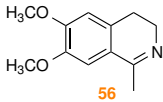
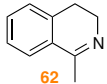
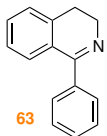
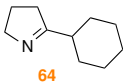
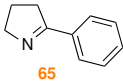
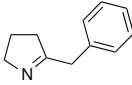
The artificial transfer hydrogenase (ATHase) was then subjected to genetic optimisation by introducing single-point mutations of amino acids flanking the biotin-binding pocket. X-ray crystal structure analysis of the Sav-**58** complex revealed three cationic (R84, H87, and K121), one anionic (D67), and six polar (N49, S69, N85, T114, T115, N118) amino acid residues in the proximity of the piano-stool moiety. Variations at position S112 were found to have a drastic influence on the stereoselectivity of the reaction: variant S112A produced (*R*)-**57** in 96% *ee* under optimized conditions, while variant S112K afforded the opposite enantiomer in 78% *ee*.^[134] The replacement of the cationic residues R84 and K121 with apolar amino acids, on the other hand, resulted in an improved turnover rate (up to 8-fold improvement over wild-type streptavidin) and alleviated substrate inhibition.^[135]

The (*R*)-selective ATHase was subsequently used in combination with (*S*)-selective variants of monoamine oxidase from *Aspergillus niger* (MAO-N) for the deracemisation and stereoinversion of various amines (Scheme 6, B).^[136] In this context, the tight binding of the iridium complex **58** to the protein host prevented the mutual catalyst inactivation observed when MAO-N was incubated with free **58**. Exploiting the matching enantioselectivities of MAO-N in the oxidation of amines to the corresponding imines and of ATHase in the ensuing reduction, several *sec*- and *tert*-amines could be obtained as optically pure (*R*)-enantiomers in (near-)quantitative conversion.

Further research focused on alternative piano-stool complexes in which the cyclopentadienyl ring is directly tethered to biotin (**61**; Scheme 6, C). This leaves three free coordination sites on the metal, which can be filled by amino acid side chains of Sav or by small-molecule ligands. The first option was realised by introducing a histidine residue in proximity to the metal centre of the Sav-**61** (M = Rh, L = Cl) complex, resulting in a dual and more rigid anchoring of the catalytic moiety.^[137] Interestingly, by choosing either of two suitable positions for introduction of histidine (S112 or K121), two different orientations of the piano-stool complex could be realised. These resulted in opposite stereoselectivity in the reduction of **56**: The S112H variant gave the (*S*)-enantiomer of **57** in moderate excess (55% *ee*), while Sav K121H produced (*R*)-salsolidine with 79% *ee*. However, the excellent stereoselectivities observed with the initial ATHase design (SavS112A-**58**) could not

be attained in this study. The second option – combining Sav, complex **61**, and small-molecule bidentate ligands – offers unprecedented possibilities for tailoring the properties of the hybrid catalyst, as the central metal ion, the amino acid residues of the binding pocket of Sav, and the bidentate ligand can be varied independently. A systematic investigation of individual and combinatorial effects of these variables revealed optically pure α -amino amides as most promising ligands, and wild-type Sav and iridium(III) as the most suited protein variant and metal ion, respectively.^[138] The resulting ATHases were tested in the reduction of six prochiral imines and showed excellent conversions along with moderate enantioselectivities (up to 67% *ee*; Table 4).

Table 4. Selected results of the transfer hydrogenation of prochiral imines using an artificial transfer hydrogenase formed from wild-type streptavidin, piano-stool complex **61** (M = Ir), and L-amino amide ligands.^[138]

Substrate	Ligand	conv. [%]	<i>ee</i> [%]
	L-IleNH ₂	quant.	43 (S)
	L-ThrNH ₂	quant.	25 (S)
	L-ProNH ₂	47	67(S)
	L-IleNH ₂	89	65(S) 63
	L-LeuNH ₂	96	(S)
	L-ThrNH ₂	98	57 ^(a)
	L-ThrNH ₂	95	35 ^(a)
	L-LeuNH ₂	quant.	20 ^(a)

^(a) Absolute configuration not determined. General conditions: 35 mM substrate, 87 μ M Ir complex, 192 μ M ligand, 7.4 mg/mL streptavidin, 1.4 M HCO₂Na, 600 mM MOPS buffer, pH 7.8, 50 °C, 18 h.

A completely different approach for the design of artificial transfer hydrogenases was recently established using the ribonuclease S (RNase S) scaffold as anchoring protein for the organometallic complex.^[139] RNase S is formed by proteolytic cleavage of RNase A with subtilisin and consists of the N-terminal, α -helical S-peptide (comprising amino acid residues 1–20) and the C-terminal S-protein formed from amino acids 21–124 of RNase A. The two components can be readily separated by trichloroacetic acid precipitation and cation-exchange chromatography, and the ‘apo’-S-protein can be complemented with synthetic S-peptides (Fi-

Figure 5). Five 15-residue S-peptide variants were created by solid-phase synthesis and complexed with $[\text{Cp}^*\text{IrCl}_2]_2$ via metal-coordinating amino acid residues (e.g., His7, Gln10, His11). Artificial transfer hydrogenases were obtained by incubating the metal-complexed S-peptides with the 'apo'-S-protein and their catalytic performance was evaluated using the transfer hydrogenation of **56** as model reaction. All investigated ATHases showed catalytic activity, although conversions ($\leq 35\%$), turnover numbers (≤ 71) and stereoselectivities ($ee \leq 39\%$) were generally low. Interestingly, the highest ee values were observed in the absence of the S-protein.

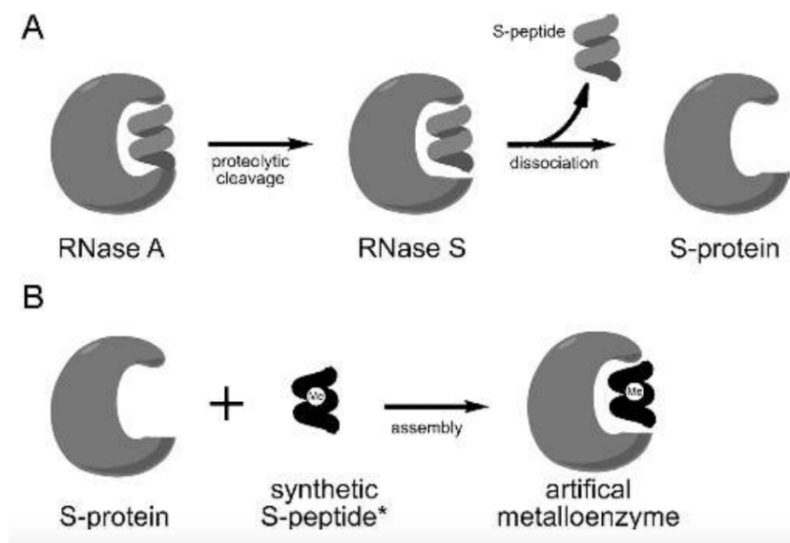
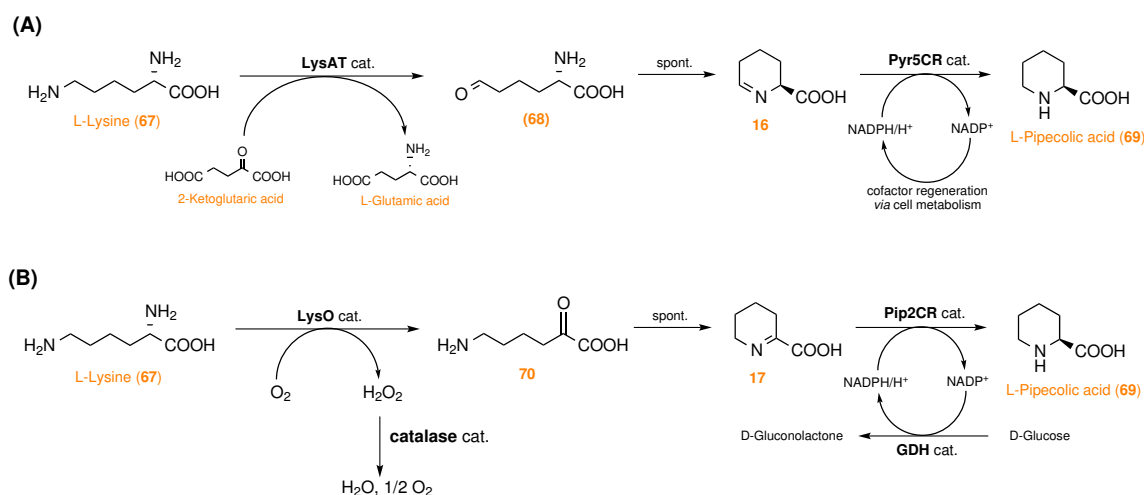


Figure 5. Formation of semisynthetic RNase S: **(A)** Proteolytic cleavage of RNase A gives RNase S, which comprises the C-terminal S-protein (amino acids 21–124) and the short α -helical S-peptide (20 amino acids). **(B)** Replacing the native S-peptide with a synthetic analogue containing a metal-binding site affords an artificial metalloenzyme. Illustration reproduced with permission of Wiley-VCH Verlag GmbH & Co. KGaA, Weinheim.

1.7 Imine Reductases and Imino Acid Reductases

1.7.1 Imino Acid Reductases

The first biocatalytic application of an imino acid reductase was reported in 2002, when the native Pyr5CR activity (Δ^1 -1-pyrroline-5-carboxylate reductase; see Section 2.3.3) of *E. coli* was exploited for the biotransformation of L-lysine (67) into L-pipecolic acid (69; Scheme 7, A).^[140]



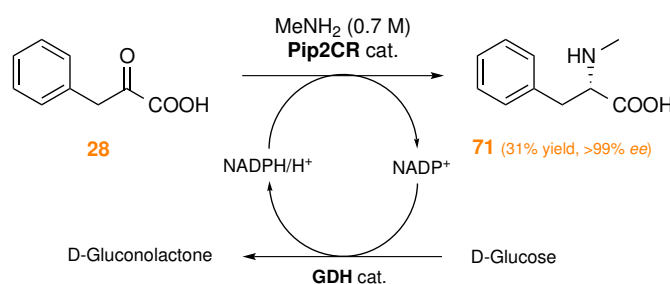
Scheme 7. Two multi-enzymatic cascade processes for the synthesis of L-pipecolic acid from L-lysine: **(A)** Transformation via L- Δ^1 -piperideine-6-carboxylic acid (16) using fermenting *E. coli* cells expressing L-lysine 6-aminotransferase (LysAT) and Δ^1 -pyrroline-5-carboxylate reductase (Pyr5CR), and **(B)** transformation via Δ^1 -piperideine-2-carboxylic acid (17) using L-lysine α -oxidase (LysO), catalase, Δ^1 -piperideine-2-carboxylate/ Δ^1 -pyrroline-2-carboxylate reductase (Pip2CR) and glucose dehydrogenase (GDH).

E. coli JM109 containing recombinant L-lysine 6-aminotransferase (LysAT) was found capable of catalyzing this two-step transformation, whereby the Pyr5CR present in the host strain was identified as the enzyme responsible for the reduction of Δ^1 -piperideine-6-carboxylate (16) in this process. Fermentation in TB medium supplemented with L-lysine (55 mM) yielded 3.9 g/L (30 mM) of L-pipecolic acid after 159 h.

In a very similar cascade, the Δ^1 -piperideine-2-carboxylate/ Δ^1 -pyrroline-2-carboxylate reductase from *Pseudomonas putida* was employed in combination with L-lysine α -oxidase from *Trichoderma viride* for the transformation of L-lysine into L-pipecolic acid (Scheme 7, B).^[141] In contrast to the previous biotransformation using LysAT (Scheme 7, A), the stereogenic centre of L-lysine is destroyed in the

oxidation step and reintroduced in the asymmetric reduction. L-Lysine was added in portions to the reaction mixture, and the acidifying effect of gluconic acid (formed from glucose by GDH) was countered by constant addition of base, resulting in a stable production of L-pipecolic acid ($ee >99.7\%$) during the 17-hour reaction. A final product titre of 210 mM (27 g/L) was obtained, corresponding to a 90% yield based on the total amount of L-lysine added. In a follow-up study, the method was extended to several five-, six-, and seven-membered cyclic L-amino acids, including thia- and oxacyclic molecules.^[142]

As mentioned in Section 2.3.3, the bacterial Δ^1 -piperideine-2-carboxylate/ Δ^1 -pyrroline-2-carboxylate reductases are not restricted to reducing cyclic imines, as they can also catalyze the reductive amination of α -keto acids with methylamine. This reductive methylation reaction has been demonstrated on preparative scale: The synthesis of *N*-methyl-L-phenylalanine (**71**) from phenylpyruvate (**28**) was performed using *E. coli* cells co-expressing Δ^1 -piperideine-2-carboxylate/ Δ^1 -pyrroline-2-carboxylate reductase from *P. putida* (Pip2CR) and glucose dehydrogenase from *Bacillus subtilis* (Scheme 8).^[89] After a 24 h reaction at 100 mL scale, *N*-methyl-L-phenylalanine (**71**) was isolated in $>99\%$ ee and 31% yield (1.1 g).

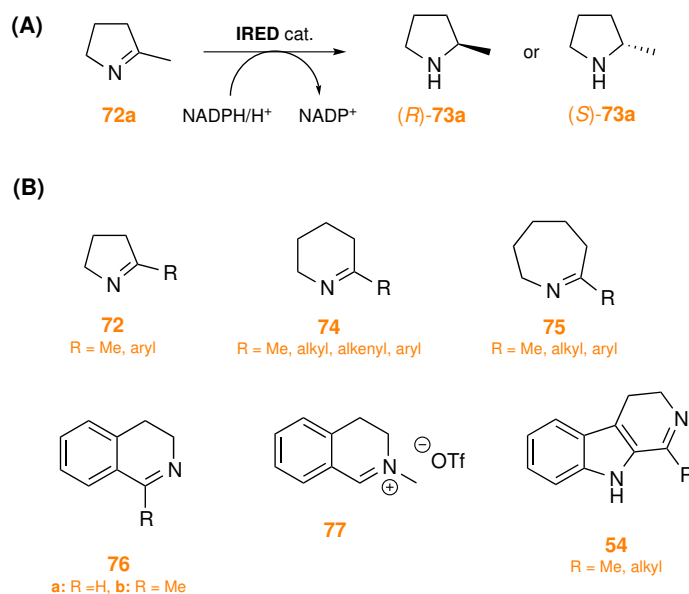


Scheme 8. Biocatalytic reductive methylation of phenylpyruvic acid (**28**) affording *N*-methyl-L-phenylalanine (**71**). Enzyme abbreviations: Pip2CR, Δ^1 -piperideine-2-carboxylate/ Δ^1 -pyrroline-2-carboxylate reductase; GDH, glucose dehydrogenase..

1.7.2 Imine Reductases

Despite the abundance of natural enzymes that reduce cyclic imines (*cf.* Section 2.3), broad-scope, NAD(P)H-dependent imine reductases have long remained unavailable. It took an immense effort of classical culture collection screening to identify biocatalysts that exhibit good activity and stereoselectivity towards prochiral, non-carboxylated cyclic imines. Mitsukura *et al.* have screened 688 microbial strains, encompassing 226 yeasts, 261 bacteria, 117 actinomycetes, and 84 fungi, for reduction activity on 2-methyl-1-pyrroline (**72**; Scheme 9).^[143] Among the tested cultures, only five *Streptomyces* sp. were found to be active on **72**, and only two of these showed a satisfactory enantioselectivity: *Streptomyces* sp. GF3587 afforded (*R*)-**73** in 99% ee , while strain GF3546 produced the (*S*)-enantiomer of

the amine in 81% *ee*. The responsible enzymes have later been purified, cloned, and heterologously expressed,^[144, 145] and they constitute the first members of the now rapidly growing enzyme family of imine reductases (IREDs). The two *Streptomyces* enzymes are homodimeric proteins with a subunit molecular mass of around 30 kDa, a pH optimum in the neutral range and a strict specificity for NADPH as cofactor. The catalyzed reaction was found to be reversible, but oxidation of amines occurred more slowly than imine reduction and only under basic conditions (pH >10). The substrate scope of the (*R*)-selective enzyme has initially been described as extremely narrow, **72a** being the only identified substrate.^[144] The (*S*)-selective IRED, on the other hand, has been found to catalyze the reduction of various cyclic imines, including (in addition to **72a**) the imino acid **15** (*cf.* Figure 4) and the 3,4-dihydroisoquinolines **56** and **62** (*cf.* Table 4).^[145] More recent investigations have revealed the substrate scope of both enzymes to be much broader, as a variety of 5-, 6-, and 7-membered cyclic imines, 3,4-dihydroisoquinolines, isoquinolinium ions, and 3,4-dihydro- β -carbolines were accepted with good conversions and excellent levels of stereoselectivity (Table 5).^[146, 147] An α,β -unsaturated imine (**74**, R = isopropenyl) was reduced chemoselectively at the carbon–nitrogen double bond with no detectable reduction of the alkene.



Scheme 9. (A) Reduction of 2-methyl-1-pyrroline (**72a**) to (*R*)- or (*S*)-2-methylpyrrolidine (**73a**) catalyzed by imine reductases (IREDs). (B) General structures of typical IRED substrates.

The discovery of the first broad-scope imine reductases in *Streptomyces* spp. has sparked an immense interest in the scientific community, and several research groups from academia as well as industry – including ourselves – have started investigating these enzymes. Based on the protein sequences of the first-discovered

IREDs, additional enzymes of this family have soon been identified *via* sequence homology search (Table 5): An (*R*)-selective imine reductase from *Streptomyces kanamyceticus* (Table 5, entry 2) was first described in a patent^[148] and was later functionally and structurally characterised.^[149] The X-ray crystal structure of this IRED was solved by molecular replacement and revealed an intertwined dimer with an N-terminal Rossmann-fold domain and overall structural similarity to known β -hydroxyacid dehydrogenases (see Section 5 (????)). The kinetics of the enzyme were studied using three substrates (**72a**, **76a**, and **77**). The observed turnover rates are low (k_{cat} between 1.1 and 0.054 per minute), but **73a** was formed in excellent optical purity (>99% *ee*). Another patent, published in 2011, describes an (*S*)-selective IRED from *Streptosporangium roseum* without disclosing any details on the enzyme's properties except its stereoselectivity in the reduction of **72a** (97.7% *ee*).^[150]

Table 5. Overview of characterized imine reductases and their kinetic properties and stereoselectivities in the reduction of 2-methyl-1-pyrroline (**72a**).

Entry	Accession code	Source organism	Kinetic parameters (72a)			<i>ee</i> (73a)
			k_{cat} [s ⁻¹]	K_m [mM]	k_{cat}/K_m [s ⁻¹ mM ⁻¹]	
1 ^[147]	M4ZRJ3 (UniProt)	<i>Streptomyces</i> sp. GF3587	0.351	1.88	0.187	99 (<i>R</i>)
2 ^[149]	Q1EQE0 (UniProt)	<i>Streptom. kanamyceticus</i>	0.018	8.21	0.0022	>99 (<i>R</i>)
3 ^[151]	YP_003336672.1 (Genebank)	<i>Streptospor. roseum</i>	0.961	1.08	0.889	98 (<i>R</i>)
4 ^[151]	WP_006374254.1 (Genebank)	<i>Streptom. turgidiscabies</i>	0.112	1.81	0.062	99 (<i>R</i>)
5 ^[152]	Q88J51 (UniProt)	<i>Pseudomonas putida</i>	<i>spec. act.</i> : 66 mU/mg ^(a)			99 (<i>R</i>)
6 ^[152]	L1KNB7 (UniProt)	<i>Streptomyces ipomoeae</i>	<i>spec. act.</i> : 27 mU/mg ^(a)			99 (<i>R</i>)
7 ^[146]	M4ZS15 (UniProt)	<i>Streptomyces</i> sp. GF3546	0.024	11.82	0.002	>95 (<i>S</i>)
8 ^[153]	S3Z901 (UniProt)	<i>Streptomyces aurantiacus</i>	<i>spec. act.</i> : 75 mU/mg ^(a)			<i>nd</i>
9 ^[151]	WP_010497949.1 (Genebank)	<i>Paenibacillus elgii</i>	0.026	1.29	0.020	95 (<i>S</i>)

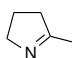
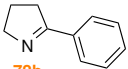
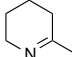
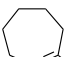
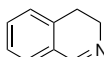
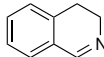
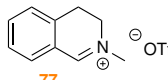
^(a) Specific activity at fixed substrate concentration (entries 5, 6: 20 mM; entry 8: 10 mM); kinetic parameters not determined. *nd*, not determined.

More recently, a novel (*S*)-selective imine reductase was identified from *Streptomyces aurantiacus* (Entry 8) and the crystal structures of this enzyme as well as its homologue, the original (*S*)-IRED from *Streptomyces* sp. GF3546, were solved.^[153] Both proteins show a high overall structural similarity to the (*R*)-selective *S. kanamyceticus* enzyme. The hitsets of BLAST searches on known IRED sequences have recently been used for generating an electronic library of almost 400 putati-

ve imine reductases, the Imine Reductase Engineering Database, which is freely available on the internet (<https://ired.biocatnet.de/>). Three proteins from this database, originating from *Streptosporangium roseum*, *Streptomyces turgidiscabies*, and *Paenibacillus elgii* (Entries 3, 4, and 9), were expressed in *E. coli* and found to be functional IREDs.^[151] In an alternative approach, an imine reductase from *Pseudomonas putida* was identified based on its 3D structural similarity to known IREDs (Entry 5).^[152] The enzyme, for which a crystal structure has been deposited in the protein data bank (PDB) in 2009 but whose function was unknown then, afforded (*R*)-**73a** from imine **72a** in 99% *ee*.

Most imine reductases known to date originate from streptomycetes, but the wealth of sequences deposited in the Imine Reductase Engineering Database suggests that these proteins are also common in other families of bacteria, e.g., *Mycobacteriaceae*, *Bacillaceae*, and *Pseudonocardiaceae*. The physiological role of IREDs, and hence their natural substrate, is currently still unknown, and it is even unclear whether the reduction of C=N bonds is their main or just a promiscuous activity.^[149] Proteins now identified as imine reductases have previously been annotated as hydroxyisobutyrate dehydrogenase, 6-phosphogluconate dehydrogenase, or glycerol-3-phosphate dehydrogenase. However, in all cases where these putative functions were tested for, the IREDs proved inactive towards the respective substrates. In general, imine reductases have been found incapable of reducing carbonyl compounds or oxidising alcohols.^[151, 152] Interestingly, imine **72a** – the compound used in the screening that led to the discovery of the IRED enzyme family – is converted only sluggishly by most known imine reductases (*cf.* Table 5, Table 6). Turnover rates of six-membered cyclic imines and 3,4-dihydroisoquinolines are often one order of magnitude higher than those of **72a** (Table 6). K_m values in the millimolar range for all these compounds suggest that they are not the natural substrates of imine reductases. Valuable indications regarding the mode of substrate binding and the catalytic mechanism of IREDs can be obtained by comparing the kinetic parameters in the reduction of 3,4-dihydroisoquinoline (**76a**) with those found for the positively charged, methylated derivative **77**. The (*S*)-selective reductase from *Streptomyces* sp. GF3546 shows no appreciable preference for one of the compounds, while the (*R*)-selective enzymes from *S. kanamyceticus* and *Streptomyces* strain GF3587 reduce the iminium ion **77** 4 times and 7.5 times faster, respectively, than the uncharged species (Table 6).

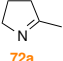
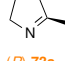
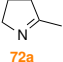
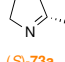
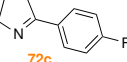
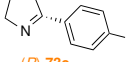
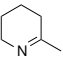
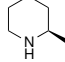
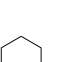
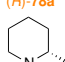
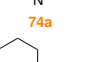
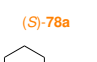

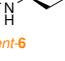
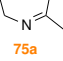
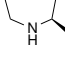
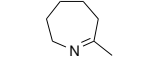
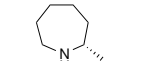


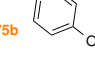
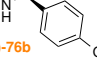
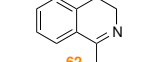
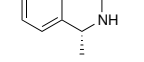
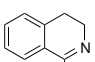
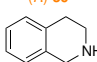
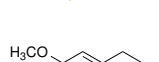

Table 6. Kinetic parameters of IREDs from *Streptomyces* sp. GF3587 (M4ZRJ3),^[147] *Streptomyces* sp. GF3546 (M4ZS15),^[146] and *Streptomyces kanamyceticus* (Q1EQE0)^[149] with selected substrates.

Substrate	IRED	Kinetic parameters		
		k_{cat} [s ⁻¹]	K_m [mM]	k_{cat}/K_m [s ⁻¹ mM ⁻¹]
 72a	M4ZRJ3	0.351	1.88	0.187
	M4ZS15	0.024	11.82	0.002
	Q1EQE0	0.018	8.21	0.0022
 72b	M4ZS15	0.004	0.54	0.007
 74a	M4ZRJ3	4.21	0.371	11.4
	M4ZS15	0.137	5.50	0.025
 75a	M4ZRJ3	3.64	5.22	0.698
	M4ZS15	0.039	8.19	0.005
 76a	M4ZRJ3	0.141	0.317	0.447
	M4ZS15	0.445	0.63	0.708
	Q1EQE0	0.0009	1.16	0.00074
 62	M4ZRJ3	0.189	0.155	1.22
	M4ZS15	0.040	1.05	0.038
 77	M4ZRJ3	1.057	0.481	2.195
	M4ZS15	0.483	0.60	0.801
	Q1EQE0	0.0038	0.724	0.0052

The stereoselectivity of imine reductases is usually high but depends on the ring and substituent size of the substrate. For instance, the (*S*)-selective IRED from *Streptomyces* sp. GF3546 reduces **72a** to (*S*)-**73a** with >95% *ee*, while the phenyl-substituted derivative **72b** is transformed into (*R*)-**73b** with only 87% *ee*.^[146] The opposite absolute configuration of the product is due to a switch in Cahn–Ingold–Prelog priorities. The influence of substituent size is even more pronounced for the (*R*)-selective enzyme from *Streptomyces* sp. GF3587, which produces optically pure (*R*)-**73a** (>98% *ee*), but nearly racemic (*S*)-**73b** (8% *ee*). A similar effect is observed with the corresponding piperidineines **74**, while the Δ^1 -azepanes **76** (R = Me, p–MeOC₆H₄) are both reduced with excellent stereoselectivity (*ee* >98%).^[147] The (*S*)-selective *S. aurantiacus* imine reductase reduces 1-methyl-3,4-dihydroisoquinoline **62** to the optically pure tetrahydroisoquinoline (*S*)-**59** (*cf.* Table 7), but reaches only 34% *ee* for its ethylsubstituted analogue. The (*R*)-IRED from *Streptomyces* strain GF3587 generally exhibits low stereoselectivity with dihydroisoquinolines, as (*R*)-**59** is formed in only 71% *ee* (*cf.* Table 7).^[147] Dihydro- β -carbolines **54** with C1-substituents ranging in size from methyl to cyclohexyl are readily accepted substrates for the (*S*)-selective enzyme from *Streptomyces* sp. GF3546 and generally afford reduction products of excellent optical purity (98% *ee*).^[146]

Biotransformations using imine reductases have thus far mainly been carried out using resting cells of *E. coli* in which the respective IRED is heterologously expressed. In this setup, the regeneration of the required NADPH cofactor is accomplished by the metabolism of the host cell, provided fresh cell preparations are used and D-glucose is added as sacrificial cosubstrate.

Table 7. Representative biotransformations using imine reductases. All reactions were performed using resting *E. coli* cells expressing the specified IRED.

Substrate	IRED	Product	Conv. [%]	ee [%]
 72a	(<i>R</i>)-IRED M4ZRJ3	 (<i>R</i>)-73a	>98 ^(a)	>98
 72a	(<i>S</i>)-IRED M4ZS15	 (<i>S</i>)-73a	57 ^(b)	>95
 72c	(<i>S</i>)-IRED M4ZS15	 (<i>R</i>)-73c	42 ^(b)	98
 74a	(<i>R</i>)-IRED M4ZRJ3	 (<i>R</i>)-78a	>98 ^(a)	>98
 74a	(<i>S</i>)-IRED M4ZS15	 (<i>S</i>)-78a	>98 ^(b)	>98
 5	(<i>R</i>)-IRED M4ZRJ3	 ent-6	>98 ^(a) (90) ^(c)	>98
 75a	(<i>R</i>)-IRED M4ZRJ3	 (<i>R</i>)-79a	>98 ^(a)	>98
 75a	(<i>S</i>)-IRED M4ZS15	 (<i>S</i>)-79a	>98 ^(b)	>98
 75b	(<i>R</i>)-IRED M4ZRJ3	 (<i>S</i>)-76b	50 ^(a)	>98
 62	(<i>R</i>)-IRED M4ZRJ3	 (<i>R</i>)-59	>98 ^(a)	98
 62	(<i>S</i>)-IRED M4ZS15	 (<i>S</i>)-59	>98 ^(b) (87) ^(d)	98
 56	(<i>S</i>)-IRED M4ZS15	 ent-57	92 ^(b)	>98
 54a	(<i>S</i>)-IRED M4ZS15	 (<i>S</i>)-55a	>98 ^(b)	>98
 54b	(<i>S</i>)-IRED M4ZS15	 (<i>S</i>)-55b	97 ^(b)	>98

(a) Data from ref. [147]; 5 mM substrate, 50 mM glucose, *E. coli* cells expressing (*R*)-IRED M4ZRJ3 added to an OD₆₀₀ of 30, 100 mM potassium phosphate buffer, pH 7.0, 30 °C, 24 h.

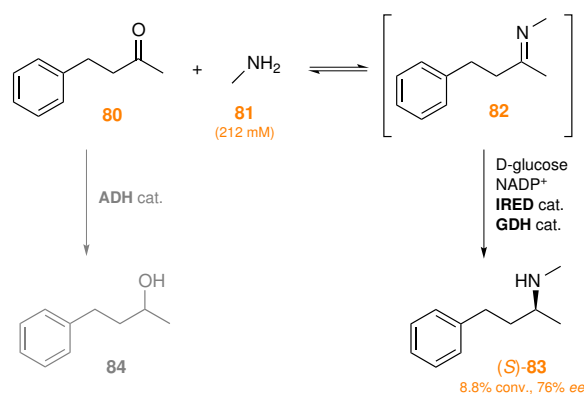
(b) Data from ref. [146]; 5 mM substrate, 50 mM glucose, *E. coli* cells expressing (*S*)-IRED M4ZS15 added to an OD₆₀₀ of 30, 100 mM potassium phosphate buffer, pH 7.0, 30 °C, 24 h.

(c) The value in parentheses is the isolated yield of a reaction performed on 1.0 g scale.

(d) The value in parentheses is the isolated yield of a reaction performed on 200 mg scale.

Besides, the limited thermal stability^[144, 145] of many imine reductases might have prompted researchers to work with a wholecell catalyst, as the cell environment may help to stabilise the enzyme. A selection of representative biotransformations is provided in Table 7. Since expression levels of the heterologous enzyme may vary, it is difficult to deduce reactivity trends for different substrates from the published conversion data. Generally, the (*R*)-selective IRED from *Streptomyces* sp. GF3587 seems to accept a wide range of piperidineines **74**, as low conversions were only observed with very bulky substituents (e.g., 1-naphthyl, 4% conversion after 24 h). The (*S*)-selective reductase from *Streptomyces* sp. GF3546, on the other hand, affords highest conversions with 3,4-dihydroisoquinolines **76** and 3,4-dihydro- β -carbolines **54**.

Despite the large number of substrates accepted by imine reductases and the promising results with respect to conversion and stereoselectivity, preparative-scale biotransformations and product isolation have only been reported in a few cases. For instance, the synthesis of both enantiomers of **72a**, isolated as hydrochloride salts, was achieved using the *Streptomyces* strains GF3587 and GF3546. (*R*)-**73a** · HCl was obtained in 73% yield (243 mg) and 99% *ee*, while the synthesis of (*S*)-**73a** · HCl was carried out on smaller scale yielding 56 mg (67%) of the product in 92% *ee*. Furthermore, *E. coli* cells expressing (*S*)-IRED from strain GF3546 were used in the synthesis of (*S*)-**59** which was obtained as free base in 87% yield (176 mg) and 98% *ee*.^[146] The asymmetric synthesis of the hemlock alkaloid (*R*)-coniine (*ent*-**6**) has even been performed on gram scale using (*R*)-IRED from *Streptomyces* sp. GF3587 as a recombinant *E. coli* cell preparation. The target alkaloid was isolated as the corresponding hydrochloride salt in 90% yield (898 mg) and >98% *ee*.^[147]



Scheme 10. Asymmetric reductive amination of ketone **80** and methylamine (**81**) catalyzed by an imine reductase (IRED) from *Streptomyces* sp. GF3546. When the IRED was used as a crude cell lysate, formation of alcohol **84** was observed, probably due to alcohol dehydrogenases (ADHs) present in the *E. coli* expression host.

A highly exciting but little explored feature of imine reductases is their ability to

reduce open-chain imines. Just like bacterial Δ^1 -piperidine-2-carboxylate/ Δ^1 -pyrroline-2-carboxylate reductases, the (*S*)-selective IREDs from *Streptomyces* sp. GF3546 and *S. aurantiacus* have been found capable of catalyzing asymmetric reductive methylation reactions. However, in the case of the imine reductases, noncarboxylated ketones (e.g., **80**; Scheme 10) were investigated as acceptors and the observed reactions were extremely slow (k_{cat} for **80** = $2.8 \times 10^{-6} \text{ s}^{-1}$), probably due to the hydrolytic instability of the intermediate imines in aqueous media. The reaction proceeded best under alkaline conditions (pH 9.5) and required a purified IRED preparation as contaminating alcohol dehydrogenases in the crude cell lysate led to carbonyl reduction of **80** to give **84**. The secondary amine **83**, formed from **80** and methylamine using (*S*)-IRED from strain GF3546, had an enantiomeric excess of 76%, representing a proof of principle for the asymmetric reductive amination of ketones using imine reductases.

1.8 Amino Acid Dehydrogenases and Amine Dehydrogenases

The reductive amination of ketone moieties is often the most efficient approach to the synthesis of chiral amine-based target molecules. As discussed in Section 2.4, natural enzymes catalyzing direct reductive amination of ketones require a carboxylic acid moiety adjacent to the carbonyl group; i.e., they need α -keto acids as substrates and are hence only applicable to the preparation of α -amino acids and their derivatives. However, enzymes that are not subject to this limitation have recently been developed by directed evolution.

1.8.1 Amino Acid Dehydrogenases

L-Selective amino acid dehydrogenases (L-AADHs) have found broad application in the asymmetric synthesis of natural and non-natural α -amino acids, either *via* reductive amination or oxidative kinetic resolution.^[98–102] A vast number of natural L-AADHs from diverse organisms as well as variants engineered for industrial production have been described, and several large-scale processes using these enzymes have been implemented.

Nicotinamide cofactor-dependent D-selective AADHs, on the other hand, have only become available recently. They have been developed *via* protein engineering of *meso*-diaminopimelic acid D-dehydrogenases from various bacterial sources, and the engineered biocatalysts have been used for the asymmetric synthesis of a variety of D-amino acids.^[154–157] The production of (*R*)-5,5,5-trifluoronorvaline, an intermediate for the γ -secretase inhibitor BMS-708163 (Figure 5), using a D-AADH has even been carried out on pilot plant scale (50 kg). Moreover, the use of an engineered D-AADH in a spectrophotometric assay for

D-isoleucine has recently been reported.^[158]

With respect to substrate scope, the engineered D-AADHs seem to be subject to the same limitations as the natural, L-selective enzymes: Ketones need to bear a carboxylic acid group in vicinal position, and ammonia is the only amine accepted as substrate. Nevertheless, due to the importance of α -amino acids in various areas of chemistry, both L- and D-selective AADHs will continue to be important enzymes in research and industrial production.

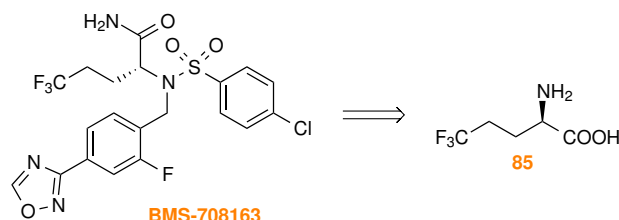
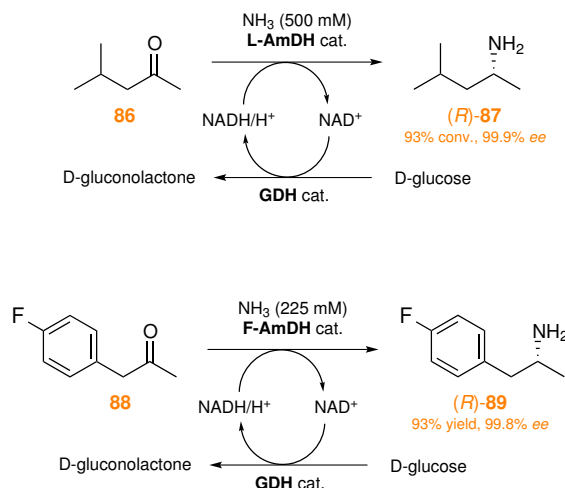


Figure 6. Structures of the γ -secretase inhibitor BMS-708163 and its synthetic precursor (*R*)-5,5,5-trifluoronorvaline (**85**), which has been prepared on multi-kilogram scale employing a D-selective AADH.

1.8.2 Amine Dehydrogenases

In analogy to amino acid dehydrogenases, which catalyse the reductive amination of α -keto acids with ammonia, enzymes able to perform the same reaction on unfunctionalised ketones can be referred to as amine dehydrogenases (AmDHs). Natural AmDHs are unknown, although at the beginning of the millennium an enzyme was described that reductively aminates keto acids, hydroxyketones as well as non-functionalised ketones and aldehydes.^[159] The reported stereoselectivities were low, however, and the experiments have not been reproduced since. Stereoselective, nicotinamide cofactor-dependent AmDHs have hence remained elusive – so much so that they have even been referred to as ‘the holy grail in biocatalysis’.^[160]



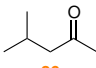
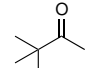
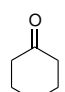
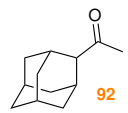
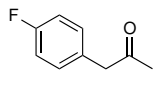
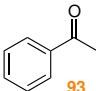
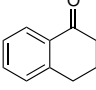
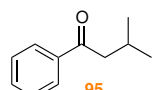
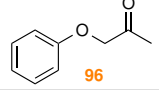
Scheme 11. Asymmetric synthesis of α -chiral primary amines *via* reductive amination using amine dehydrogenases (AmDHs) in combination with glucose dehydrogenase (GDH) for cofactor regeneration. The AmDH biocatalysts were created *via* protein engineering of L-leucine dehydrogenase (L-AmDH) and L-phenylalanine dehydrogenase (F-AmDH).

While natural AmDHs have not yet been identified, artificial amine dehydrogenases have been created *via* semi-rational protein engineering of existing amino acid dehydrogenase scaffolds. In a first ground-breaking study, L-leucine dehydrogenase from *Bacillus stearothermophilus* was chosen as starting point for directed evolution.^[161] Since a holo-structure of this enzyme was not available, the X-ray crystal structure of an analogous L-phenylalanine dehydrogenase was used for identifying potentially important positions in the amino acid sequence. A total of 19 residues was selected for mutagenesis, whereby some amino acid positions were grouped according to CAST (combinatorial active site saturation test) principles. The best variant obtained after several rounds of directed evolution contained four mutations (K68S, E114V, N261L, V291C) and showed a specific activity of 0.69 U/mg in the reductive amination of ketone **86**, producing the (R) -amine **87** in 99.8% *ee* (Scheme 11). Not surprisingly, two of the introduced mutations (K68S, N261L) exchanged the residues involved in binding of the natural substrate's carboxylate group with more apolar amino acids. As a consequence, the natural activity of the enzyme was completely abolished.

Following a similar strategy, the same authors converted L-phenylalanine dehydrogenase from *Bacillus badius* into an AmDH suitable for the reductive amination of aromatic ketones (F-AmDH).^[162] A two point variant (K77S, N276L) transformed *p*-fluorophenylacetone (**88**), for instance, into the corresponding amine (R) -**89** (Scheme 11) with 93.8% conversion, 74% (212 mg) isolated yield, and an *ee* of >99.8%. Moreover, a range of other aromatic and aliphatic ketones were shown to be accepted (Table 9). To alleviate issues arising from the low water-solubility of the apolar substrates, the use of F-AmDH in biphasic aqueous–organic media

has also been investigated.^[163] To further broaden the scope of accessible amines, a chimeric AmDH was generated from the two initially developed biocatalysts *via* domain shuffling: The N-terminal substrate-binding domain of F-AmDH was fused to the C-terminal cofactor-binding domain of L-AmDH, creating a chimeric enzyme called cFL1-AmDH.^[164] Unlike the parent enzymes, cFL1-AmDH showed substantial activity towards aryl-conjugated ketones, e.g., acetophenone (85) and 1-tetralone (86; Table 9). Besides, it exhibited a profoundly altered temperature profile, reaching maximum activity only above 70 °C, a temperature at which its half-life time was 40 min. The excellent stereoselectivity of the parent enzymes was conserved in the chimeric protein.

Table 8. Specific activities of amine dehydrogenases (AmDHs) with selected substrates.

Substrate	Specific Activity [mU/mg]		
	L-AmDH ^(a)	F-AmDH ^(b)	cFL1-AmDH ^(c)
 86	690	73	<i>nd</i>
 90	<i>nd</i>	0	133
 91	123	28	<i>nd</i>
 92	<i>nd</i>	0	69
 88	0	4000	1725
 93	59	0	301
 94	<i>nd</i>	0	107
 95	<i>nd</i>	0	30
 96	<i>nd</i>	541	<i>nd</i>

(a) Data from ref. [161, 164]; 20 mM substrate, 200 μM NADH, 500 mM NH₄Cl/NH₄OH buffer, pH 9.6, 25 °C.

(b) Data from ref. [162, 164]; 20 mM substrate, 200 μM NADH, 225 mM NH₄Cl/NH₄OH buffer, pH 9.6, 25 °C.

(c) Data from ref. [164]; 20 mM substrate, 5 M NH₄Cl buffer, pH 9.6, 60 °C, NADH conc. not specified. *nd*, not determined.

1.9 Opine Dehydrogenases and ‘Reductive Aminases’

Enzymes that can catalyze the reductive amination of ketones with more complex amines than ammonia or methylamine would be highly attractive and versatile biocatalysts. Opine dehydrogenases are able to couple α -keto acids with a broad range of α -amino acids, but show limited acceptance for less functionalized amines (see Section 2.4.2). More flexible biocatalysts can be obtained by directed evolution, although the expansion of both amine and ketone scope represents a formidable challenge. Nevertheless, researchers from industry have recently succeeded in engineering an opine dehydrogenase into a broad-scope ‘reductive aminase’.

1.9.1 Opine Dehydrogenases

The recombinant opine dehydrogenase from *Arthrobacter* sp. 1C has been used in the asymmetric synthesis of various opines by reacting the amine group of L-amino acids with the ketone moiety of pyruvate, 2-oxobutyrate, or glyoxylate (Figure 7).^[120, 165] The products were generally obtained as single stereoisomers (*ee, de* >99%) in moderate to good isolated yields (16–71%). The reductive coupling of phenylalaninol with pyruvate was also successful, providing *N*-1-(*R*)-carboxyethyl-(*S*)-phenylalaninol in 88% isolated yield.

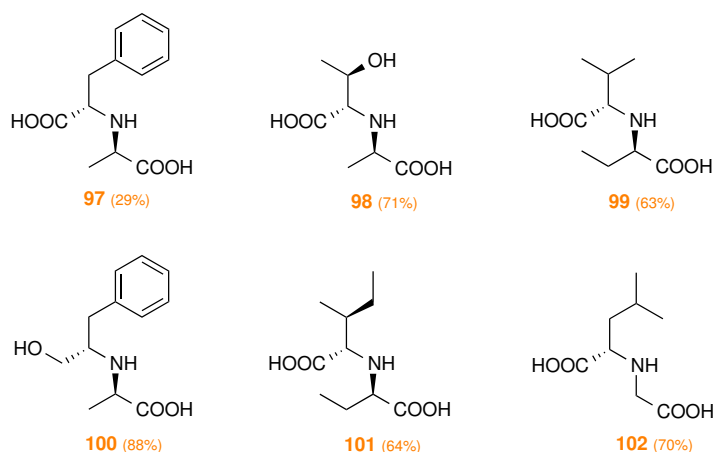
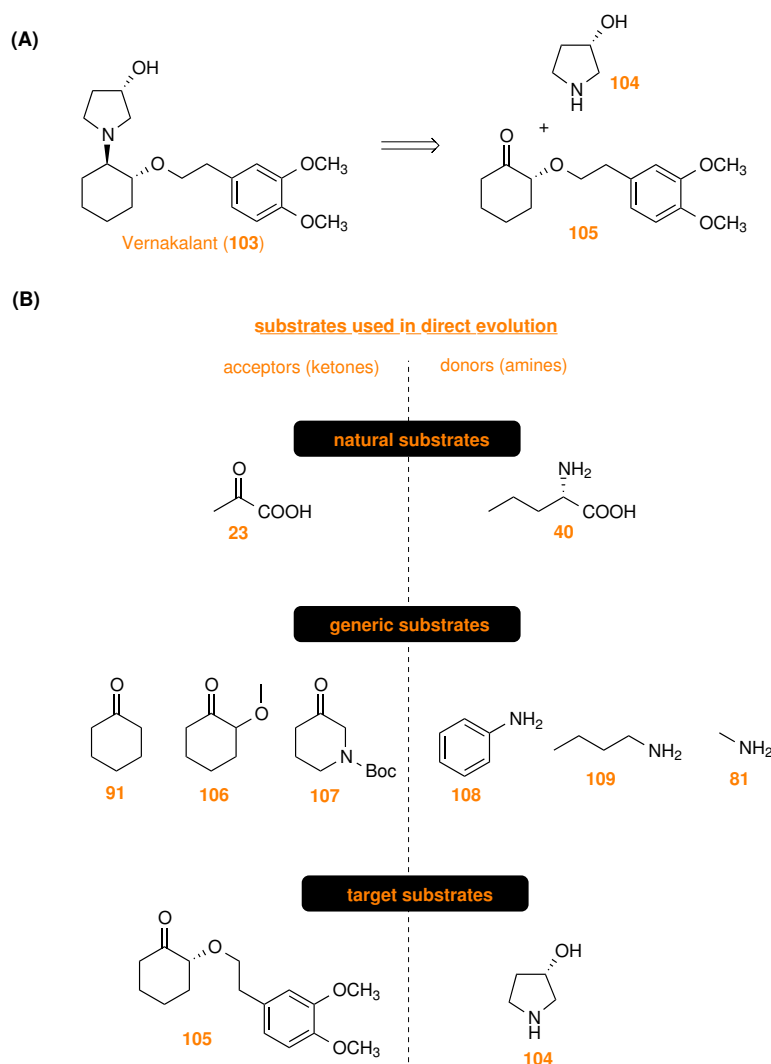


Figure 7. Examples of amino acid conjugates obtained *via* opine dehydrogenase-catalysed reductive amination on preparative scale. Isolated yields are given in parentheses..

1.9.2 Engineering of a 'Reductive Aminase's

An enzymatic reductive amination process was desired for the production of the antiarrhythmic drug vernakalant (**103**; Scheme 12, A). Since natural enzymes catalyzing this transformation are unknown, a suitable biocatalyst was developed by means of an extensive directed evolution program, for which the above-mentioned opine dehydrogenase from *Arthrobacter* sp. 1C served as the starting point.^[166–168]



Scheme 12. (A) Structures of vernakalant (**103**), an antiarrhythmic drug, and two building blocks (**104** and **105**) from which vernakalant can be derived via asymmetric reductive amination. (B) Substrates used for evolving an opine dehydrogenase into a 'reductive aminase' for vernakalant synthesis.

The early rounds of protein engineering were aimed at increasing the stability and specific activity of the enzyme, while the substrate specificity was tackled in

later rounds. To maximize the chances of identifying positive clones, the engineering program followed a ‘substrate walking’^[42] approach: Initially, the reductive coupling of the natural substrates (pyruvate and L-norvaline) was used as assay reaction. One of the two compounds was then replaced with various non-natural derivatives, before moving on to reactions between two non-natural substrates. Eleven rounds of directed evolution afforded a variant that carries 29 mutations spread over the 359-residue protein sequence (corresponding to a mutation rate of 8%) and produces the target compound vernakalant in approx. 80% *de*. Using a glucose/GDH system for cofactor regeneration, complete conversion of precursor **105** (50 mM) into **103** was achieved within 24 h, but the reaction required a large excess of amine **104** (1.6 M) and a high reductase loading (10 g/L). Continuing evolution of the biocatalyst can be expected to further improve the selectivity and efficiency of the target reaction, while muteins from intermediate stages of the protein engineering program showed broad substrate scope and might hence provide starting points for the development of other ‘reductive aminases’.

1.10 Structural and Mechanistic Aspects

Many of the imine-reducing enzymes discussed in the previous sections have been characterized not only with regard to their catalytic function but also with regard to their three-dimensional structure. X-ray crystal structures have been solved for various enzymes, including dihydrofolate reductases, pteridine reductases, Δ^1 -pyrroline-5-carboxylate reductases, L-amino acid dehydrogenases, opine dehydrogenases, a bacterial Δ^1 -piperidine-2-carboxylate/ Δ^1 -pyrroline-2-carboxylate reductase, (*R*)- and (*S*)-selective imine reductases, and even a thiazoline reductase (Table 9). In several cases it was also possible to obtain structures for ternary complexes of the enzyme, its cofactor, and a substrate, product, or inhibitor molecule. This wealth of structural information, combined with kinetic studies and computational methods (*e.g.* protein–ligand docking, molecular dynamics simulations) has contributed to a detailed understanding of the active-site architecture and catalytic mechanism of some of these enzymes (*e.g.*, DHFR). Others, like the only recently discovered family of imine reductases, are currently not so well understood.

The imine-reducing enzymes encountered in nature are structurally diverse. They range in size and complexity from small monomeric proteins, *e.g.*, human dihydrofolate reductase (21 kDa), to large assemblies like human Δ^1 -pyrroline-5-carboxylate reductase, whose native form is a homodecamer (pentamer of dimers) with a total molecular mass of approx. 370 kDa.^[169] In general, dimeric structures or substructures are common among imine-reducing enzymes, but there seems to be no privileged fold for C=N-reducing activity (see Figure 7 for selected struc-

tures). In some cases, enzymes catalysing the same imine reduction reaction can even be based on entirely different protein scaffolds – an example of divergent evolution of enzyme function.

Table 9. Available X-ray crystal structures of imine-reducing enzymes. For dihydrofolate reductase, dihydropteridine reductase, and Δ^1 -pyrroline-5- carboxylate reductase only selected examples are listed..

Enzyme	Source Organism	PDB Codes			Ref.
		<i>apo</i>	<i>holo</i>	<i>ternary</i>	
Dihydrofolate reductase (384) ^(a)	<i>Homo sapiens</i>	-	4M6J	4M6K 4M6L	[170]
Dihydropteridine reductase (4)	<i>Rattus norvegicus</i>	-	1DHR	-	[171]
Thiazoline reductase (2)	<i>Yersinia enterocolitica</i>	4GMF	4GMG	-	[172]
Δ^1 -Pyrroline-5-carboxylate reductase (12)	<i>Homo sapiens</i>	2GER	2GRA	2GR9	[169]
Δ^1 -Piperidine-2-carboxylate reductase (3)	<i>Pseudomonas syringae</i>	1WTJ	2CWF	2CWH	[85]
L-Leucine dehydrogenase (2)	<i>Bacillus sphaericus</i>	1LEH	-	-	[173]
L-Phenylalanine dehydrogenase (4)	<i>Sporosarcina psychrophila</i> <i>Rhodococcus</i> sp. M4	3VPX -	- -	- 1BW9 1BXG 1C1D 1C1X	[174] [175, 176]
Opine dehydrogenase (4)	<i>Pecten maximus</i>	-	3C7A	3C7C 3C7D	[119]
(R)-imine reductase (3)	<i>Streptomyces kanamyceticus</i>	3ZGY	3ZHB	-	[149]
	<i>Pseudomonas putida</i>	3L6D	-	-	[152]
(S)-imine reductase (2)	<i>Streptomyces</i> sp. GF3546	-	4OQY	-	[153]
	<i>Streptomyces aurantiacus</i>	4OQZ	-	-	

^(a) Total number of structures available in the protein data bank (PDB) as of February 2015.

For instance, the dihydrofolate reductase encoded on the so-called R-plasmid of trimethoprim-resistant bacteria is structurally unrelated to other DHFRs, including the chromosomal bacterial enzymes.^[52] Opine dehydrogenases from marine

invertebrates and *Agrobacteria*, on the other hand, are structurally homologous despite showing distinct substrate spectra and fulfilling vastly different roles in the metabolism of their respective source organisms.^[119, 177] All currently known imine reductases share the same overall architecture, irrespective of their source organism and stereoselectivity: they are homodimeric proteins showing extensive reciprocal domain swapping between the two subunits, each binding one molecule of NADPH via a Rossmann-fold motif (Figure 8). The active site is a cleft formed by residues from both subunits.^[149, 152, 153]

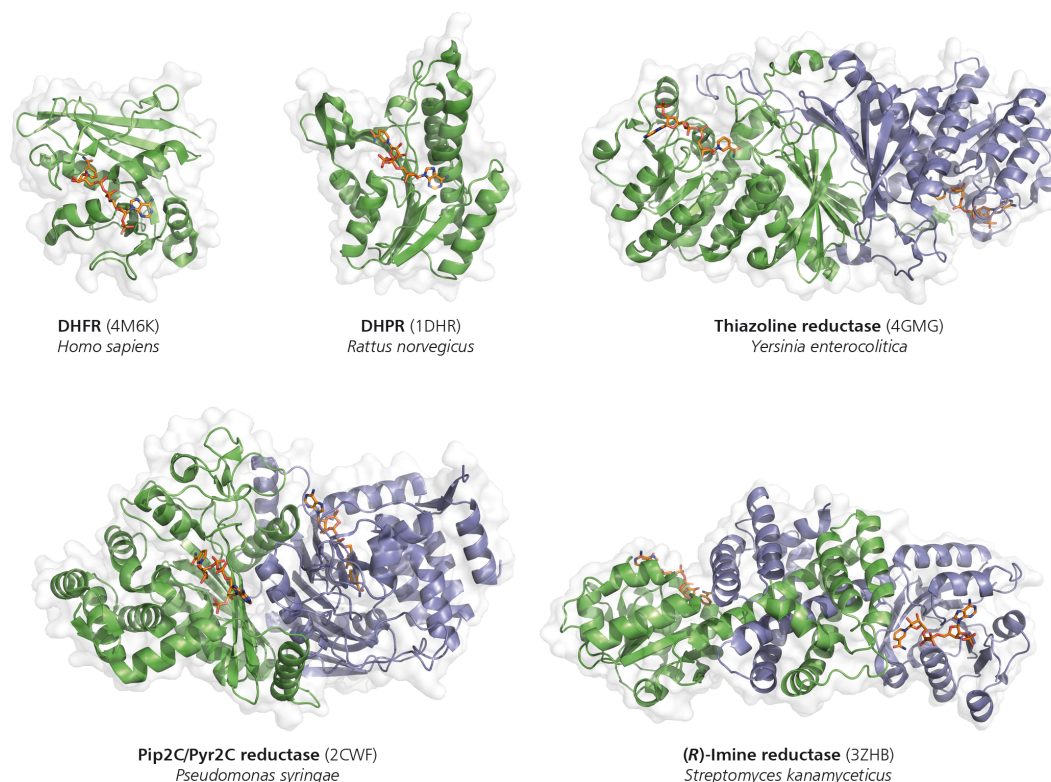
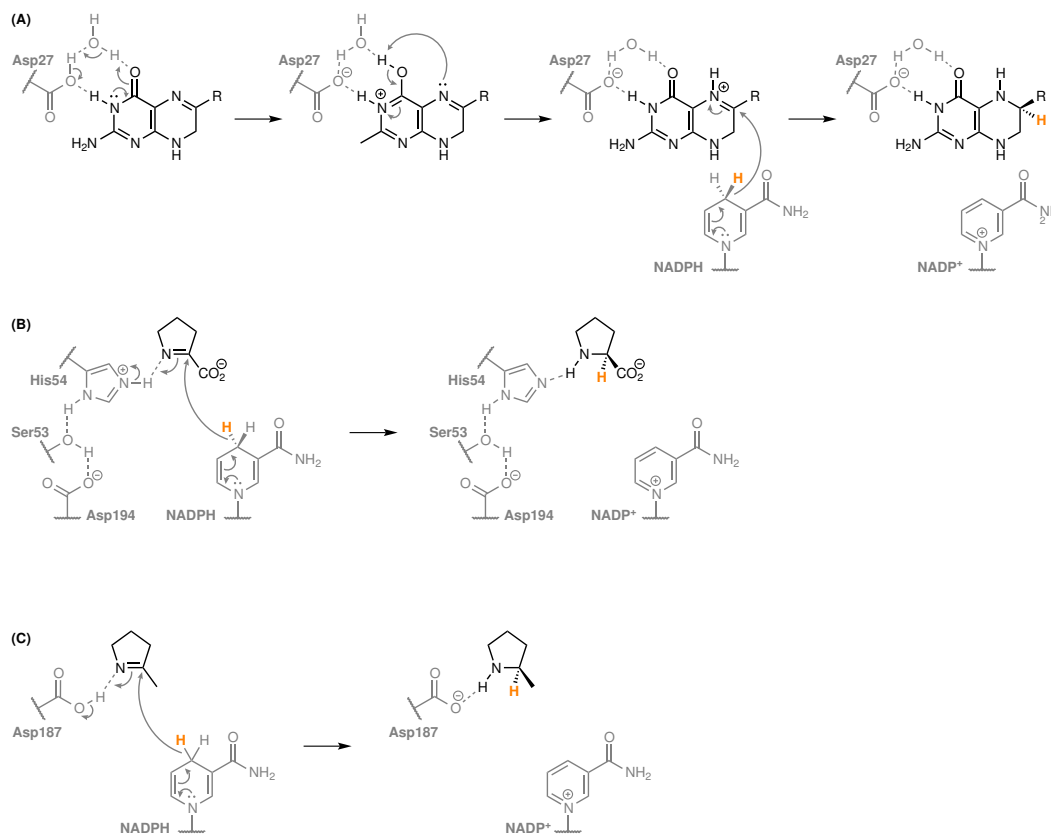


Figure 8. Three-dimensional structures of imine-reducing enzymes. 6,7-Dihydrofolate reductase (DHFR) and 6,7-dihydropteridine reductase (DHPR) are monomers, while thiazoline reductase, Δ^1 -piperideine-2-carboxylate/ Δ^1 -pyrroline-2-carboxylate reductase (Pip2C/Pyr2C reductase), and (*R*)-imine reductase are dimers. Cofactors are shown in orange, and subunits A and B of the dimeric enzymes are colored green and blue, respectively.

In general, NAD(P)H-dependent imine-reducing enzymes bind their cofactor *via* an N-terminal Rossmann fold motif containing the typical GxGxxG/A consensus sequence. An exception is Δ^1 -piperideine-2-carboxylate/ Δ^1 -pyrroline-2-carboxylate reductase from *Pseudomonas syringae*: its NADPH-binding domain is formed by a seven-stranded, mostly antiparallel β -sheet fold referred to as ‘SESAS’ fold by the authors who solved the protein’s crystal structure (Figure 8).^[85] Despite the structural variety among C=N-reducing enzymes and the broad range of substrates they act upon, their basic reaction mechanisms appear to be related. Active-site metal ions, as commonly found in alcohol dehydrogenases, have so far not

been observed in imine-reducing enzymes, and their reactivity seems to rely on general acid–base catalysis. Generally speaking, the reduction of an imine by an NAD(P)H-dependent enzyme comprises two elemental steps: (i) the transfer of a hydride from C4 of the cofactor’s nicotinamide ring to the imine carbon atom, and (ii) the transfer of a proton onto the nitrogen atom of the imine moiety. The chronology of these steps can vary, although it seems unlikely that hydride transfer precedes protonation, as the amide intermediate (R_2N^-) that would be formed in this case is a very basic species and consequently difficult to stabilize. This leaves two options for a basic order of events: either the imine is protonated first to generate an iminium ion, to which the hydride is then added, or hydride and proton transfer occur in a concerted fashion. In both cases it is reasonable to assume that a protic amino acid residue of the enzyme is involved in substrate protonation. A ‘protonation first’ mechanism has been proposed for dihydrofolate reductase from *E. coli* based on kinetic isotope effects observed with deuterated water and NADPD.^[178] An aspartic acid residue (Asp27) is thought to promote the enolisation of the substrate dihydrofolate via a water molecule. Further transfer of the enol proton onto N5 converts the substrate into an iminium ion, to which the hydride from NADPH is then thought to be delivered (Scheme 13, A). The rate-determining step of the catalytic cycle is product release.^[52, 178, 179] Interestingly, molecular dynamics simulations suggest an alternative reaction pathway in which protonation occurs by the solvent directly after hydride transfer.^[180]



Scheme 13. Proposed mechanisms for imine-reducing enzymes: **(A)** dihydrofolate reductase from *E. coli*, **(B)** Δ^1 -piperidine-2-carboxylate/ Δ^1 -pyrroline-2-carboxylate reductase from *Pseudomonas syringae*, and **(C)** imine reductase from *Streptomyces kanamyceticus*.

The proposed mechanisms for most other imine-reducing enzymes involve – either explicitly or implicitly – a concerted hydride transfer from NAD(P)H and protonation of the nascent amine by a protic active site residue. In Δ^1 -piperidine-2-carboxylate/ Δ^1 -pyrroline-2-carboxylate reductase from *Pseudomonas syringae* the alleged proton donor is His54, the pK_a of which is thought to be lowered by interactions with Ser53 and Asp194 as the three residues form a catalytic triad (Scheme 13, B). In bacterial Δ^1 -pyrroline-5-carboxylate reductases, the proton is thought to be derived from a serine or threonine residue, although the possibility that substrate protonation occurs by water is not excluded,^[181] and for the pteridine reductase from *Leishmania major* a tyrosine residue (Tyr194) has been proposed to be the proton donor.^[182] In the X-ray crystal structure of thiazoline reductase from *Yersinia enterocolitica*, His101 and Tyr128 have been identified as potential proton-donating residues.^[172] Since the carboxylate groups of cyclic imino acids have no mechanistic role in the reduction of these compounds by NAD(P)H-dependent enzymes, imine reductases – which act on analogous non-carboxylate imines – are thought to operate *via* a related mechanism. For (*R*)-selective IREDs, it was first proposed that an aspartic acid residue (Asp187) protonates the nascent ami-

ne formed upon hydride transfer from NADPH (Scheme 13, C; Figure 8).^[149] This assumption was supported by mutagenesis experiments in which Asp187 was replaced with an alanine or asparagine residue, rendering the enzyme inactive. In stark contrast to this finding, the analogous D → A mutation in (R)-IREDs from *Streptosporangium roseum* (D170A) and *Streptomyces turgidiscabies* (D172A) affected the enzymes' activity and stereoselectivity only to a limited extent: The rate of product formation was reduced to 15% and 4%, respectively, of the values observed with the wild-type IREDs, and the *ee* values of reduction product **73a** declined from 98% and 99% to 91% and 94%, respectively.^[151] One plausible reason for these conflicting observations is the already poor activity of the wild-type enzyme used in the first study, which might have caused the activities of the mutants to drop below detection limit. Besides, the distance of Asp187 to the nicotinamide ring of NADPH in the crystal structure of *S. kanamyceticus* IRED (7.9 Å from O-carboxyl to C4) seems too large for direct proton transfer from the aspartic acid side-chain onto the substrate and hence suggests that this transfer might be mediated by a water molecule.^[183] (S)-Selective IREDs bear a conserved tyrosine residue in the position equivalent to Asp187 of the *S. kanamyceticus* enzyme (Figure 9).

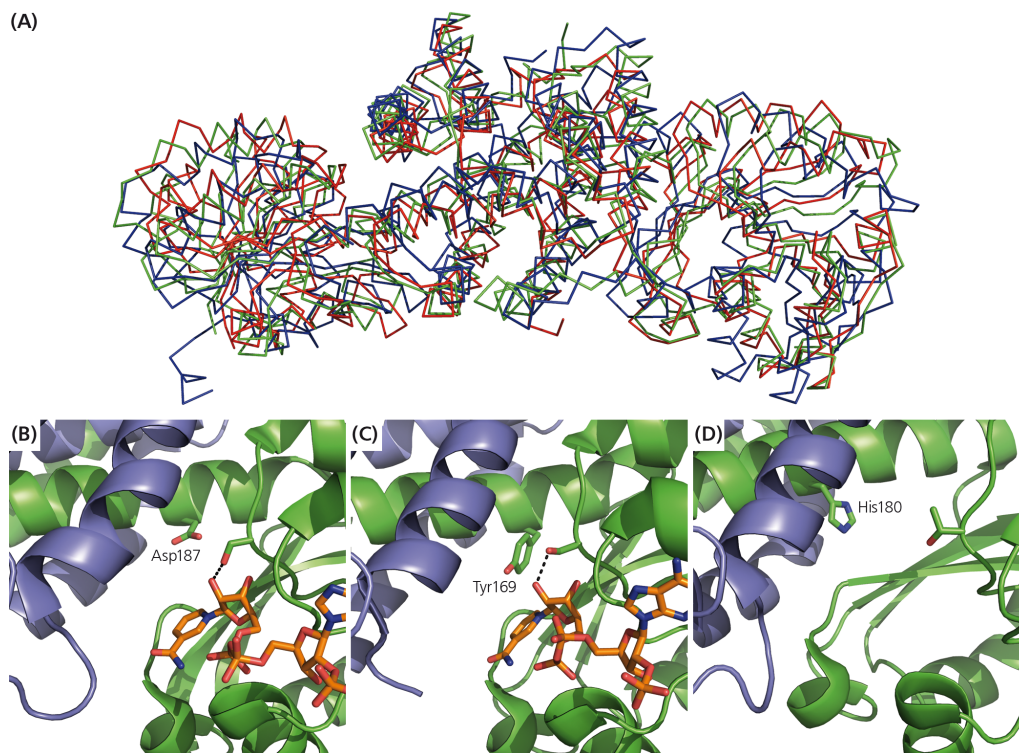


Figure 9. Structural comparison of imine reductases (IREDs): **(A)** aligned backbone traces of the IREDS from *Streptomyces kanamyceticus* (3ZHB, holo-enzyme; green), *Streptomyces* sp. GF3546 (4OQY, holo-enzyme; red), and *Pseudomonas putida* (3L6D, apo-enzyme; blue). **(B–D)** Active-site close-ups of the IREDS from *Streptomyces kanamyceticus* **(B)**, *Streptomyces* sp. GF3546 **(C)**, and *Pseudomonas putida* **(D)**. The catalytically important Asp, Tyr, and His residues are labelled. NADPH cofactors are shown in orange and hydrogen-bonding interactions of a conserved serine residue with the ribose moiety of the cofactor are shown as dashed lines.

In the crystal structure of the (*S*)-imine reductase from *Streptomyces* sp. GF3546, this tyrosine residue is located within a distance of 4.9 Å from the nicotinamide ring of the cofactor and is hence appropriately positioned for acting as a direct proton donor to the nascent amine. Replacement of Tyr187 with phenylalanine in the (*S*)-IRED from *Paenibacillus elgii* rendered the protein almost entirely inactive, supporting the hypothesis of this residue having an important role in catalysis.^[151] Intriguingly, the catalytically important aspartate and tyrosine residues are conserved among known or putative members of the (*R*)-IRED and (*S*)-IRED families.^[151] One might hence be tempted to assume that these residues are involved in determining the stereoselectivity of imine reductases. The real picture is more complex, however, since the recently described (*R*)-selective IRED from *Pseudomonas putida* bears neither of these amino acids at the respective position. Instead, a histidine residue located one turn of an α -helix downstream (His180) occupies roughly the same space in the enzyme's active site as Asp187 does in other (*R*)-IREDs (Figure 9). This histidine can therefore be considered to function as proton shuttling residue in the *P. putida* enzyme.^[152] Additional, as

yet unpublished data suggest that other amino acid residues (including asparagine) can be found at the 'proton-donor position' in functional, naturally occurring IREDs, and that the stereoselectivity of imine reductases is not easily predicted based on polar active-site residues alone.^[183] In summary, imine-reducing enzymes – including the recently discovered family of imine reductases – are structurally diverse but mechanistically related. The main structural determinants of C=N-reducing activity are the enzymes' ability to bind substrate and cofactor in an orientation favorable for hydride transfer and the existence of a protic active-site residue that mediates proton transfer onto the nascent amine. In this respect, they do not seem to differ much from alcohol dehydrogenases of the short-chain dehydrogenase/reductase family (e.g., hydroxysteroid dehydrogenases, ADHs from *Lactobacillus kefir* and *Lactobacillus brevis*).^[184, 185] However, imine reduction by alcohol dehydrogenases is unknown, while imine reductases are incapable of reducing ketones. The reasons for this exclusive chemoselectivity remain to be elucidated.

2 Results and Discussion



2.1 Characterization of Novel Imine Reductases

To expand the scope of already known and characterized imine reductases (IREDs) several novel imine reducing enzymes were heterologously expressed, purified and characterized in terms of temperature stability, pH optimum, substrate spectrum and stereoselectivity. Figure 10 shows a phylogenetic tree of possible imine reductases including enzymes with known C=N bond reducing activity and the IREDs that have been studied throughout this work.

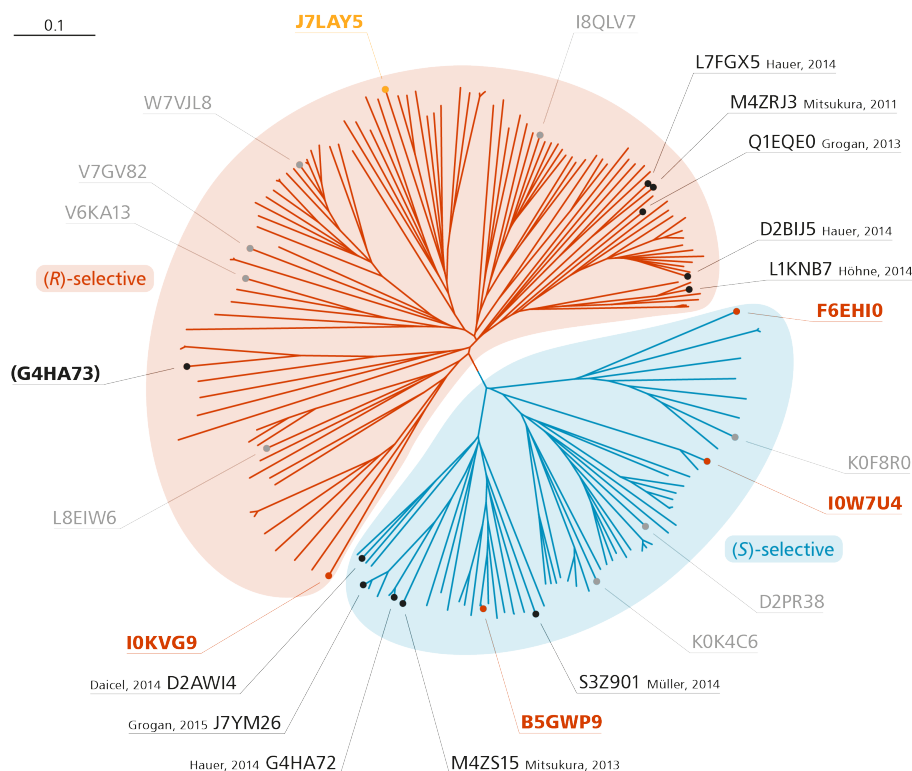


Figure 10. Phylogenetic tree of imine reductases. Enzymes highlighted in red were insoluble or unstable after desalting or thawing. R-IRED G4HA73 (bold black in parentheses) could not be investigated due to a wrong gene provided by the supplier.

All new imine reductases (light grey) displayed in Figure 10 were identified through a sequence database search which was based on the overall sequence homology including functional key motifs derived from available crystal structures. Suitable candidates representing major branches of the phylogenetic tree were heterologously expressed in *E. coli* and characterized.

The enzymes marked in red were either found to be localized in the cell pellet after SDS-PAGE analysis or precipitated after desalting or thawing. In some cases the instability problem could have been overcome by applying a buffer system featuring a higher salt concentration, to stabilize soluble proteins.

Besides insoluble and unstable enzymes the (*R*)-selective imine reductase J7LAY5

was found to be inactive towards several tested substrates (see Section 3.6). Despite these inaccessible proteins several novel potential biocatalysts have been investigated and characterized for future applications.

2.2 Gene Subcloning and Plasmid Transformation

All of the herein described and characterized IREDs were already subcloned by Jörg Schrittwieser and successfully transformed into *E. coli* BL21 (DE3) cells except of two: the (*S*)-selective imine reductase K0K4C6 and the (*R*)-selective imine reductase G4HA73. These two genes had to be subcloned into a pET28a(+) vector and transformed into competent cells.

In a first attempt, the IRED genes and the vector were digested using XhoI and NdeI endonucleases as described in the procedures section of this work. Analysis of the restricted vector on a TAE agarose gel under blue light showed completely digested samples. For the ligation of the desired reductase genes and the expression vector, a standard procedure was applied as described in Section 4.2.1. The samples were initially transformed into chemically competent *E. coli* NEB 5 α cells since this strain shows a better uptake of DNA. Unfortunately no colonies were obtained for neither the (*R*) nor the (*S*) gene.

By preparing a newly digested vector solution, a successful transformation was achieved and each agar plate contained several colonies, three of which were picked randomly and used for sequence analysis. Transformants harboring the (*S*)-IRED gene were found to be active clones, however, the picked colonies of the (*R*)-selective enzyme contained only truncated gene inserts, based on the sequence analysis results. To investigate if full length inserts were cloned into the vector and transformed, 12 colonies of the (*R*)-IRED plate were picked, used for singularisation and analyzed *via* colony PCR.

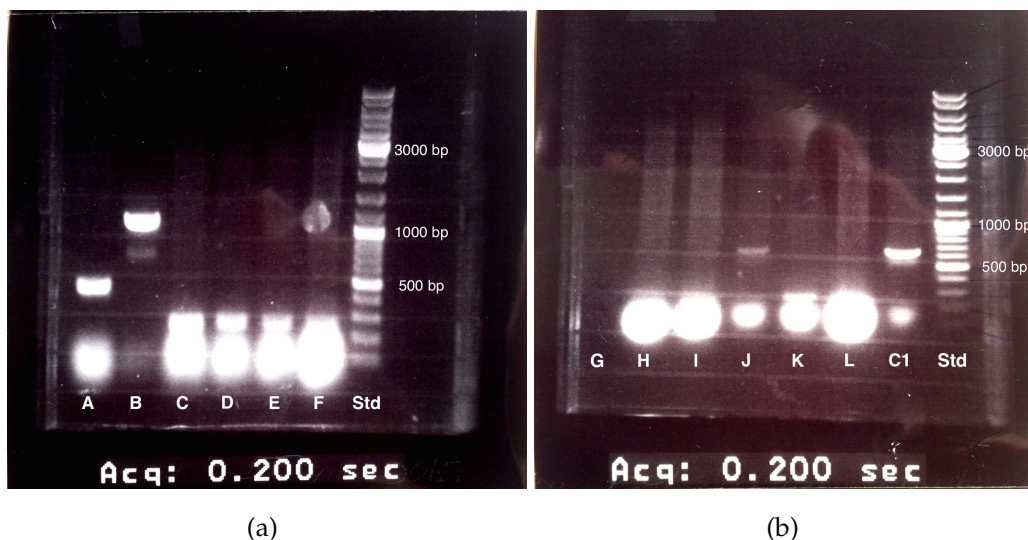


Figure 11. Colony PCR results of (*R*)-IRED G4HA73. Picked colonies were labeled A-L. Sample C1 represents the reference harboring only a truncated insert.

As can be seen in Figure 11 nearly all transformants contained religation products of the vector (colonies C-F, H, I, K, L). Samples A and J showed bands at around 500 bp, meaning that half of the desired gene was incorporated into the plasmid whereas colony B was the only sample to have seemingly taken up an intact vector encoding for the imine reductase.

A DNA sequence analysis of this colony, though, showed that a different kind of imine reductase was ligated with the vector, which suggested that a wrong batch of the IRED gene was synthesized by the supplier. For this reason, only the (*S*)-selective reductase was used for further experiments and characterization.

2.3 Heterologous Protein Expression and Protein Purification

All of the transformed imine reductases were successfully expressed in *E. coli* and the soluble proteins were purified and concentrated by HisTrap Ni²⁺-affinity chromatography using an FPLC system. Hereinafter only a few examples of enzymes are shown that were localized in the supernatant fraction as well as those that were found to be concentrated in the cell pellet.

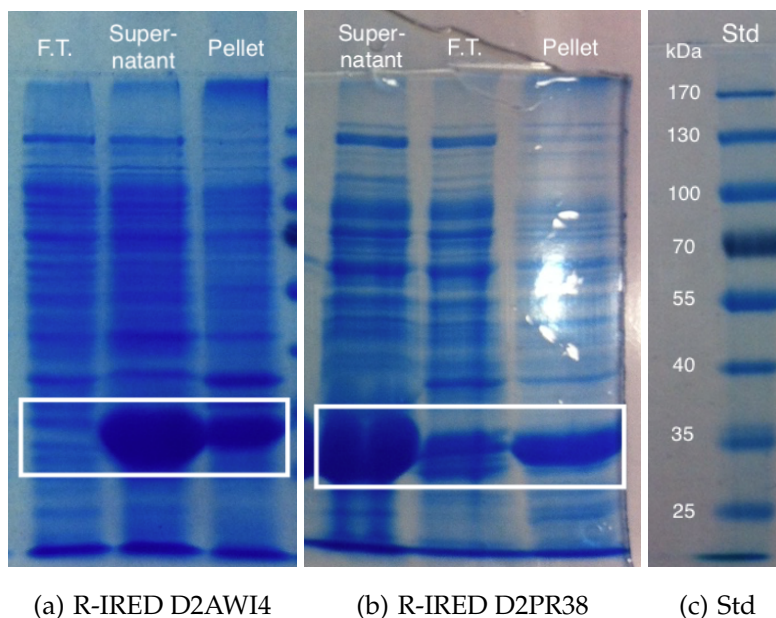


Figure 12. SDS-PAGE results of imine reductases that appeared to be soluble proteins. The higher amount is found in the supernatant after centrifugation. F.T. = flow through of the HisTrap column after loading the enzyme containing supernatant.

The annotated molecular masses of 30-32 kDa in the UniProt database correlated perfectly with the detected sizes on the polyacrylamide gel when compared to a protein standard. In most cases, bands of the expressed protein were also visible in the cell pellet after centrifugation, however, the major part of the desired enzyme was detected in the soluble fraction (see Figure 12).

For insoluble IREDs, on the other hand, the main protein fraction was seen in the cell pellet, due to formation of inclusion bodies (see Figure 13).

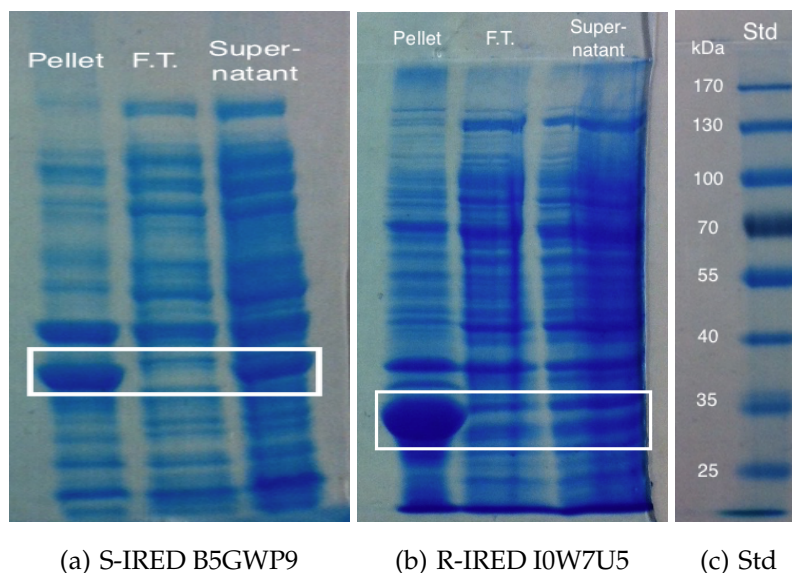


Figure 13. Acrylamide gels of insoluble imine reductases. The majority of the catalytic enzyme is located in the cell pellet. F.T. = flow through of the HisTrap column after loading the enzyme containing supernatant.

When looking at the source organisms of the different imine reductases, a wide range of various prokaryotes is covered, particularly bacteria seem to provide the vast majority of functional enzymes. *Streptomyces* sp. account for nearly half of the proteins described in this thesis but also other Actinobacteria like *Nocardia*, *Frankia*, *Micromonospora* and *Kribbella* were found to contain genes of this class of enzymes. The following table gives an overview of catalytically active proteins, that were studied during this work, with their specific activity and source organism.

Table 10. Catalytically active imine reductases, their specific activities and source organism.

Enzyme (UniProt No.)	Specific Activity [U/mg]	Source Organism
R-IRED M4ZRJ3	0.0782 ^(a)	<i>Streptomyces</i> sp. GF3587
R-IRED V6KA13	0.768 ^(b)	<i>Streptomyces niveus</i> NCIMB 11891
R-IRED W7VJL8	2.30 ^(b)	<i>Micromonospora</i> sp. M42
R-IRED V7GV82	0.187 ^(a)	<i>Mesorhizobium</i> sp. L2C089B000
R-IRED L8EIW6	0.175 ^(a)	<i>Streptomyces rimosus</i> subsp. <i>rimosus</i> ATCC 10970
R-IRED J7LAY5	0.0765 ^(b)	<i>Nocardiosis alba</i> (strain ATCC BAA-2165 / BE74)
R-IRED Q1EQE0	1.33 ^(c)	<i>Streptomyces kanamyceticus</i>
R-IRED I8QLV7	1.98 ^(c)	<i>Frankia</i> sp. QA3
S-IRED M4ZS15	2.10 ^(b)	<i>Streptomyces</i> sp. GF3546
S-IRED D2PR38	1.70 ^(b)	<i>Kribbella flavida</i> (strain DSM 17836)
S-IRED D2AWI4	0.0390 ^(a)	<i>Streptosporangium roseum</i> (strain ATCC 12428)
S-IRED J7YM26	0.312 ^(b)	<i>Bacillus cereus</i> BAG3X2-2
S-IRED K0F8R0	1.16 ^(b)	<i>Nocardia brasiliensis</i> ATCC 700358
S-IRED K0K4C6	0.102 ^(c)	<i>Saccharothrix espanaensis</i> (strain ATCC 51144)

^(a) Substrate: 2-methyl-1-pyrroline (**72a**).

^(b) Substrate: 3,4-dihydroisoquinoline (**76a**).

^(c) Substrate: 6-methyl-2,3,4,5-tetrahydropyridine (**74a**).

2.4 Temperature Stability of Selected Enzymes

The stability of enzymes at higher temperatures is an important characteristic, since unstable or temperature labile enzymes mean a loss of function and therefore are unsuitable for biocatalytic applications. Therefore the remaining activity of the imine reductases was investigated when exposed to a heat treatment at various temperatures.

Aliquots of only the purified enzyme solution were incubated at varying temperatures for one hour and the remaining activity was determined via triplicate measurements.

The following examples were picked to give a short overview of the temperature profile of selected enzymes.

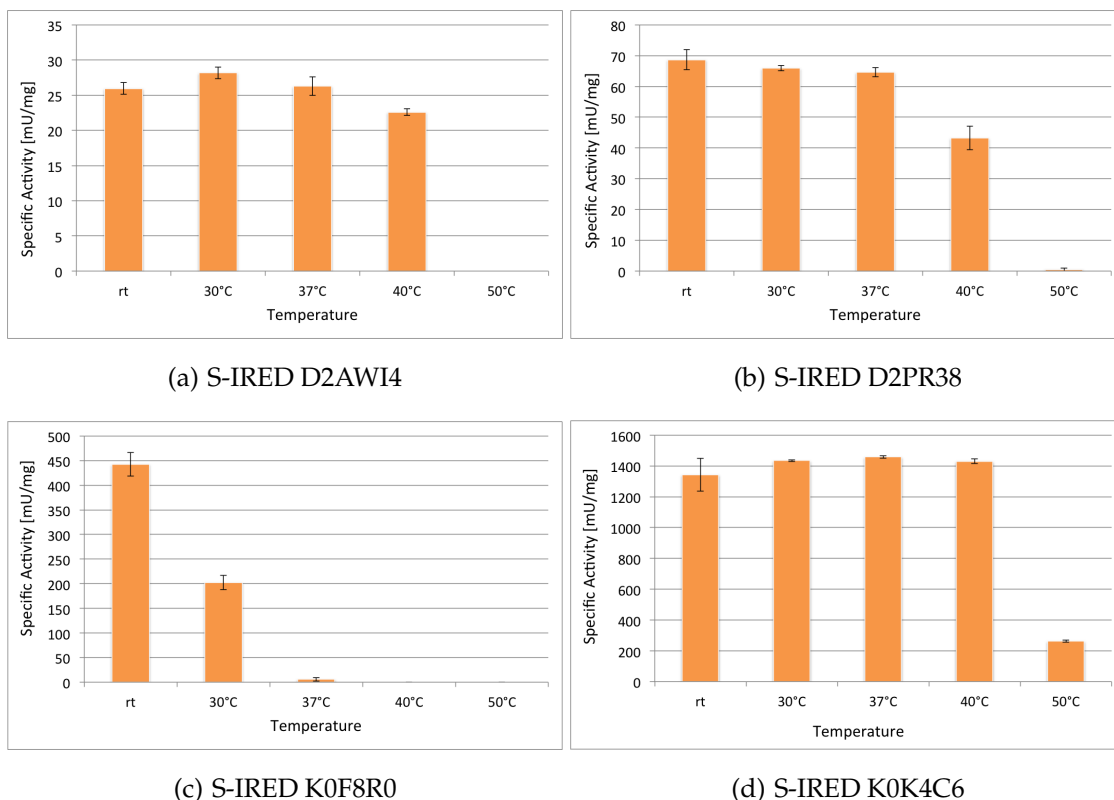


Figure 14. Results of the temperature stability assay measurements of (*S*)-selective enzymes using the novel procedure. Error bars represent standard deviation of triplicate measurements.

All (*S*)-selective enzymes show nearly the same behavior regarding their temperature profile, with a few exceptions (Figure 14). In most of the cases the enzymatic activity remained nearly unaltered below 40 °C, as can be observed with S-IREDs D2AWI4 and D2PR38 (see Figure 14 (a) and (b)).

The imine reductase with the UniProt accession number K0F8R0 on the contrary appeared to be rather temperature labile, since a loss of activity of more than 50% was observed even at 30 °C.

With S-IRED K0K4C6, on the other hand, a slight increase in activity was visible at higher temperatures, compared to the room temperature value. Even at 50 °C about 20% of its initial activity was measurable.

The (*R*)-selective enzymes showed a similar behavior, when heat-treated, with a few exceptions as well.

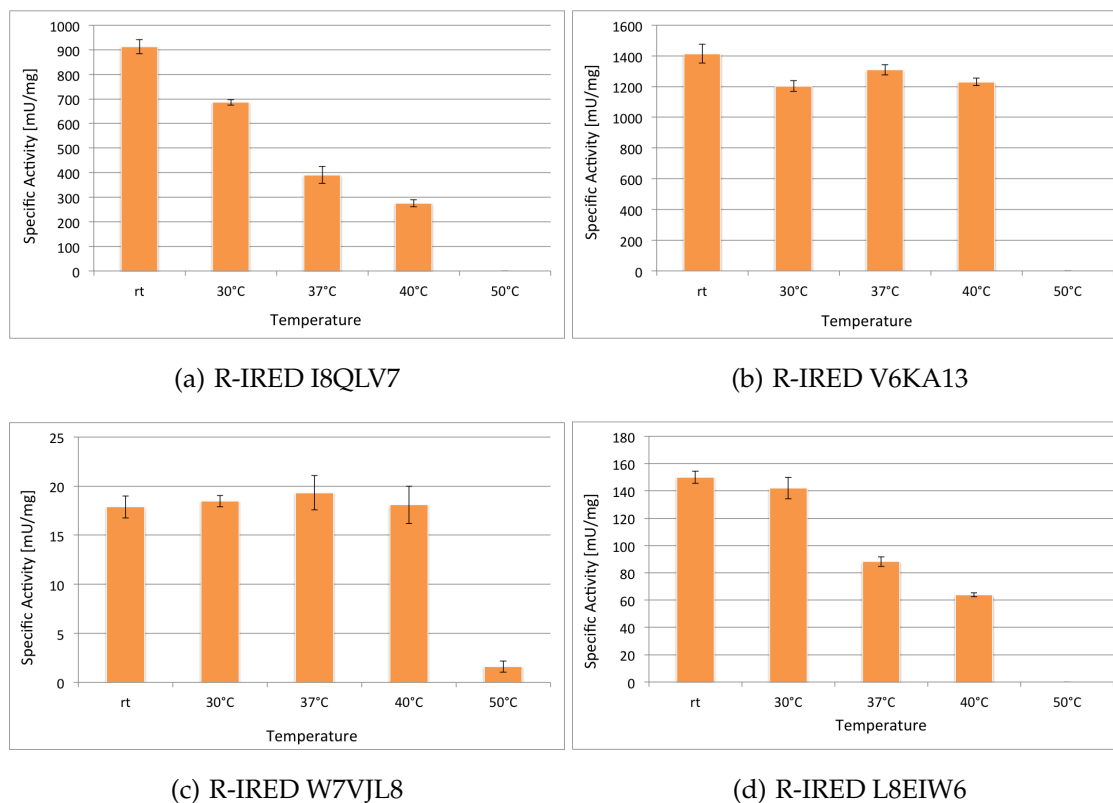


Figure 15. Results of the temperature stability assay measurements of (*R*)-selective enzymes using the novel procedure. Error bars represent standard deviation of triplicate measurements.

The general trend in heat resistance was comparable with that observed for (*S*)-selective enzymes, with a more or less stable activity below 40 °C. R-IRED I8QLV7, however, showed an almost continuous decline in its activity as did R-IRED L8EIW6, even though the drop at 30 °C is not as significant as with the first-mentioned enzyme.

In literature only little data is available regarding the influence of temperature on the activity. MITSUKURA *et al.* investigated the (*S*)-imine reductase M4ZS15 from *Streptomyces* sp. GF3546 which showed an optimum temperature at 40 °C, but the applied procedure differs from the assay used in this work.^[145] Researchers from the same group also characterized the (*R*)-imine reductase from *Streptomyces* sp. GF3587 (UniProt accession number M4ZRJ3) which in turn was found to be stable below 35 °C, however the incubation time was shorter, with only 30 min.^[144] For both of these enzymes, a temperature study was done within this thesis as well (see Figure 16) whereby the (*S*)-selective reductase didn't show any remaining activity at 40 °C. The enantiocomplementary enzyme showed some altered behavior as well, with a near unchanged activity for all the tested temperatures and only a slight decrease at 30 °C, compared to the untreated sample.

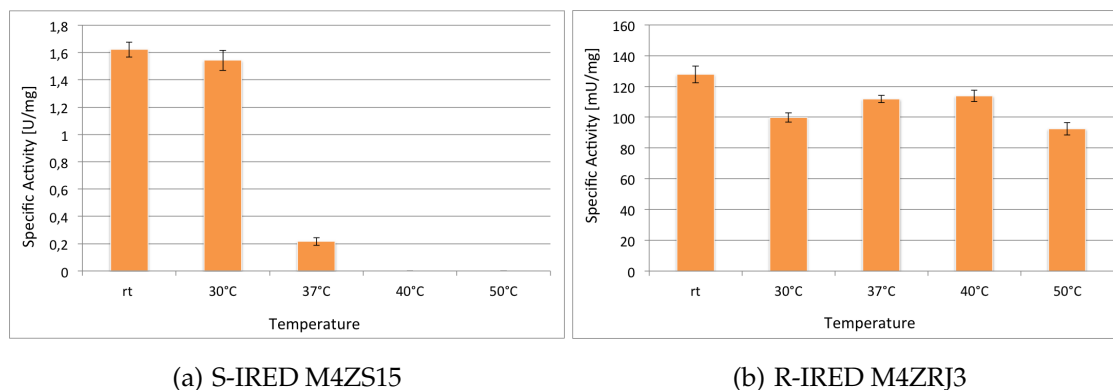


Figure 16. Temperature stability results obtained in this work of literature-known imine reductases M4ZS15 and M4ZRJ3. Error bars represent standard deviation of triplicate measurements.

Another interesting and also necessary parameter regarding enzyme activity is the optimal pH of the protein environment, which will be discussed in the following section.

2.5 pH Dependence of Imine Reduction

The optimal pH value of each protein plays an important role for its activity, since changes in proton concentration affect the stability and therefore the 3D structure of an enzyme due to protonation or deprotonation events on amino acid side chains. Moreover, the presence of acids or bases in the protein environment also has a direct influence on the enzymatic activity as many biocatalytic reactions depend on the transfer or the abstraction of a proton.

For this purpose the pH dependence of isolated and purified (*R*)- and (*S*)-selective imine reductases was investigated during this master thesis.

Figure 17 shows the results of S-IRED enzymes over the range of pH 6 - pH 11. For the majority of the studied proteins the optimum pH for the reduction of imines was found to be around 6 - 7.5. S-IRED K0F8R0 has its highest activity at even higher pH values, namely between 8 - 8.5. In the case of the imine reductase K0K4C6, on the other hand, the maximum activity was achieved at a more acidic pH, therefore, the measurements were expanded to much lower values to see, if a further increase in activity was detectable (see Figure 17 (d)).

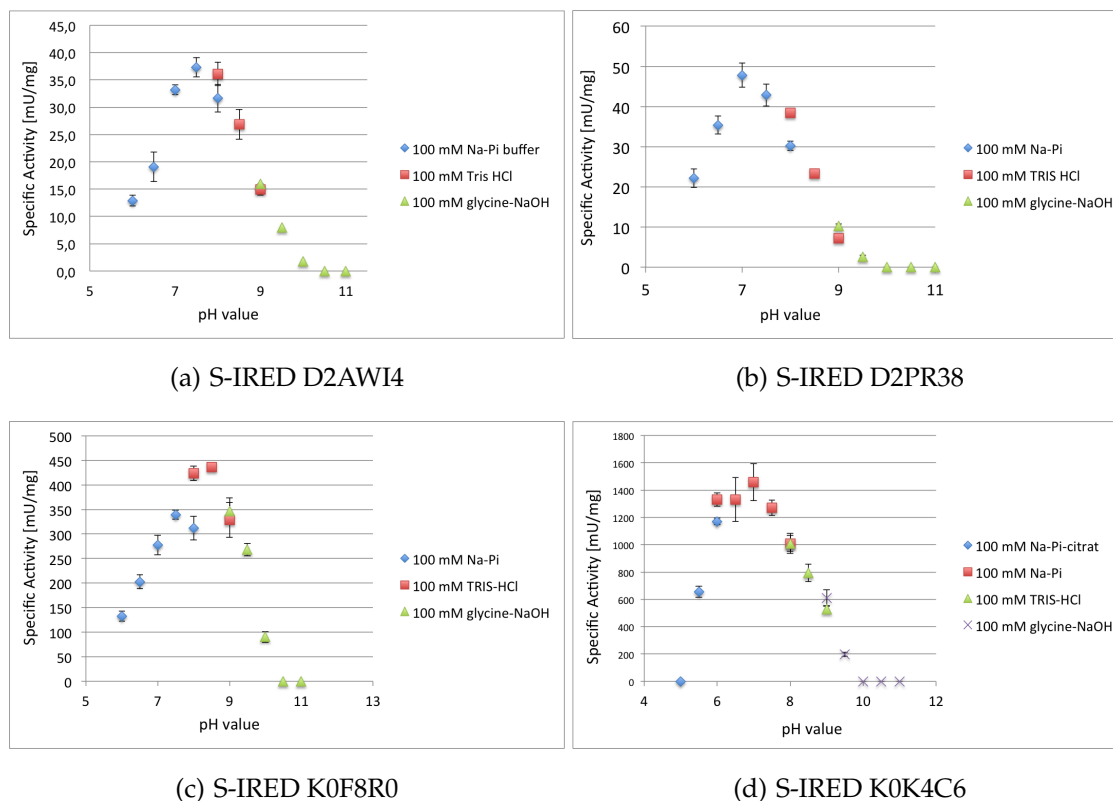


Figure 17. pH dependence of (S)-selective imine reductases. Error bars represent standard deviation of triplicate measurements.

(R)-Imine reductases show their highest reduction activity at about the same pH range as S-IREDs do, with the highest pH optimum at 8 for reductase W7VJL8. In Figure 18 the results of these measurements are shown.

R-IREDs I8QLV7 and V6KA13 behaved in a similar manner as their enantiocomplementary enzyme K0K4C6, displaying an activity maximum at pH 6. By measuring their enzymatic activity at even lower values, no further increase was visible at all [see Figure 18 (a) and (b)].

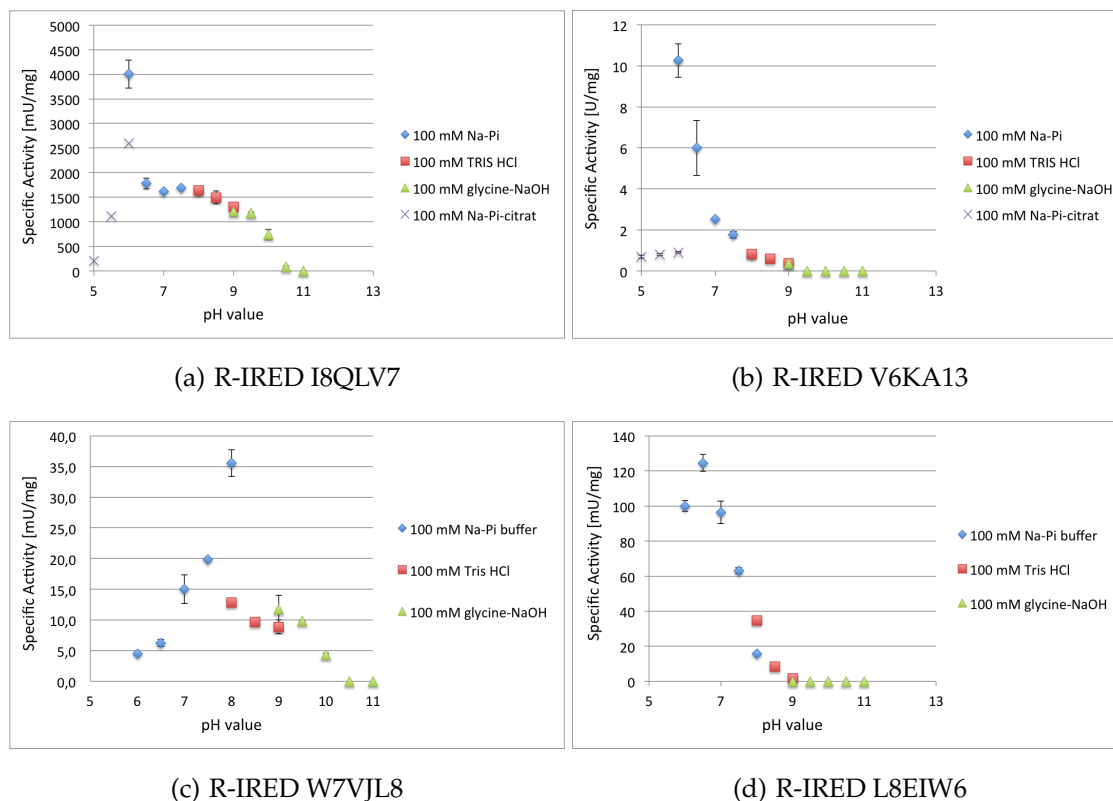


Figure 18. pH dependence of (*R*)-selective imine reductases. Error bars represent standard deviation of triplicate measurements.

Another interesting observation that arose from these experiments was an apparent correlation between the buffer composition and measured activity. At pH 6, 8 and 9 a change in the buffer system had to be done, due to different buffer capacities at various pH values.

When looking at Figure 18 (a) and (b) this correlation is rather obvious at pH 6, when switching from the sodium phosphate-citrate to the sodium phosphate buffer. At this point R-IRED I8QLV7 increased its activity in reducing 6-methyl-2,3,4,5-tetrahydropyridine (**74a**) by more than 1.4 U/mg whereas R-IRED V6KA13 showed an even higher increase in reduction activity of more than 9 U/mg.

A similar effect was also observed for the (*R*)-selective reductase W7VJL8, although at pH 8, as can be seen in Figure 18 (c), where more than 50% more activity was measured with the Na-Pi buffer system.

For the *S*-IREDD family proteins such a dramatic change in enzymatic activity is missing, although a slight difference at pH 8 in Figure 17 (b) and (c) was observed.

The literature provides more information about pH optima than it does for temperature stability. Data is available for the already mentioned (*S*)-imine reductase M4ZS15 and the (*R*)-selective enzyme M4ZRJ3, which show a pH optimum at 7.0 and 6.5 for the reduction of 2-methyl-1-pyrroline, respectively.^[144, 145]

Figure 19 represents the results obtained during this work for the just mentioned enzymes, which were comparable with the values claimed in the literature.

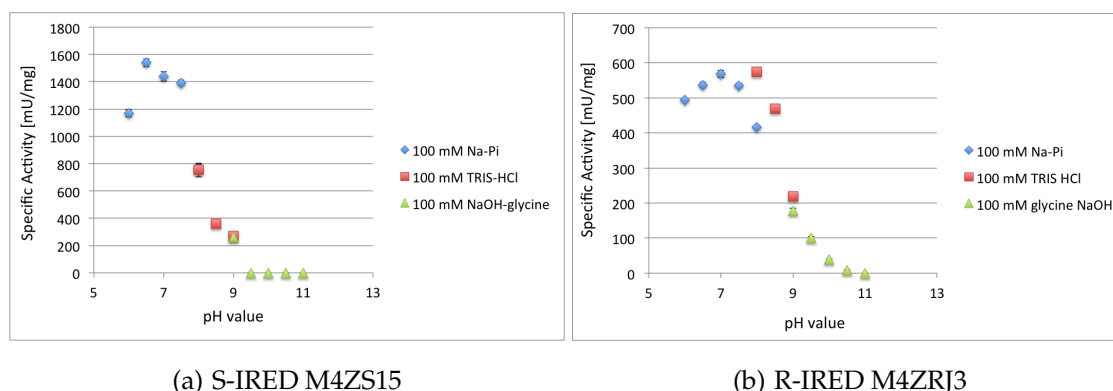


Figure 19. pH dependence of literature known imine reductases M4ZS15 and M4ZRJ3.

Some more information was made available by GAND *et al.* who characterized three novel imine reductases from *Paenibacillus elgii* B69, *Streptomyces ipomoeae* 91-03 and *Pseudomonas putida* KT2440.^[152]

The optimal pH values for these enzymes were found to be 7.0, 6.5 and 6.5, respectively, which is in agreement with the values found during this study, whereas GAND *et al.* also noticed the change in activity with different buffer systems.

2.6 Substrate Scope Determination & Cofactor Dependence of R- and S-IREDs

The substrate spectrum of an enzyme of interest is an important property, since a wider range of accepted molecules means a potentially broader application in biocatalysis.

Therefore, the newly characterized imine reductases were subjected to a substrate screening, which included a large bandwidth of different cyclic secondary imine compounds, such as five-, six- and seven-membered rings, as well as bicyclic systems of the dihydroisoquinoline type. Figure 20 gives a summary of the compounds used in this screening.

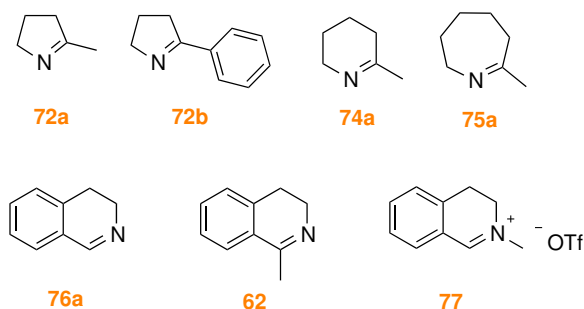


Figure 20. Imine compounds used in the substrate screening assay for novel imine reductases.

The substrate screening revealed-for the greater part of the enzymes-a rather clear trend of accepted molecules. The following table summarizes the obtained activities towards the different imines whereas the diagrams shown on the next page display an graphical overview of the measured activities for each compound with (*R*)- and (*S*)-imine reductases.

Table 11. Overview of obtained activities, with standard-deviations, for (*R*)- and (*S*)-imine reductases using different types of cyclic imines.

Enzymes	Substrates			
	72a	72b	74a	76a
	Specific Activities [U/mg] \pm Standard Deviation			
R-IREN M4ZRJ3	0.286 \pm 0.0638	1.40 \pm 0.204	0.757 \pm 0.0811	1.92 \pm 0.0307
R-IREN V6KA13	0.00797 \pm 0.0225	0.122 \pm 0.219	0.0345 \pm 0.00920	0.505 \pm 0.157
R-IREN W7VJL8	0.0276 \pm 0.0361	0.0197 \pm 0.00683	0.446 \pm 0.0355	5.41 \pm 0.273
R-IREN V7GV82	0.165 \pm 0.0146	0.0653 \pm 0.0146	1.10 \pm 0.0802	3.48 \pm 0.124
R-IREN L8EIW6	0.175 \pm 0.0206	0.0654 \pm 0.0358	0.430 \pm 0.000	0.292 \pm 0.00596
R-IREN J7LAY5	0.0280 \pm 0.0132	0.0761 \pm 0.00659	0.109 \pm 0.0161	0.0590 \pm 0.0194
R-IREN Q1EQE0	no activity	0.0777 \pm 0.00538	0.497 \pm 0.0353	0.162 \pm 0.0427
R-IREN I8QLV7	0.538 \pm 0.00932	0.202 \pm 0.00	1.88 \pm 0.111	0.159 \pm 0.00538
S-IREN J7YM26	0.0175 \pm 0.00	0.0336 \pm 0.00877	0.0979 \pm 0.00506	0.184 \pm 0.0101
S-IREN M4ZS15	0.0543 \pm 0.0256	0.214 \pm 0.109	0.367 \pm 0.0306	0.479 \pm 0.0156
S-IREN D2PR38	0.0493 \pm 0.0131	0.0796 \pm 0.00656	0.425 \pm 0.0473	2.84 \pm 0.282
S-IREN D2AWI4	0.0527 \pm 0.0279	0.0984 \pm 0.0327	0.116 \pm 0.0150	0.246 \pm 0.0715
S-IREN K0F8R0	0.168 \pm 0.0336	0.133 \pm 0.0645	0.746 \pm 0.0440	0.709 \pm 0.0132
S-IREN K0K4C6	0.0497 \pm 0.0108	0.0466 \pm 0.00538	0.180 \pm 0.0142	0.889 \pm 0.120

Table 11 continued.

Enzymes	Substrates		
	62	77	75a
	Specific Activities [U/mg] ± Standard Deviation		
R-IREN M4ZRJ3	5.30 ± 0.477	2.85 ± 0.336	7.02 ± 0.716
R-IREN V6KA13	1.08 ± 0.193	0.0292 ± 0.0302	0.0266 ± 0.0138
R-IREN W7VJL8	0.584 ± 0.0205	0.237 ± 0.00683	1.05 ± 0.118
R-IREN V7GV82	1.21 ± 0.0219	0.388 ± 0.0146	0.826 ± 0.0364
R-IREN L8EIW6	0.254 ± 0.000	0.196 ± 0.0119	0.365 ± 0.00596
R-IREN J7LAY5	0.0373 ± 0.00932	0.0466 ± 0.0142	0.00312 ± 0.0215
R-IREN Q1EQE0	0.0249 ± 0.00538	0.00311 ± 0.00	0.0280 ± 0.0142
R-IREN I8QLV7	0.224 ± 0.00	0.460 ± 0.00	0.221 ± 0.0247
S-IREN J7YM26	0.0146 ± 0.0101	0.199 ± 0.0101	0.133 ± 0.00506
S-IREN M4ZS15	0.166 ± 0.0156	1.15 ± 0.0270	0.360 ± 0.0212
S-IREN D2PR38	2.62 ± 0.153	0.515 ± 0.0656	0.455 ± 0.0473
S-IREN D2AWI4	0.0387 ± 0.115	0.137 ± 0.0572	0.130 ± 0.00544
S-IREN K0F8R0	4.19 ± 0.158	0.298 ± 0.0285	0.298 ± 0.0132
S-IREN K0K4C6	1.49 ± 0.0635	0.34 ± 0.0377	0.0995 ± 0.00538

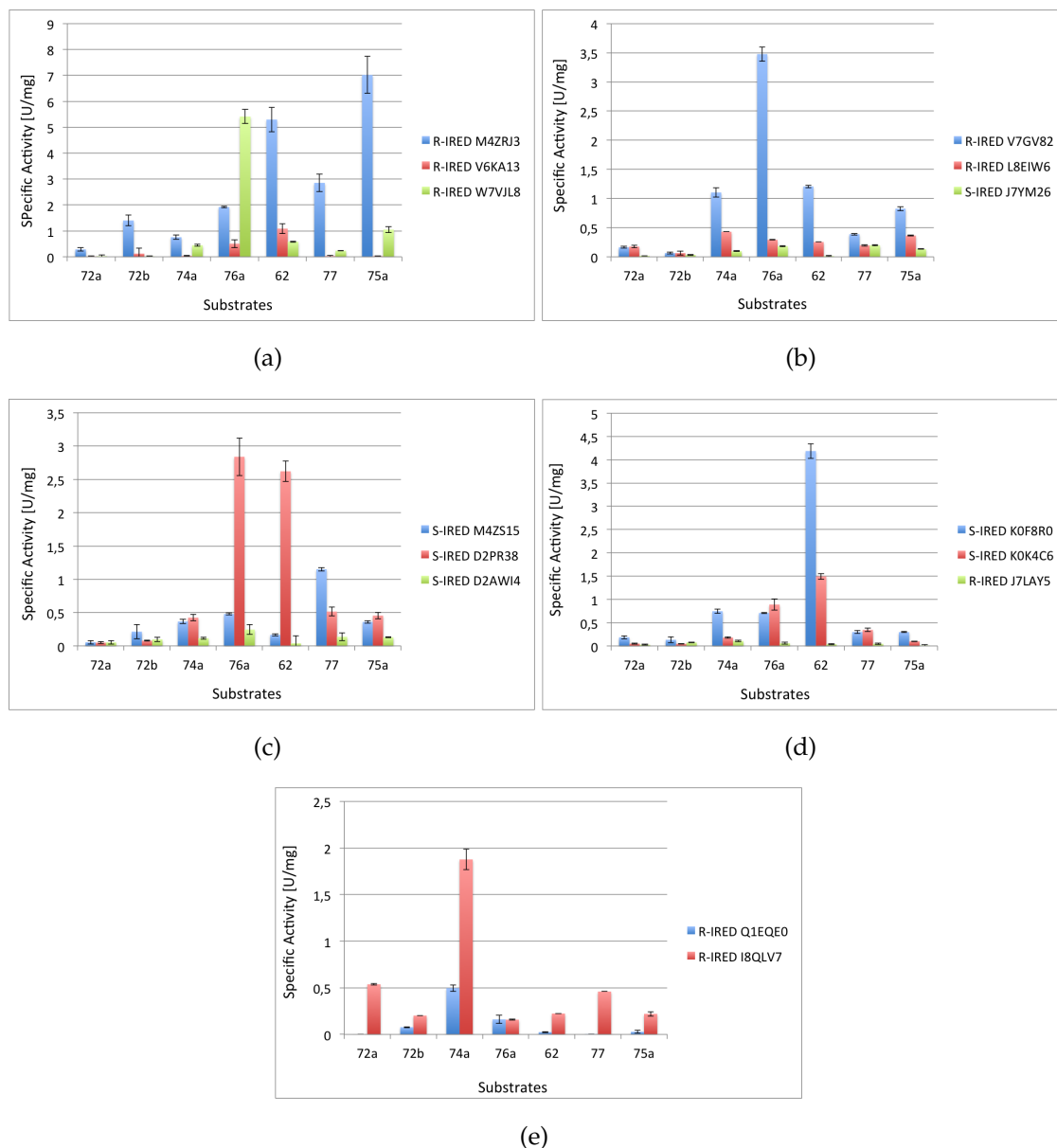


Figure 21. Specific activity of IREDs with various substrates. Error bars represent standard deviation of triplicate measurements.

The covered substrate range should give some more details about the influence of different parameters of the converted molecules, such as ring size, substituent hindrance and polarity. From the results in Figure 21 it can be noticed that a distinct preference for dihydroisoquinoline compounds **62**, **76a** and **77** is detectable for nearly all tested enzymes, with the highest activity of over 5 U/mg for R-IREDs W7VJL8 and M4ZRJ3 [see Figure 21 (a)], which may allude to the natural function of this class of enzymes.

When looking at the influence of the substituent at the imine carbon for these substrates no obvious tendency can be observed. A few enzymes seem to prefer the methyl-substituted 3,4-dihydroisoquinoline (**62**) over the unsubstituted one (R-IREDs M4ZRJ3 and V6KA13 as well as S-IREDs K0F8R0 and K0K4C6) with ac-

tivities ranging from 1 to over 5 U/mg. Others like the R-IREDs W7VJL8, V7GV82 and the (S)-selective ones M4ZS15 and D2AWI4 show their highest reduction potential with unsubstituted 3,4-dihydroisoquinoline (**76a**).

For three of the tested proteins (S-IRED D2PR38 and R-IREDs L8EIW6, I8QLV7) no real preference was observed between compounds **76a** and **62**. Furthermore iminium substrate **77** was accepted by nearly all of the enzymes, though the measured activity remained below 0.5 U/mg in most of the cases. The consideration behind this molecule as substrate was based on the proposed mechanism of imine reduction by RODRÍGUEZ-MATA *et. al*^[149], where the imine is protonated first to form the iminium ion which is then reduced by hydride transfer from NADPH (see Scheme 13). Therefore the provided iminium ion **77** should have been reduced more easily however the obtained data does not support this.

Only one of the investigated enzymes was proven to show a strongly reduced activity as potential imine reductase, namely R-IRED J7LAY5, as already mentioned in Section 3.1. Its highest activity of ca. 109 mU/mg was measured with 6-membered ring imine 2-methylpiperidine, unfortunately, no crystal structure is available for this particular enzyme, which might have given a better view on the reduced imine reduction activity.

By comparing the determined activities of 5-membered ring compound 2-methyl-1-pyrroline (**72a**) with 6-membered ring substrate 6-methyl-1-piperidine (**74a**) the influence of the ring size can be clearly seen. This relationship is represented in Figure 22.

In the best case an 8.6-fold increase in enzymatic activity was observed for S-IRED D2PR38 using the piperidine compound instead of the 5-membered ring system. The (R)-selective reductase M4ZRJ3 even showed its highest activity with the 7-membered azepine substrate **75a** [see Figure 21 (a)].

A similar behavior is reported in literature^[146, 147], where kinetic constants of S-IRED M4ZS15 and R-IRED M4ZRJ3 were determined, showing an over 5-fold and 10-fold increase in activity, respectively, when providing the piperidine substrate.

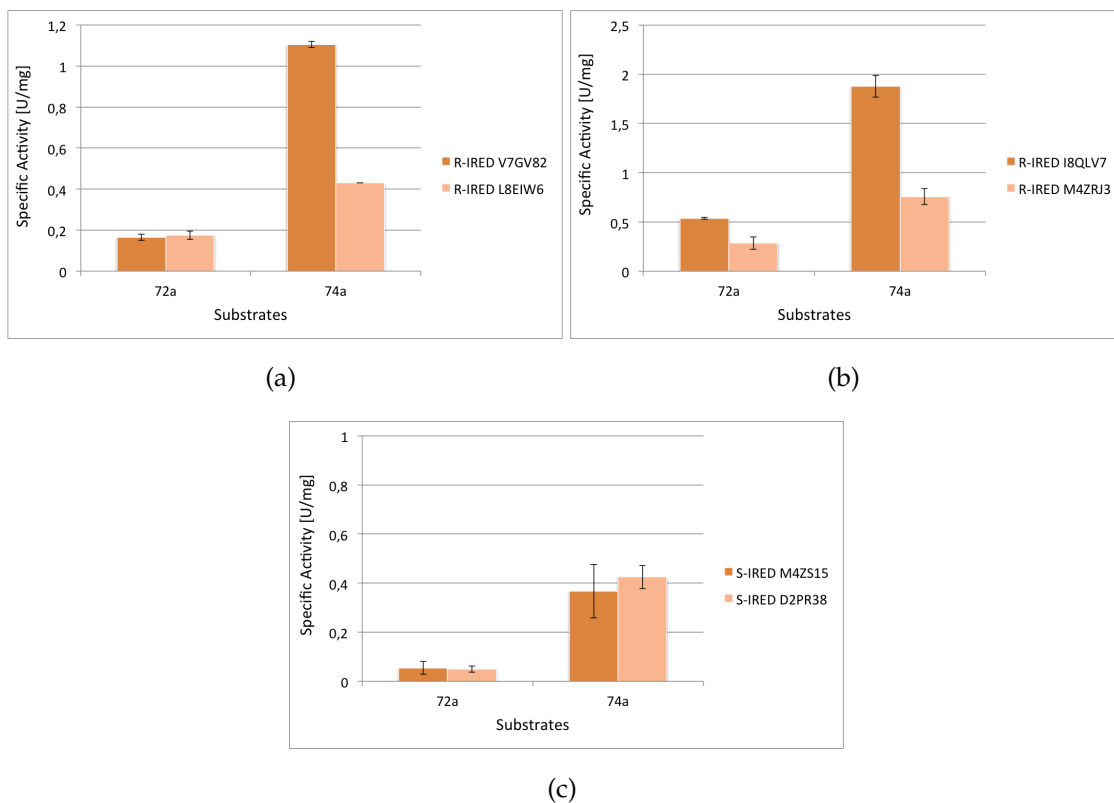


Figure 22. Influence of the ring size of imine compounds on the measured activity of IRED enzymes.

Interestingly, the size of the substituent on the imine-carbon of pyrroline compound **72a** seem to have only little influence on the observed activity, although (*R*)-imine reductase M4ZRJ3 showed a significant increase in the reduction of substrate **72b** whereas for R-IRED I8QLV7 reduction activity dropped by more than 50% compared to 2-methyl-1-pyrroline [compare Figure 21 (a) and (e)]

All of the herein tested enzymes were found to depend on the phosphorylated cofactor as electron donor. To investigate if the more expensive NADPH could be replaced with its dephosphorylated analogue, the activity of selected enzymes was measured with NADH as the hydride source. In Figure 23 the results of this measurement are shown.

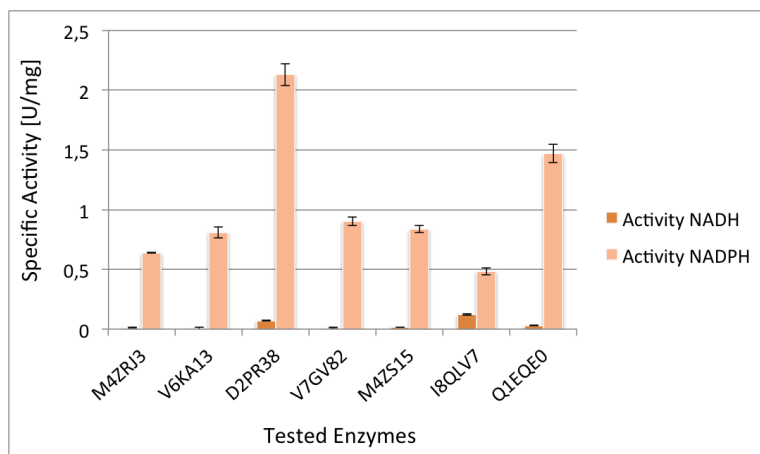


Figure 23. Comparison of enzymatic activity using NADH as reduction equivalent.

The results in Figure 23 clearly outline the strict dependence on NADPH as the required cofactor for all the tested reductases. R-IRED V7GV82 only showed 0.4% of its actual activity when supplied with the non-phosphorylated nicotinamide whereas R-IRED I8QLV7 retained more than 27% of its reduction activity. All the other enzymes however, showed a highly decreased reactivity towards their substrates, ranging from 0.85 - 3.4%. This circumstance is made even more clear, when looking at the amino acids surrounding the additional phosphate group of the NADPH molecule. The crystal structures of R-IRED Q1EQE0 and S-IRED M4ZS15 revealed conserved side chains, namely positively charged arginine and lysine as well as hydrogen bond forming threonine and serine residues in the proximity. Hence the PO_4^{2-} group, and as a consequence the whole NADPH molecule, is stabilized by these residues whereas the dephosphorylated NADH interacts only loosely with the enzyme leading to a decreased reduction activity.

These amino acids were also found in R-IRED V6KA13 and S-IRED D2PR38 at equivalent positions, by a sequence alignment with M4ZS15. Reductase D2PR38 even showed the same Rossmann-fold sequence as its homologue with residues GLGPMGQ being highly conserved in both enzymes. However the Rossmann-fold found in (*R*)-selective enzyme V7GV82 only resembles 5 out of 7 amino acids of the M4ZS15 protein.

2.7 Biotransformations and Enantioselectivity

To further investigate the substrate scope of the herein described R- and S-IREDs, lyophilized cell-free extracts were used for biotransformations, with higher-substituted 3,4-dihydroisoquinoline compounds as well as an indoleine derivative. In Figure 24 the tested molecules are shown.

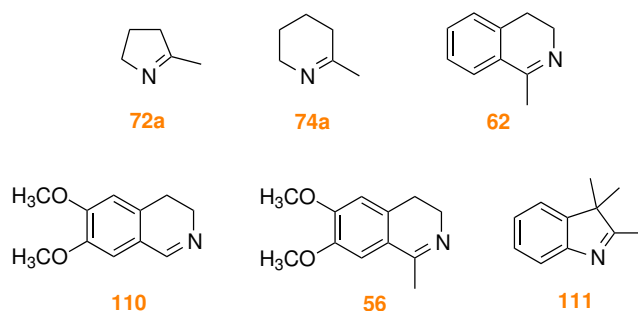
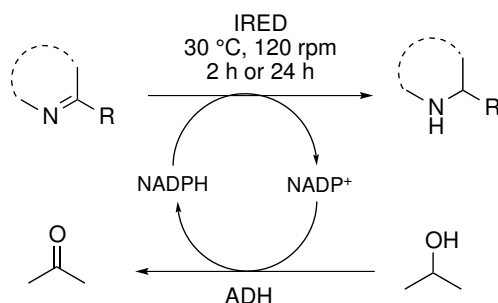


Figure 24. Imine compounds used for biotransformations with new imine reductases.

The biotransformations were allowed to proceed for 2 and 24 h respectively by using a NADPH regenerating system of recombinantly expressed alcohol dehydrogenase from *Lactobacillus brevis* (*Lb*-ADH)^[186, 187] and isopropanol (see Scheme 14).



Scheme 14. Exemplary biotransformation of an imine using an ADH/isopropanol cofactor recycling system.

Pyrroline **72a** and piperidine compound **74a** were both converted after 2 h with almost full conversion by most of the investigated enzymes, yielding (*R/S*)-2-methylpyrrolidine and (*R/S*)-2-methylpiperidine, respectively, with (*R*)-2-methylpyrrolidine as an important building block for new histamine H₃ receptor antagonists.^[188, 189]

Enantioselectivities for these two compounds varied with the applied enzyme, unfortunately not all biotransformations yielded interpretable chromatograms due to insufficient extraction or incomplete derivatization. Perfect *e.e.* values of

over 99% for (*S*)-2-methylpyrrolidine (**73a**) were observed with S-IRED K0F8R0 as well as for the (*R*)-enantiomer by using R-IRED W7VJL8 as biocatalyst. Another (*R*)-selective reductase, J7LAY5, showed full conversion after 2 h with the 5-membered ring, although the obtained *e.e.* was rather low, with only 31.8% for the (*R*)-enantiomer. For the same enzyme, on the other hand, complete conversion of the piperidine compound was detected after 2 h with good enantiomeric excess of over 94%. Other tested imine reductases, such as S-IREDs D2PR38, M4ZS15 and R-IRED V7GV82 also showed good to excellent enantiomeric preferences with 89, 97 and >98% for the corresponding enantiomer.

Dihydroisoquinoline derivative **62** showed good conversions with all of the applied enzymes after 24 h, which is in agreement with the above discussed substrate scope findings, however only two reductases (R-IRED V6KA13 & R-IRED M4ZRJ3) converted the compound completely after 2 h incubation. Conversely the *e.e.s* were found to be perfect for almost all reductases tested, with >99% for the (*R*)- as well as the (*S*)-enantiomer. To the present day, only (*S*)-selective reductases are known that show good to excellent conversions as well as near perfect *e.e.s* for compound **62**^[146, 153, 190], whereas literature-known (*R*)-imine reductase M4ZRJ3 only afforded 71% enantiomeric excess of (*R*)-**59**.^[147] The herein investigated R-IREDs not only converted compound **62** with 95-100% measured conversion, but also afforded the (*R*)-amine with >99% *e.e.*, which represents a significant improvement.

By introducing electron donating methoxy groups to compound **62**, affording molecule **56**, a decrease in conversion was detectable for the greater part of the tested enzymes with conversions ranging from 0-88%. The highest amount of formed amine was measured with S-IRED D2PR38, showing 90% of formed product after 24 h. The relatively low substrate conversion rates may also be traced back to the sterical hindrance of the -OCH₃ groups at positions 6 and 7, suggesting a difference in the size of the active site cleft for the various reductases. For (*S*)-imine reductases D2PR38 and M4ZS15 the obtained *e.e.s* were perfect, with >99% for the (*S*)-enantiomer, in both cases. On the contrary, the enantiocomplementary enzymes V7GV82 and V6KA13 produced the (*R*)-enantiomer with 59 and 75 % *e.e.*, respectively. For the other tested enzymes no or only tiny amounts of formed product were observed.

Indoleine compound **111** was also confirmed to be a substrate for the investigated proteins with the highest conversion of 88% detected with S-IRED J7YM26. Enantiomeric excesses for the given molecule were rather difficult to determine, since no real satisfying separation technique was found as for the other molecules. Furthermore literature^[191] only provides data for the (+) and (-) enantiomers of the

indole product therefore this nomenclature is used for the described biotransformations. When looking at the molecule itself, the imine bearing 5-membered ring is heavily substituted with methyl groups which seem to have an influence on the enantioselectivity of some of the enzymes. High enantiomeric excesses were observed for (*R*)-imine reductases V6KA13, V7GV82 and W7VJL8 with >99% measured for the (-) enantiomer. Interestingly the same enantiomer was formed with S-IREDs J7YM26 and M4ZS15 in good yields of more than 99%. A strong decrease in the selectivity was detected with R-IREDs L8EIW6, M4ZRJ3 and (S)-imine reductase D2PR38 with observed *e.e.s* of 93 (+), 18 (+) and 61 % also for the (+) enantiomer.

These results indicate a contribution of the substitution pattern of the imine in the reduction process.

Table 12 summarizes the results of the biotransformation experiments.

Table 12. Summary of the obtained results of biotransformational reactions after 2 h and 24 h, respectively.

Enzymes	Substrates					
	72a	74a	62	110	56	111
	2 h Conversion [%]; <i>e.e.</i> [%]					
R-IRED V6KA13	n.c. ^(a)	n.c. ^(a)	>99; >99% (R)	92; n.a.	10; 75 (R)	63; >99 (-)
R-IRED L8EIW6	n.c. ^(a)	30; n.d. ^(b)	n.c. ^(a)	n.c. ^(a)	n.c. ^(a)	81; 93 (+)
R-IRED M4ZRJ3	n.c. ^(a)	>99; n.d. ^(b)	>99; 66 (R)	n.c. ^(a)	n.c. ^(a)	47; 18 (+)
R-IRED V7GV82	n.c. ^(a)	n.c. ^(a)	96; >99 (R)	n.c. ^(a)	25; 59 (R)	13; >99 (-)
R-IRED J7LAY5	>99; 32 (R)	>99; 94 (R)	86; >99 (R)	14; n.a.	n.c. ^(a)	n.d. ^(c)
R-IRED W7VJL8	>99; >99 (R)	>99; >98 (R)	95; >99 (R)	n.c. ^(a)	n.c. ^(a)	25; >99 (-)
S-IRED K0F8R0	>99; >99 (S)	>99; >99 (S)	94; >99 (S)	51; n.a.	37; n.d. ^(b)	n.c. ^(a)
S-IRED D2PR38	>99; n.d. ^(b)	>99; 89 (S)	95; >99 (S)	93; n.a.	90; >99 (S)	49; 61 (+)
S-IRED M4ZS15	52; n.d. ^(b)	>99; 97	92; >99 (S)	45; n.a.	35; >99 (S)	85; >99 (-)
S-IRED J7YM26	n.c. ^(a)	38; n.d. ^(a)	26; >99 (S)	n.c. ^(a)	n.c. ^(a)	86; >99 (+)
	24 h Conversion [%]; <i>e.e.</i> [%]					
R-IRED V6KA13	>99; n.d. ^(b)	>99; n.d. ^(b)	>99; >99 (R)	85; n.a.	4; 75 (R)	85; (-)
R-IRED L8EIW6	n.c. ^(a)	>99; n.d. ^(b)	n.c. ^(a)	n.c. ^(a)	7; n.d. ^(b)	78; 93 (+)
R-IRED M4ZRJ3	n.c. ^(a)	>99; n.d. ^(b)	100; 66 (R)	n.c. ^(a)	n.c. ^(a)	72; 18 (+)
R-IRED V7GV82	n.c. ^(a)	>99; >99 (R)	96; >99 (R)	56; n.a.	55; 59 (R)	46; >99 (-)
R-IRED J7LAY5	>99; 32 (R)	>99; 94 (R)	95; >99 (R)	38; n.a.	46; n.d. ^(b)	12; n.d. ^(c)
R-IRED W7VJL8	n.c. ^(a)	>99; >98 (R)	96; >99 (R)	n.c. ^(a)	n.c. ^(a)	85; >99 (-)
S-IRED K0F8R0	>99; >99 (S)	>99; (S)	95; >99 (S)	>99; n.a.	76; n.d. ^(b)	9; n.d. ^(b)
S-IRED D2PR38	n.c. ^(a)	>99; 89 (S)	95; >99 (S)	>99; n.a.	90; >99 (S)	83; 61 (+)
S-IRED M4ZS15	>99; n.d. ^(b)	>99; 97 (S)	96; >99 (S)	95; n.a.	89; >99 (S)	86; >99 (-)
S-IRED J7YM26	n.c. ^(a)	>99; n.d. ^(b)	>99; n.d. ^(b)	45; n.a.	3; n.d. ^(b)	88; >99 (-)

^(a) n.c. = no conversion^(b) n.d. = not determined (insufficient peak size in GC/HPLC chromatogram).^(c) n.d. = sample spilled.

2.8 Summary

In total, 10 novel imine reductases, 6 (*R*)- and 4 (*S*)-selective enzymes, were characterized in terms of their temperature stability, pH optimum and their substrate scope. Seven of these were also subjected to biotransformation studies including their enantioselectivities. It was shown that many of the new reductases described herein showed their stability and activity maximum at temperatures below 40 °C and needed a neutral to slight acidic pH for optimal reduction conditions. Most of the investigated proteins accepted a vast set of cyclic imine compounds with broad structural features, with the highest activities observed for 6-membered ring **74a** and 3,4-dihydroisoquinolines **62**, **76a** as well as iminium substrate **77**. For at least 7 of the newly discovered enzymes, the substrate scope could be extended to methoxy-substituted dihydroisoquinolines **56** and **110** with good to excellent conversions as well as good to perfect enantiomeric excesses for all the tested molecules used in biontransformational reactions.

With these novel reductases in hand, several cyclic secondary amines were accessible, not only in good yields but also in high enantiomeric purity form, thus the herein described enzymes would also provide a greener alternative to access these compounds on an industrial scale.

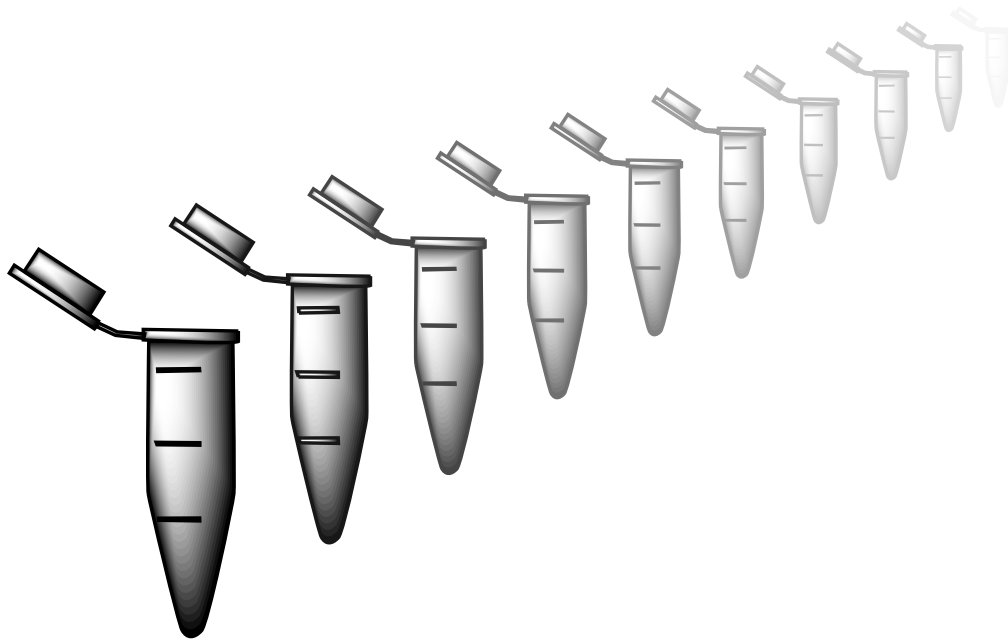
2.9 Outlook

The herein described novel imine reductases were investigated in terms of various important parameters, yet there are still some more questions that need to be answered.

For future studies it would be desirable to expand the substrate scope to another class of relevant imine compounds, namely β -carbolines, which are not only found in many natural sources but also show known pharmacological effects.^[192] Furthermore the above discussed influence of the substituent size on the imine carbon should be further investigated with pyrroline **72a**, piperidine **74a** and azepine **75a** compounds bearing different alkyl, alkenyl or phenyl groups. Additionally, kinetic data such as K_M , k_{cat} and k_{cat}/K_M would give some more insight into substrate affinity and catalytic efficiency with different substrates used.

Hence, the final steps in imine reductase characterization would be the upscale of a biocatalytic transformation on a gram scale as well as the elucidation of the crystal structure of these newly discovered reductases.

3 Experimental



3.1 Materials

3.1.1 Compounds Used for Buffer Solutions

Compound	Purity (%)	Supplier	Lot No.	Unit Size
EDTA–Na ₂ dihydrate	99.0	Sigma-Aldrich	SLBF7702V	500 g
Glycine	>99	Roth	n.a.	5 kg
Imidazole	>99.5	Sigma-Aldrich	SZBE0500V	1 kg
K ₂ HPO ₄ anhydr.	n.a.	Merck	AMO0430204445	1 kg
KH ₂ PO ₄ anhydr.	99.5	Sigma-Aldrich	SZBE0870V	1 kg
Na ₂ HPO ₄ anhydr.	>98	Fluka	BCBC4969V	1 kg
NaH ₂ PO ₄ anhydr.	n.a.	Fluka	0001403084	1 kg
NaCl	>99.8	Roth	9265.1	1 kg
NaOH pellets	n.a.	Merck	0656540	1 kg
TRIS pufferan	>99.9	Roth	4855.2	1 kg

3.1.2 Compounds Used for Cell Cultivation

Compound	Purity (%)	Supplier	Lot No.	Unit Size
Agar bacteriological	n.a.	Oxoid	n.a.	500 g
Glycerol	>99.5	Sigma-Aldrich	BCP0365V	1 L
Isopropyl-β-D-1-thiogalactoside (IPTG)	n.a.	peqlab	13411043	25 g
Kanamycin sulfate	n.a.	Sigma-Aldrich	SLBB0945V	25 g
NaCl	>99.8	Roth	9265.1	1 kg
Tryptone	n.a.	Oxoid	n.a.	500 g
Yeast extract	n.a.	Oxoid	n.a.	500 g

3.1.3 Chemicals Used for Activity Assay, Substrate Screening & Biotransformations

No.	Compound	Purity (%)	Supplier	Lot No.	Unit Size
76a	3,4-Dihydroisoquinoline	>97.5	Sigma-Aldrich	STBC3516V	1 g
62	1-Methyl-3,4-dihydroisoquinoline HCl · H ₂ O	n.a.	Acros Organics	A0222435	1 g
72a	2-Methyl-1-pyrroline	95	Sigma-Aldrich	MKBD7277V	5 mL
72b	2-Phenyl-1-pyrroline	n.a.	Jörg Schrittwieser	n.a.	n.a.
74a	6-Methyl-2,3,4,5-tetrahydropyridine	n.a.	Jörg Schrittwieser	n.a.	n.a.
77	2-Methyl-3,4-dihydroisoquinolinium triflat	n.a.	Jörg Schrittwieser	n.a.	n.a.
75a	7-Methyl-3,4,5,6-tetrahydro-2H-azepine	n.a.	Jörg Schrittwieser	n.a.	n.a.
-	NADPH–Na ₄	n.a.	AppliChem	4P005190	500 mg
-	NADP ⁺ –Na ₂	n.a.	Roche	n.a.	10 g
-	Methanol	> 99	Roth	n.a.	1 L
-	Isopropanol	> 99.9	Sigma-Aldrich	n.a.	1 L

3.1.4 Materials Used for DNA Isolation and Ligation

Material	Purity (%)	Supplier	Lot No.	Unit Size
QIAquick Gel Extraction Kit (250)	n.a.	QIAGEN	148017448	n.a.
QIAquick PCR Purification Kit (250)	n.a.	QIAGEN	145036739	n.a.
QIAprep Spin Miniprep Kit (250)	n.a.	QIAGEN	148047164	n.a.
T4 DNA ligase	n.a.	Thermo Scientific	00157494	n.a.
10x T4 DNA ligase buffer	n.a.	Thermo Scientific	00136629	1.5 mL
SYBR safe DNA gel stain	n.a.	invitrogen	1621150	400 μ L

3.1.5 Materials Used for Restriction Digest and Colony PCR

Material	Purity (%)	Supplier	Lot No.	Unit Size
Fast Digest XhoI endonuclease	n.a.	Thermo Scientific	00240103	400 μ L
Fast Digest NdeI endonuclease	n.a.	Thermo Scientific	00173608	300 μ L
Fast Digest buffer 10x	n.a.	Fermentas	n.a.	1 mL
Dream Taq green PCR master mix (2x)	n.a.	Thermo Scientific	00177836	1.25 mL
T7 primer mix (2 μ M each forward and reverse)	n.a.	Thermo Scientific	n.a.	2 μ g

3.2 Procedures

3.2.1 Gene Subcloning & Plasmid Transformation

The synthetic genes, encoding R- and S-IREDs, were obtained as linear double-stranded DNA from GeneArt and were codon-optimized for *E. coli*. Each gene contained restriction sites for XhoI and NdeI and was subcloned into a pET28a(+) vector, if not otherwise specified, according to following procedure.

About 200 ng of the corresponding IRED DNA or 500 ng of the vector DNA were mixed with the restriction enzymes (1 μ L each), water (depending on the volume of DNA solution) and 10 x restriction buffer (2 μ L) each, to a total volume of 20 μ L. Target gene and vector were incubated at 37 °C for 1.5 h and 30 min, respectively. The restriction digest of the pET28a(+) vector was analyzed on a 1 % agarose TAE gel and the bands were extracted using the QIAquick Gel Extraction Kit (250). The digested IRED genes were purified with the QIAquick PCR purification kit.

For gene subcloning about 40 ng of the digested insert and 35 ng of the vector were mixed with T4 ligase (1 μ L), water (2 μ L) and ligation buffer (10x) (2 μ L) to a total volume of 20 μ L and were incubated at room temperature for 3 hours. For the religation control, the insert was replaced with water. An aliquot of 10 μ L of the ligation reaction was transferred to a fresh Eppendorf vial and heat-deactivated at 65 °C for 10 min. The sample was cooled on ice and transformed into chemically competent *E. coli* BL21 (DE3) cells as follows.

The cell suspension was thawed on ice and an aliquot of 100 μ L was mixed with the heat deactivated ligation aliquot. The mixture was incubated on ice for 30 min, for negative control no plasmid was added. After heat treatment at 42 °C for 1 min the cells were cooled on ice for 5 min and 900 μ L LB-medium were added followed by incubation at 37 °C and 300 rpm for 1 hour. The cells were pelleted by centrifugation, 900 μ L of the supernatant were discarded and the cell pellet was resuspended in the remaining 100 μ L. The suspension was plated on LB-agar plates containing 50 μ g/mL kanamycin and were incubated at 37 °C over night.

3.2.2 Colony Polymerase Chain Reaction (Colony PCR)

As proof of successful gene ligation a colony PCR was performed as follows. Several colonies from the agar plate were picked and each resuspended in 15 μ L water. The suspension was heat treated at 95 °C for 15 min and centrifuged. In PCR tubes, components were mixed in following amounts and order:

1. **T7 primer mix, 2 μ M:** 2.5 μ L
2. **PCR master mix:** 12.5 μ L
3. **colony supernatant:** 10.0 μ L

The PCR was run with following specifications:

Step	Temperatur [°C]	Time [min]	Cycles
initial activation	95	5	
amplification	94	0.5	} 30
	55	0.5	
	72	2	
final extension	72	10	
storage	4		

Analysis of the samples was done *via* agarose gel electrophoresis. Aliquots of 15 μ L were loaded onto a 1 % TAE agarose gel and run at 100 V for 40 min. The DNA bands were rendered visible under blue light using Sybr Safe DNA gel stain.

3.2.3 Protein Expression, Protein Purification & Desalting

For the overnight culture (ONC) a single colony from the agar plate was picked and transferred aseptically to 10 mL LB-medium containing 50 μ g/mL kanamycin and incubated at 30 °C and 120 rpm overnight. On the next day, 300 mL of sterile TB-medium, containing 50 μ g/mL kanamycin, were inoculated with 2 mL of the ONC and shaken at 30 °C and 150 rpm. When the OD₆₀₀ reached 0.8, protein expression was induced by adding IPTG to a final concentration of 1 mM and incubation at 20 °C and 120 rpm. After 12 hours, the cells were harvested by centrifugation for 20 min, 4000 rpm and 4 °C. The pellet was washed once with 20 mL 20 mM KPi-buffer, pH 7.0 and stored at -20 °C.

The frozen cell pellet was thawed and resuspended in 10 mL His-Trap buffer A, supplemented with 1 mg/mL lysozyme, and incubated at 30 °C for 30 min. Then, the cell suspension was sonicated using Branson digital sonifier 250 with following specifications: pulse: 2 sec, pause: 4 sec, 20% amplitude, total pulse time: 2:30 min, 75 cycles in total. This cell lysate was transferred to a 50 mL centrifuge beaker and centrifuged at 16000 rpm for 20 min at 4 °C. The supernatant was decanted from the pellet and used for protein purification via His-Trap Ni²⁺ affinity

chromatography.

To this end, the supernatant was supplemented with 500 μ L His-Trap buffer B and loaded onto a 5 mL His-Trap column. The protein of interest was eluted by using a Fast Protein Liquid Chromatography (FPLC) system with following elution profile:

Step	Volume [mL]	Buffer A [%] ^(a)	Buffer B [%] ^(b)	Mode of Elution
1	50	95	5	isocratic
2	100	95 to 0	5 to 100	linear gradient
3	50	0	100	isocratic

^(a) 100 mM K-Pi buffer with 300 mM NaCl.

^(b) 100 mM K-Pi buffer with 300 mM NaCl and 500 mM imidazole.

Equilibration of the column and the FPLC system was performed with 50 mL 95% buffer A/5% buffer B, respectively. After protein elution the column was stored in 20% ethanol.

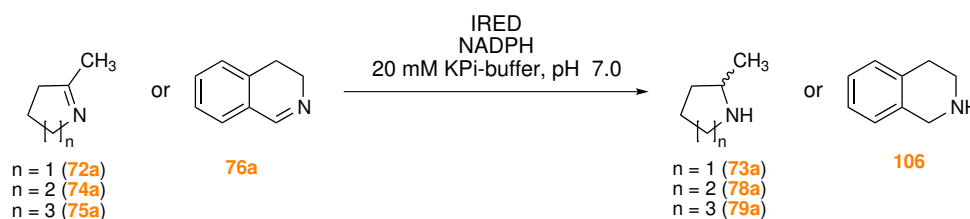
The enzyme containing fractions were pooled, concentrated and desalted using a PD-10 desalting column (GE healthcare, Lot# 9611730). To this end, the column was equilibrated with 25 mL buffer (20 mM K-Pi, pH 7.0 or 50 mM TRIS-HCl, 300 mM NaCl, pH 7.5) and loaded with 2.5 mL enzyme concentrate. The enzyme was eluted with 3.5 mL of the corresponding equilibration buffer and stored at -20 °C. The His-Trap column was cleansed with stripping buffer after approx. 5 uses and recharged with 0.1 M NiSO₄ for reuse.

3.2.4 SDS-PAGE analysis & Bradford assay

Protein expression was detected by SDS-polyacrylamide gel electrophoresis (PAGE) with subsequent staining using Coomassie Brilliant Blue Silver stain. 20 μL of the sample were mixed with 20 μL sample buffer, Laemmli (2x) and denatured at 95 $^{\circ}\text{C}$ for 15 min. 10 μL of the cooled samples and 5 μL of PageRuler, prestained protein ladder standard (Thermo Scientific, Lot# 00207069) were loaded onto the gel and developed at 180 V for 50 min. The bands were rendered visible with Coomassie Brilliant Blue Silver stain (20% ethanol, 1.6% phosphoric acid, 8% ammonium sulfate, 0.08% Coomassie Brilliant Blue G-250) for 30 min and destained with dd-H₂O overnight.

Protein concentrations were determined using the Bio-Rad protein assay. 20 μL of the diluted sample (1:5, 1:20, 1:100) were mixed with 980 μL of the reagent (1:5 dilution) followed by 15 min incubation at room temperature. The absorbance was measured at 595 nm with an Eppendorf BioPhotometer *plus* which provided the concentration in mg/mL.

3.2.5 Activity Assay



The purified enzymes were screened for imine reducing activity by using a photometrical assay based on the decrease of NADPH absorbance at 340 and 370 nm (depending on the substrate), respectively. For this purpose 10 μL of the desalted enzyme and 10 μL of NADPH stock (final concentration = 0.2 mM) were mixed with 930 μL of reaction buffer (20 mM K-Pi, pH 7.0). The reaction was started by adding 50 μL imine substrate stock, in methanol (final concentration = 10 mM) to a total volume of 1 mL and the decrease of NADPH absorbance was measured over 5 min with a Thermo GeneSys Spectrophotometer. To calculate the enzyme activity (U/mL) the following formula was used:

$$U/mL = \frac{\Delta AU/min * V}{\epsilon * d * v}$$

$\Delta AU/min$ = decrease in absorbance units/min

V = reaction volume (1 mL)

ϵ = extinction coefficient of NADPH

d = cuvette diameter

v = sample volume (10 μ L)

The specific activity (U/mg) of each enzyme was obtained as quotient of its activity (U/mL) and its protein concentration (mg/mL).

3.2.6 Biotransformations

To investigate the actual stereospecificity and conversion of each enzyme, biotransformations on an analytical scale were performed as follows.

In a 2 mL Eppendorf vial, 500 μ L of the reaction mixture contained following components:

1. **(R/S)-IRED lyophilized cell free extract:** 1 mg
2. **ADH lyophilized cell free extract:** 2 mg
3. **NADP⁺ cofactor:** 0.4 mg
4. **Imine substrate in 2-propanol:** 10 mM
5. **100 mM TRIS-HCl buffer, pH 7.5:** 500 μ L

An ADH/2-propanol system was used for cofactor regeneration. By adding the imine, dissolved in 2-propanol, the reaction contained 5% (v/v) of alcohol for regenerating the cofactor. The biotransformations were allowed to proceed at 30 °C and 120 rpm for 2 h and 24 h, respectively. The reaction was stopped by adding 200 μ L sat. Na₂CO₃ solution and the aqueous phase was extracted two times each with 500 μ L ethyl acetate supplemented with 9.921 mM *n*-dodecane as internal standard. The combined organic layers were dried over MgSO₄ and transferred to 1.5 mL GC vials for subsequent measurements.

3.2.7 Buffer Recipes and Media Preparation

20 mM K-Pi buffer, pH 7.0: 2.14 g K_2HPO_4 (12.3 mM) and 1.05 g KH_2PO_4 (7.7 mM) were dissolved in 1 L dd-H₂O and stored at room temperature.

100 mM K-Pi buffer, pH 7.0: 10.7 g K_2HPO_4 (61.5 mM) and 5.2 g KH_2PO_4 (38.5 mM) were dissolved in 1 L dd-H₂O and stored at room temperature. For pH optimum measurements, aliquots of 45 mL were taken and the pH was adjusted with 85% H_3PO_4 to the desired value (pH 6 - 8). Dion. Water was added to a final volume of 50 mL.

His-Trap buffer A, pH 7.0: 10.7 g K_2HPO_4 (61.5 mM), 5.2 g KH_2PO_4 (38.5 mM) and 17.5 g NaCl (300 mM) were dissolved in 1 L dd-H₂O and stored at 4 °C.

His-Trap buffer B, pH 7.0. 10.7 g K_2HPO_4 (61.5 mM), 5.2 g KH_2PO_4 (38.5 mM), 17.5 g NaCl (300 mM) and 34.1 g imidazole (500 mM) were dissolved in 950 mL dd-H₂O. The pH was adjusted with 85% H_3PO_4 and dion. water was added to a final volume of 1 L. The solution was stored at 4 °C.

100 mM TRIS-HCl buffer, pH 8 - 9: 12.1 g tris(hydroxymethyl)aminomethane (TRIS) were dissolved in 1 L dd-H₂O and stored at room temperature. For pH optimum measurements aliquots of 45 mL were taken and the pH was adjusted with HCl to the desired value. The solution was filled up with dion. water to a final volume of 50 mL.

100 mM glycine-NaOH buffer, pH 9-11: 7.5 g glycine were dissolved in 1 L dd-H₂O and stored at room temperature. For pH optimum measurements aliquots of 45 mL were taken and the pH was adjusted with 10 M NaOH to the desired value. Water was added to a final volume of 50 mL.

Citric acid-Na₂HPO₄ buffer, pH 5-6: pH 5: 24.3 mL 0.1 M citric acid and 25.7 mL 0.2 M Na₂HPO₄ were mixed and stored at room temperature. pH 5.5: 21 mL 0.1 M citric acid and 29 mL 0.2 M Na₂HPO₄ were mixed and stored at room temperature. pH 6: 18.4 mL 0.1 M citric acid and 31.6 mL 0.2 M Na₂HPO₄ were mixed and stored at room temperature.

His-Trap stripping buffer, pH 7.4: 3.27 g Na₂HPO₄ · 7 H₂O (12.2. mM), 0.94 g NaH₂PO₄ (7.8 mM), 29.2 g NaCl (500 mM) and 18.6 g EDTANa₂ (50 mM) were

dissolved in 1 L dd-H₂O and stored at room temperature.

Lysogeny broth (LB) medium: 5 g/L yeast extract, 5 g/L NaCl and 10 g/L tryptone were mixed and autoclaved. For plates, 15 g/L agar was added.

Terrific broth (TB) medium: TB base: 24 g/L yeast extract, 12 g/L tryptone and 4 mL/L glycerol were mixed and autoclaved.

10 x K-Pi buffer (1 M), pH 7.5: 23.1 g/L KH₂PO₄ and K₂HPO₄ were mixed and autoclaved.

TB medium: 900 mL TB base and 100 mL 10 x K-Pi buffer were mixed just before use.

3.2.8 GC-FID Methods

Throughout this thesis all substrate conversion measurements and *e.e.* determinations of compounds **73a** and **74a** were performed with GC-FID. Substrate imines and product amines were calibrated in a range from 0.5 to 50 mM with standard concentrations of 0.5, 2.5, 10, 25 and 50 mM. Dodecane was used as an internal standard. Standard preparation and dilution was done on a scale with 0.1 mg accuracy. The conversion of calibrated compounds was calculated based on their measured concentrations according to the following equation:

$$c = \frac{A_P}{A_P + A_E} * 100\%$$

$$c = \text{conversion in \%}$$

$$A_{P,E} = \text{concentration (mM) of product or educt peak in chromatogram}$$

The enantiomeric excess (*e.e.*) for compounds **73a** and **74a** was solely derived from GC-FID areas of the peaks assigned to the N-acetylated enantiomers according to the following formula:

$$e.e. = \frac{|A_R - A_S|}{A_R + A_S} * 100\%$$

e.e. = enantiomeric excess in %

A_R = area of (R)-enantiomer peak in chromatogram

A_S = area of (S)-enantiomer peak in chromatogram

Derivatization was performed as follows: 500 μ L of the ethylacetate extract from the conversion measurement were mixed with 200 μ L sat. Na_2CO_3 solution and 20 μ L acethanhydride. The mixture was shaken vigorously for 1 min and dried over K_2CO_3 .

Achiral GC-Methods used within this work

Method: TMI_HP-5

Column: HP-5: Agilent J&W GC columns, 19091J-413, 30 m, 0.250 mm, 0.25 μ m

Temperature Program: 60 $^{\circ}\text{C}$ (0.5 min) $-[10^{\circ}\text{C}/\text{min}] \rightarrow 160^{\circ}\text{C}$ (0 min) $-[40^{\circ}\text{C}/\text{min}] \rightarrow 300^{\circ}\text{C}$ (1 min)

Carrier Gas Flow: (He) 1 mL/min

Split Ratio: 30:1

Injector Temperature: 300 $^{\circ}\text{C}$

Method: 2-MP_HP-5

Column: HP-5: Agilent J&W GC columns, 19091J-413, 30 m, 0.250 mm, 0.25 μ m

Temperature Program: 40 $^{\circ}\text{C}$ (0.5 min) $-[10^{\circ}\text{C}/\text{min}] \rightarrow 90^{\circ}\text{C}$ (0 min) $-[30^{\circ}\text{C}/\text{min}] \rightarrow 300^{\circ}\text{C}$ (1 min)

Carrier Gas Flow: (He) 1 mL/min

Split Ratio: 30:1

Injector Temperature: 300 $^{\circ}\text{C}$

Method: 2-MPI_HP-5

Column: HP-5: Agilent J&W GC columns, 19091J-413, 30 m, 0.250 mm, 0.25 μ m

Temperature Program: 40 $^{\circ}\text{C}$ (0.5 min) $-[10^{\circ}\text{C}/\text{min}] \rightarrow 90^{\circ}\text{C}$ (0 min) $-[30^{\circ}\text{C}/\text{min}] \rightarrow 300^{\circ}\text{C}$ (1 min)

Carrier Gas Flow: (He) 1 mL/min

Split Ratio: 30:1

Injector Temperature: 300 $^{\circ}\text{C}$

Method: 1M-DHIQ_DB-1701

Column: DB-1701: Agilent J&W GC columns, 122-0732, 30 m, 0.250 mm, 0.25 μ m

Temperature Program: 80 °C (1 min) –[10 °C/min]–> 250 °C (1 min)

Carrier Gas Flow: (He) 1 mL/min

Split Ratio: 15:1

Injector Temperature: 280 °C

Method: 1M-DM-DHIQ_DB-1701

Column: DB-1701: Agilent J&W GC columns, 122-0732, 30 m, 0.250 mm, 0.25 μ m

Temperature Program: 80 °C (1 min) –[10 °C/min]–> 250 °C (1 min)

Carrier Gas Flow: (He) 1 mL/min

Split Ratio: 15:1

Injector Temperature: 280 °C

Method: DM-DHIQ_DB-1701

Column: DB-1701: Agilent J&W GC columns, 122-0732, 30 m, 0.250 mm, 0.25 μ m

Temperature Program: 80 °C (1 min) –[10 °C/min]–> 250 °C (1 min)

Carrier Gas Flow: (He) 1 mL/min

Split Ratio: 15:1

Injector Temperature: 280 °C

Chiral GC-Method used within this work

Method: TBDAc_2-MP-Ac

Column: Hydrodex- β -TBDAC: Macherey-Nagel, 723 384.50, 50 m, 0.25 mm

Temperature Program: 70 °C (1 min) –[20 °C/min]–> 150 °C (10 min) –[20 °C/min]–> 210 °C (2 min)

Carrier Gas Flow: (H₂) 1 mL/min

Split Ratio: 20:1

Injector Temperature: 230 °C

3.2.9 HPLC Methods

Enantiomeric excess (*e.e.*) determination of dihydroisoquinoline compounds **56** and **62** as well as compound **111** was done by chiral HPLC measurements. For the calculation of the *e.e.* value, see the formula above. The investigated compounds were analyzed without any further derivatization using following methods:

Chiral HPLC-Methods used within this work

Method: A

Column: Daicel Chiracel OD-H, 0.46 cm Øx 25 cm

Solvent ratio [%]: 99 heptane/1 *i*-propanol, 0.1 diethylamine

Solvent Flow: 0.5 mL/min

Oven Temperature: 30 °C

Method: B

Column: Daicel Chiracel OD-H, 0.46 cm Øx 25 cm

Solvent ratio [%]: 90 heptane/10 *i*-propanol, 0.1 diethylamine

Solvent Flow: 1 mL/min

Oven Temperature: 30 °C

Method: C

Column: Daicel Chiracel OD-H, 0.46 cm Øx 25 cm

Solvent ratio [%]: 97 heptane/3 *i*-propanol, 0.1 diethylamine

Solvent Flow: 1 mL/min

Oven Temperature: 30 °C

3.2.10 Determination of Absolute Configurations

The absolute configurations of chiral compounds were determined by means of comparing the elution order of biotransformational reactions with known GC-FID elution orders of reference substances.

Table 13 summarizes the used references for each compound.

Table 13. Summary of references used for the determination of absolute configurations of chiral compounds.

Compound	Reference
(<i>R/S</i>) 73a & 78a	[147]
(<i>R/S</i>) 59	[193]
(<i>R/S</i>) 57	[146]
(+)/(−) 111	[191]

4 Appendix

4.1 Protein and DNA Sequences of Characterized IREDs

R-IRED M4ZRJ3

Protein Sequence

MGDNRTPVTVIGLGLMGQALAAAFLEAGHTTTVWNRSAKAEQLVSQGA-
 QAATPADAVA ASELVVVCLSTYDNMHDVIGSLGESLRGKVVNLTSGSSDQGRE-
 TAAWAQKQVEYLDGA IMITPPGIGTETAVLFYAGTQSVFEKYEPALKLLGGGT-
 TYLGTDHGMPALYDVSLGLMW GTLNSFLHGVAVVETAGVGAQQFLPWAHMW-
 LEAIKMFTADYAAQIDAGDGKFPANDATLE THLAALKHLVHESEALGIDAEL-
 PKYSEALMERVISQGHAKNSYAAVLKAFRKPSE

ORF	Protected sites	Protected areas	Motifs to avoid
22-906 [GGT...TAA]	<u>16-21 NdeI [CATATG]</u> <u>907-912 XhoI [CTCGAG]</u>		NdeI [CATATG] XhoI [CTCGAG]

1.	GTGCCGCGCGGCAGC	CATATG	GGGTGATAATCGTACACCGGTTACCGTTATTGGTCTGGGTCTGATGGGT
76.	Q A L A A A F L E A G H T T T V W N R S A G K		CAGGCACTGGCAGCAGCATTCTGGAAGCAGGTCATACCACCACCGTTTGGAAATCGTAGCCGAGGTAAA
139.	A E Q L V S Q G A V Q A A T P A D A V A A S E		GCAGAACAGCTGGTTAGCCAGGGTGCAGTTCAGGCAGCAACACCGGCAGATGCAGTTGCAGCAAGCGAA
208.	L V V V C L S T Y D N M H D V I G S L G E S L		CTGGTTGTTGTTGTCTGAGCACCTATGATAATATGCATGATGTTATTGGTAGCCTGGGTGAAAGCCTG
277.	R G K V I V N L T S G S S D Q G R E T A A W A		CGTGGTAAAGTTATTGTTAATCTGACCAGCGGTAGCAGCGATCAGGGTCGTGAAACCGCAGCATGGGCA
346.	E K Q G V E Y L D G A I M I T P P G I G T E T		GAAAAACAGGGTGTGAAATATCTGGATGGTGCCATTATGATTACCCCTCCGGGTATTGGCACCGAAACA
415.	A V L F Y A G T Q S V F E K Y E P A L K L L G		GCAGTTCTGTTTTATGCAGGCACCCAGAGCGTTTTTGAAAAATATGAACCGGCACTGAAACTGCTGGGT
484.	G G T T Y L G T D H G M P A L Y D V S L L G L		GGTGGCACCATATCTGGGCACCGATCATGGTATGCCTGCACTGTATGATGTTAGCCTGCTGGGCCTG
553.	M W G T L N S F L H G V A V V E T A G V G A Q		ATGTGGGGCACCTGAATAGCTTTCTGCATGGTGTTCAGTTGTTGAAACAGCGGGTGTGGTGCACAG
622.	Q F L P W A H M W L E A I K M F T A D Y A A Q		CAATTTCTGCCGTGGGCACACATGTGGCTGGAAGCCATTAATAATGTTTACCGCAGATTATGCAGCACAG
691.	I D A G D G K F P A N D A T L E T H L A A L K		ATTGATGCCGGTGATGGTAAATTTCCGGCAAATGATGCAACCCTGGAAACCCATCTGGCAGCCCTGAAA
760.	H L V H E S E A L G I D A E L P K Y S E A L M		CATCTGGTTCATGAAAGCGAAGCACTGGGTATTGATGCAGAAGTCCGAAATATTCTGAAGCACTGATG
829.	E R V I S Q G G H A K N S Y A A V L K A F R K P		GAACGTGTTATTAGTCAGGGTCATGCCAAAATAGCTATGCAGCCGTTCTGAAAAGCATTTCGTA AACCG
898.	S E *	CTCGAG	AGCGAATAA

R-IRED V6KA13

Protein Sequence

MTTEPSLPTVSIVGLGNLGRALAGAFLDQGYRRTTVWNRSPAKADDLVARGAHRRA-
 TTAAEA LAAGELVIVCVLDYDTVNRLLLTPAADALRGRVLLNLTSGTPEPARELAA-
 WVTGQGADYLD GAVYAVPQTIGTADAFVLYSGSSAVFETYREQLDLLGAPTFVGTD-
 PGLASLYDVALLSGM YGMFAGFFQSVAVADSAQIKATDITALLVPWLNGAAAAL-
 PGFAAEIDSGDYTTETSNDI NTVGLANILTATKAQGVGVDLLTPLQLTFERQIAQG-
 HGASSLSRAIESLRPPR

ORF	Protected sites	Protected areas	Motifs to avoid
22-900 [ACC...TAA]	<u>16-21 NdeI [CATATG]</u> <u>901-906 XhoI [CTCGAG]</u>		NdeI [CATATG] XhoI [CTCGAG]

1.	GTGCCGCGCGGCAGCC	CATATG	T T E P S L P T V S I V G L G N
70.	L G R A L A G A F L D Q G Y R T T V W N R S P		
139.	CTGGGTCGTGCACTGGCAGGCATTTCTGGATCAGGGTTATCGTACCACCGTTTGGAAATCGTAGTCCG		
208.	A K A D D L V A R G A H R A T T A A E A L A A		
277.	GCAAAAAGCAGATGATCTGGTTGCACGTGGTGCACATCGTGCCACCACCGCAGCCGAAGCTCTGGCAGCC		
346.	G E L V I V C V L D Y D T V N R L L T P A A D		
415.	GGTGAACCTGGTTATTGTTTGTGTTCTGGATTATGATACCGTGAATCGTCTGCTGACACCGGCAGCAGAT		
484.	A L R G R V L L N L T S G T P E P A R E L A A		
553.	GCACTGCGTGGTCTGTTCTGCTGAATCTGACCAGCGGTACACCGGAACCGGCACGTGAACTGGCAGCA		
622.	W V T G Q G A D Y L D G A V Y A V P Q T I G T		
691.	TGGGTTACCGGTGAGGGTGCAGATTATCTGGATGGTGCAGTTTATGCAGTTCCCGCAGACCATTGGCACC		
760.	A D A F V L Y S G S S A V F E T Y R E Q L D L		
829.	GCAGATGCATTTGTTCTGTATAGCGGTAGCAGCGCAGTTTTTGAACCTATCGTGAACAGCTGGATCTG		
898.	L G A P T F V G T D P G L A S L Y D V A L L S		
	CTGGGTGCACCGACCTTTGTTGGCACCAGTCCGGTCTGGCAAGCCTGTATGATGTTGCACTGCTGAGC		
	G M Y G M F A G F F Q S V A V A D S A Q I K A		
	GGTATGTATGGTATGTTTGCAGGTTTTTTTCAGAGCGTTGCAGTTGCAGATAGCGCACAGATTAAGCA		
	T D I T A L L V P W L N G A A A A L P G F A A		
	ACCGATATTACCGCACTGCTGGTTCCGTGGCTGAATGGTGCAGCAGCAGCCCTGCCTGGTTTTGCAGCA		
	E I D S G D Y T T E T S N L D I N T V G L A N		
	GAAATTGATAGCGGTGATTATACCACCGAAACAGCAATCTGGATATTAACACCGTGGGTCTGGCCAAT		
	I L T A T K A Q G V G V D L L T P L Q T L F E		
	ATTCTGACCGCAACCAAAGCACAGGGTGTGGTGTGATCTGCTGACTCCGCTGCAGACCCTGTTTGAA		
	R Q I A Q G H G A S S L S R A I E S L R P P R		
	CGTGAGATTGCACAGGGTCATGGTGCAAGCAGTCTGAGCCGTGCAATTGAAAGCCTGCGTCCGCCTCGT		
	*		
	TAACTCGAG		
	CCCACTGAGATCCGGC		

R-IRED W7VJL8

Protein Sequence

MAPDTVEKTPVTLGLGAMGAALARAWLAARHPLTVWNRTPTRAAAISAEGATV-
 ADSAAE AVAANTLVVVCLLDDASVEEVLAGADLAGRDVNLTTGTPAQARA-
 RADWARERGARYLDG GIMAVPPMIGVPDAGGYVVFYSGSRELFERHRETLAVPAGT-
 TYVGRDAGFAALHDVALLSA MYGMFAGAAHAFALIRREDIDPASLAPLLADW-
 LVAMAPT VHQTADQLRSGDYTKGVVSNL AMQVAGTPTFLRTAAEQGVSPILLS-
 PYFELMRRRLAEGSGEEDLTGVIDLLVR

ORF	Protected sites	Protected areas	Motifs to avoid
22-900 [GCA...TAA]	<u>16-21 NdeI [CATATG]</u> <u>901-906 XhoI [CTCGAG]</u>		NdeI [CATATG] XhoI [CTCGAG]

1.	GTGCCGCGCGGCGAGCCATATGGCACCCGGATACCGTTGAAAAAACACCGGTTACCCCTGCTGGGCTCGGGT
70.	A M G A A L A R A W L A A R H P L T V W N R T GCAATGGGTGCAGCACTGGCACGTGCATGGCTGGCAGCACGTCATCCGCTGACCGTTTTGGAATCGTACC
139.	P T R A A A I S A E G A T V A D S A A E A V A CCGACCCGTGCAGCAGCAATTAGCGCAGAAGGTGCAACCGTTGCAGATAGCGCAGCAGAAGCAGTTGCA
208.	A N T L V V V C L L D D A S V E E V L A G A D GCAAATACCCCTGGTTGTTGTTGCTGCTGGATGATGCAAGCGTTGAAGAAGTTCTGGCAGGCGCAGAT
277.	L A G R D L V N L T T G T P A Q A R A R A D W CTGGCAGGTCGTGATCTGGTTAATCTGACCACCGGTACACCGGCACAGGCACGGCAGGTCAGATTGG
346.	A R E R G A R Y L D G G I M A V P P M I G V P GCACGTGAACGTGGTGCACGTTATCTGGATGGTGGTATTATGGCAGTTCGGCCTATGATTGGTGTTCG
415.	D A G G Y V F Y S G S R E L F E R H R E T L A GATGCCGGTGGTTATGTGTTTTATAGCGGTAGCCGTGAACTGTTTGAACGTCATCGTGAACCCCTGGCC
484.	V P A G T T Y V G R D A G F A A L H D V A L L GTTCCGGCAGGCACCACCTATGTTGGTCGTGATGCAGGTTTTGCAGCCCTGCATGATGTTGCACTGCTG
553.	S A M Y G M F A G A A H A F A L I R R E D I D AGCGCAATGTATGGTATGTTTGCCGGTGCCGCACATGCATTTGCACTGATTTCGTGCGTGAAGATATTGAT
622.	P A S L A P L L A D W L V A M A P T V H Q T A CCGGCAAGCCTGGCACCGCTGCTGGCAGATTGGCTGGTTGCAATGGCACCGACCGTTTCATCAGACCGCA
691.	D Q L R S G D Y T K G V V S N L A M Q V A G T GATCAGCTGCGTAGCGGTGATTATACCAAAGGTGTTGTTAGCAATCTGGCAATGCAGGTTGCAGGCACC
760.	P T F L R T A A E Q G V S P E L L S P Y F E L CCGACCTTTCTGCGTACCGCAGCCGAACAGGGTGTTAGTCCGGAAGTCTGAGTCCGATTTTTGAACTG
829.	M R R R L A E G S G E E D L T G V I D L L V R ATGCGTCGCGCTGCGCCGAAGGTAGTGGTGAAGAGGATCTGACCAGGTTATTGATCTGCTGGTTGCT
898.	* TAACTCGAGC CCACTGAGATCCGGC

R-IRED V7GV82

Protein Sequence

MSDITVIGLGAMGTALAEAFLNQGHAVTVWNRSPAKAEALAAKGATVAKSVEEA-
 VRSSPL IVACLLVYDTVREVLGSPRDALSGRTLNLNTNGTPEQARAMSGWAVS-
 QGASYIDGGIMAV PPMIGGPHALILYSGSRQAFDACSGQLGALGTSKFLGEDAGLA-
 PLYDISLLTGMYGMFAG VLQALALTGAAGIPAGEFMPLLASWLQSMQGLLPK-
 WAEQIDSGDHTSNVVSNLGMQVDAY VNLIDASRSADVSTELVLPMQSLMKRG-
 VAAGQANADLTSLVALLQLSKQGA

ORF	Protected sites	Protected areas	Motifs to avoid
22-894 [AGC...TAA]	<u>16-21 NdeI [CATATG]</u> <u>895-900 XhoI [CTCGAG]</u>		NdeI [CATATG] XhoI [CTCGAG]

		S D I T V I G L G A M G T A L A	
1.	GTGCCGCGCGGGCAGCC	CATATGAGCGGATATTACCGTTATTGGTCTGGGTGCAATGGGCACCGCACTGGCA	
	E A F L N Q G H A V T V W N R S P A K A E A L		
70.	GAAGCATTTCGAATCAGGGTCATGCAGTTACCGTTTGGAAATCGTAGTCCGGCAAAAGCAGAAGCCCTG		
	A A K G A T V A K S V E E A V R S S P L I V A		
139.	GCAGCAAAAGGTGCAACCGTTGCAAAAAGCGTTGAAAGAAGCAGTTCGTAGCAGTCCGCTGATTGTTGCA		
	C L L V Y D T V R E V L G P S R D A L S G R T		
208.	TGCTCTGGTGGTTTATGATACCGTTCTGTAAGTTCTGGTCCGAGCCGTGATGCACTGAGCGGTGCTACC		
	L V N L T N G T P E Q A R A M S G W A V S Q G		
277.	CTGGTTAATCTGACCAATGGTACACCGGAACAGGCACGTGCAATGAGCGGTTGGGCAGTTAGCCAGGGT		
	A S Y I D G G I M A V P P M I G G P H A L I L		
346.	GCAAGCTATATTGATGGTGGTATTATGGCAGTTCGCTATGATTGGTGGTCCGCATGCACTGATTCTG		
	Y S G S R Q A F D A C S G Q L G A L G T S K F		
415.	TATAGCGGTAGCCGTGAGGCATTTGATGCGTGTAGCGGTGAGTGGGTGCCCTGGGTACAAGCAAAATT		
	L G E D A G L A P L Y D I S L L T G M Y G M F		
484.	CTGGGTGAAGATGCAGGTCTGGCACCGCTGTATGATATTAGCCTGCTGACCGGTATGTATGGTATGTTT		
	A G V L Q A L A L T G A A G I P A G E F M P L		
553.	GCCGGTGTCTGCAGGCCTGGCACTGACCGGTGCAAGCCGGTATTCCGGCAGGCGAATTTATGCCGCTG		
	L A S W L Q S M Q G L L P K W A E Q I D S G D		
622.	CTGGCAAGCTGGCTGCAGAGCATGCAGGGTCTGCTGCCGAAATGGGCAGAGCAGATTGATAGCGGTGAT		
	H T S N V V S N L G M Q V D A Y V N L I D A S		
691.	CATACCAGCAATGTTGTTAGCAATCTGGGTATGCAGTTGATGCTATGTGAATCTGATTGATGCAAGC		
	R S A D V S T E L V L P M Q S L M K R G V A A		
760.	CGTAGCGCAGATGTTAGCACCGAAGCTGGTCTGCCGATGCAGAGCCTGATGAAACGTGGTGTTCAGCA		
	G Q A N A D L T S L V A L L Q L S K Q G A *		
829.	GGTCAGGCAAATGCAGATCTGACCAGCCTGGTTGCACTGCTGCACTGAGCAAAACAGGGTGCATAA	CTC	
898.	GAGCCACTGAGATCCGGC		

R-IRED L8EIW6

Protein Sequence

MAATPTNPSTDSGKTPVTVLGLGAMGRALAGAFKAGHPTTVWNRSEHKADEL-
 VARGAVR AGSVAEAVAASPLIVVCVVDYEVSHRILEPVGADLAGRVLVNLTSDT-
 PVRSRRAEWAAG HGVEYLDGAIMVPTPVIGTPEATVLYSGSRRAFDTYEETL-
 KALGGKAPFLGTDHGVAAYV DLAMLSFFYSGMAGLAHAFTLAGEEGVPATD-
 LAPFLDVITGIFPIAKGMADDLVGGRLD GAGEGNIVMEAAGIAHIVEASRDRGV-
 NTDVLDALKALMDRTIAAGHGESEFVVRVTEAMRG AYA

ORF	Protected sites	Protected areas	Motifs to avoid
22-930 [GCA...TAA]	<u>16-21 NdeI [CATATG]</u> <u>931-936 XhoI [CTCGAG]</u>		NdeI [CATATG] XhoI [CTCGAG]

1.	GTGCCGCGCGGGCAGCCATATGGCAGCAACCCCGACCAATCCGAGCACCGATAGCGGTAAAAACACCGGTT
70.	T V L G L G A M G R A L A G A F L K A G H P T ACCGTTCTGGGTCTGGGTGCAATGGGTGCGTGCACCTGGCAAGCGCATTCTGAAAAGCAGGTCATCCGACC
139.	T V W N R S E H K A D E L V A R G A V R A G S ACCGTTTGGAAATCGTAGCGAACATAAAGCAGATGAACTGGTTGCACGTTGGTGCAGTTCGTGCAGGTTAGC
208.	V A E A V A A S P L I V V C V V D Y E V S H R GTTGCAGAAGCAGTTGCAGCAAGTCCGCTGATTGTTGTTTGTGTTGTTGATTATGAAGTGAGCCATCGT
277.	I L E P V G A D L A G R V L V N L T S D T P V ATTCTGGAACCGGTTGGTGCAGATCTGGCAGGTCGTGTTCTGGTTAATCTGACCAGCGATACACCGGTT
346.	R S R R A A E W A A G H G V E Y L D G A I M V CGTAGCCGTCGTGCAGCAGAATGGGCAGCCGGTCATGGTGGTGAATATCTGGATGGTGCAATTATGGTT
415.	P T P V I G T P E A T V L Y S G S R R A F D T CCGACACCGGTTGATTGGTACACCGGAAGCAACCGTTCTGTATAGCGGTTACGTCGTGCATTTGATACC
484.	Y E E T L K A L G G K A P F L G T D H G V A A TATGAAGAAACCTGAAAAGCACTGGGTGGTAAAAGCACCGTTTCTGGGTACAGATCATGGTGTGGCAGCA
553.	V Y D L A M L S F F Y S G M A G L A H A F T L GTTTATGATCTGGCAATGCTGAGCTTTTTCTATAGCGGTATGGCAGGTCCTGGCACATGCATTTACCCCTG
622.	A G E E G V P A T D L A P F L D V I T G I F P GCTGGTGAAGAAGGTGTTCCGGCAACCGATCTGGCACCTTTTCTGGATGTTATTACCGGTTATTTTCCG
691.	P I A K A G M A D D L V G G R L D G A G E G N I CCTATTGCAAAAGGTATGGCCGATGATCTGGTTGGTGGTCTGGATGGCGCAGGCGAAGGTAATATT
760.	V M E A A G I A H I V E A S R D R G V N T D V GTTATGGAAGCAGCAGGTATTGCCCATATTGTTGAAGCAAGCCGTGATCGTGGTGGTGAATACCGATGTT
829.	L D A L K A L M D R T I A A G H G E S E F V R CTGGATGCACCTGAAAAGCCCTGATGGATCGTACCATTGCCGCAGGTCATGGCGAAAAGCGAATTTGTTTCGT
898.	V T E A M R G A Y A * GTTACCGAAGCAATGCGTGGTGCCTATGCATAACTCGAGCCACTGAGATCCGGC

R-IRED J7LAY5

Protein Sequence

MKNDGVTKGSVALLGLGEMGRVLAERLLDAGYPVTVWNRTTPGRDTALVERGAR-
 RAETVRE AVTAATTVVTCLFDHASVRETLEPVGADLAGRTLVDLTTTTPNEARWLG-
 GWAEERGIEHL DGAIMATPSMIGAPEASLLYSGSAEAFGRHRTLFEVWGSATYD-
 GADHGAASLFDLALLSG MYTMFTGFAHGAAMVTSAGVTAEEFAHRSARLL-
 SAMTGVFPMTAKVIDEGDYTGPGQSLE WTATALDTIARASAEQGVSPGPIEM-
 TRALVLAQIEAGYGNENS DRIYEELRAG

ORF	Protected sites	Protected areas	Motifs to avoid
22-900 [AAA...TAA]	<u>16-21 NdeI [CATATG]</u> <u>901-906 XhoI [CTCGAG]</u>		NdeI [CATATG] XhoI [CTCGAG]

1.	GTGCCGCGCGGGCAGG	<u>CATATG</u>	AAAAATGATGGTGTACCAAAGGTAGCGTTGCACTGCTGGGTCTGGGT
70.	E M G R V L A E R L L D A G Y P V T V W N R T		GAAATGGGTCTGTGTTCTGGCAGAACGCTGCTGGATGCAGGTTATCCGGTTACCGTTTGGAAATCGTACA
139.	P G R D T A L V E R G A R R A E T V R E A V T		CCGGGTCGTGATACCGCACTGGTTGAACGTGGTGCACGTCGTGCAGAAACCGTTCCGTGAAGCAGTTACC
208.	A A T T V V T C L F D H A S V R E T L E P V G		GCAGCAACCACCGTTGTTACCTGTCTGTTTGATCATGCAAGCGTGCCTGAAACCCCTGGAACCGGTTGGT
277.	A D L A G R T L V D L T T T T P N E A R W L G		GCAGATCTGGCAGGTCGTACCCTGGTTGATCTGACCACCACCACCCGAATGAAGCACGTTGGCTGGGT
346.	G W A E E R G I E H L D G A I M A T P S M I G		GGTTGGGCAGAAGAACGCGGTATTGAACATCTGGATGGTGCAATTATGGCAACCCCGAGCATGATTGGT
415.	A P E A S L L Y S G S A E A F G R H R T L F E		GCACCGGAAGCAAGCCTGCTGTATAGCGGTAGCGCAGAAGCATTGGTTCGTCATCGTACACTGTTTGAA
484.	V W G S A T Y D G A D H G A A S L F D L A L L		GTTTGGGGTAGCGCAACCTATGATGGTGCCGATCATGGTGCAGCCAGCCTGTTCCGATCTGGCACTGCTG
553.	S G M Y T M F T G F A H G A A M V T S A G V T		AGCGGTATGTATACCATGTTTACCGGTTTTGCACATGGTGCCGCAATGGTTACCAGTGCCGGTGTGACC
622.	A E E F A H R S A R L L S A M T G V F P M T A		GCTGAAGAATTTGCACATCGTAGCGCACGCCTGCTGAGTGCAATGACCGGTGTTTTTCCGATGACCGCA
691.	K V I D E G D Y T G P G Q S L E W T A T A L D		AAAGTTATTGATGAAGGTGATTATACCGGTCCGGGTCAGAGCCTGGAATGGACCGCAACAGCACTGGAT
760.	T I A R A S A E Q G V S P G P I E M T R A L V		ACAATTGCACGTGCCAGCGCAGAACAGGGTGTTAGTCCGGGTCGGATTGAAATGACCCGTGCACTGGTT
829.	L A Q I E A G Y G N E N S D R I Y E E L R A G		CTGGCACAGATTGAAGCAGGTTATGGTAATGAAAATAGCGATCGCATCTATGAAGAAGTGCCTGCAGGT
898.	TAA <u>CTCGAG</u> CCCACTGAGATCCGGC		

R-IRED Q1EQE0Protein Sequence

MPDNPSTKGRMMRNQQAETHPTVTVIGLGLMGQALAGAF LGAGHPPTVWNRTA-
 AKAEPLVA RGAKSAGSVAEAVAASPLVVVCVSDYDAVHALLDPLDGTALQGRT-
 LVNLTSGTSAQARER AAWADGRGADYLDGAILAGPAAIGTADAVVLLSGPRSAFD-
 PHASALGGLGAGTTYLGADH GLASLYDAAGLVMMWSILNGFLQGAALLGTAGV-
 DATTFAPFITQGIGTVADWLPGYARQI DDGAYPADDA AIDTHLATMEHLIHE-
 SEFLGVNAELPRFIKALADRAVADGHGGSGYPALI EQFRTHSGK

R-IRED I8QLV7Protein Sequence

MNSHPPAVTVIGLGLMG SALAAVLLDAGCPTTVWNRS AHKAQSLVDRGARLTGTP-
 REAVE ASPFVIVCVLDYDVLVSLAPSVDALAGKVLVNLTSGSPEQAREAMA-
 WARSHGADYLDGA IMTPPGVGSPEMMFLYGGPDDVFD AHRQTLAFLGDPLHLG-
 DDPGLASLYDVAL LGLMWS TLGWLHGTALVGA EKTSATTFPF AVRWLTA VAG-
 FLTTYAPQVDAG RYPGDDATVDVQI ASIDHLLHAAASRGVDNALPELLKSVME-
 QARAAGHGSDSYASVIEVLRSPAPDPDEHNR

ORF	Protected sites	Protected areas	Motifs to avoid
4-903 [ATG...TAA]	1-6 NdeI [CATATG] 904-909 XhoI [CTCGAG]		NdeI [CATATG] XhoI [CTCGAG]

1.	M N S H P P A V T V I G L G L M G S A L A A
	CATATG AATAGCCATCCGCCTGCAGTTACCGTTATTGGTCTGGGTCTGATGGGTAGCGCACTGGCAGCA
70.	V L L D A G C P T T V W N R S A H K A Q S L V
	GTTCTGCTGGATGCAGGTTGTCCGACCACCGTTTGGAAATCGTAGCGCACATAAAGCACAGAGCCTGGTT
139.	D R G A R L T G T P R E A V E A S P F V I V C
	GATCGTGGTGCACGCTGACCGGTACACCGCGTGAAGCAGTTGAAGCAAGCCCGTTTGTATTGTTTGT
208.	V L D Y D V L Y S V L A P S V D A L A G K V L
	GTGCTGGATTATGATGTCCTGTATAGCGTTCTGGCACCAGCGTTGATGCCCTGGCAGGTAAGTTCTG
277.	V N L T S G S P E Q A R E A M A W A R S H G A
	GTTAATCTGACCAGCGGTAGTCCGGAACAGGCACGTGAAGCAATGGCATGGGCACGTAGCCATGGTGCA
346.	D Y L D G A I M T T P P G V G S P E M M F L Y
	GATTATCTGGATGGTGCCATTATGACCACCCCTCCGGGTGTTGGTTCACCGGAAATGATGTTTCTGTAT
415.	G G P D D V F D A H R Q T L A F L G D P L H L
	GGTGGTCCGGATGATGTTTTTGTATGCACATCGTCAGACCCTGGCATTCTGGGTGATCCGCTGCACCTG
484.	G D D P G L A S L Y D V A L L G L M W S T L T
	GGTGATGATCCGGGTCTGGCAAGCCTGTATGATGTTGCACTGCTGGGCCTGATGTGGTCAACCCTGACC
553.	G W L H G T A L V G A E K T S A T T F T P F A
	GGTTGGCTGCATGGCACCAGCGTGGTGGTCAGAAAAAACAGCGCAACCACCTTTACCCCGTTTGC
622.	V R W L T A V A G F L T T Y A P Q V D A G R Y
	GTTCTGGTGGCTGACCGCAGTTGCAGGCTTTCTGACCACCTATGCACCTCAGGTTGATGCAGGTCGTTAT
691.	P G D D A T V D V Q I A S I D H L L H A A A S
	CCTGGTGATGATGCAACCGTTGATGTTTCAGATTGCAAGCATTGATCATCTGCTGCATGCCGCAGCAAGC
760.	R G V D N A L P E L L K S V M E Q A R A A G H
	CGTGGTGTGATAATGCACTGCCGGAAGTCTGAAAAGCGTTATGGAACAAGCCCGTGCAGCAGGTCAT
829.	G S D S Y A S V I E V L R S P A P D P D E H N
	GGTAGCGATAGCTATGCAAGCGTTATTGAAGTCTGCGTAGTCCGGCACCGGATCCTGATGAACATAAT
898.	R * CGTTAACTCGAG

S-IRED M4ZS15

Protein Sequence

MSKQSVTVIGLGPMGQAMVNTFLDNGHEVTVWNRTASKAEALVARGAVLAPTV-
 EDALSAN ELIVLSLTDYDAVYAILEPVTGSLSGKVIANLSSDTPDKAREAAKWAAK-
 HGAKHLTGGVQ VPPPLIGKPESSTYYSGPKDVFDAHEDTLKVLTNADYRGEDAGL-
 AAMYYQAQMTIFWTTMLSYQTLALGQANGVSAKELLPYATMMTSMMPH-
 FLELYAQHVDSADYPGDVDRLAMGAASVDHVLHTHQDAGVSTVLPAAVAEIF-
 KAGMEKGF AENSFSSLIEVLK KPAV

ORF	Protected sites	Protected areas	Motifs to avoid
7-876 [AGC...TAA]	1-6 Ndel [CATATG] 877-882 XhoI [CTCGAG]		Ndel [CATATG] XhoI [CTCGAG]

1.	S K Q S V T V I G L G P M G Q A M V N T F
	CATATGAGCAAAACAGAGCGTTACCGTTATTGGTCTGGGTC CGATGGGTCAGGCAATGGTTAATACCTTT
70.	L D N G H E V T V W N R T A S K A E A L V A R
	CTGGATAATGGTCATGAAGTGACCGTTTGGAAATCGTACCGCAAGCAAAGCCGAAAGCACTGGTTGCACGT
139.	G A V L A P T V E D A L S A N E L I V L S L T
	GGTGCAGTTCTGGCACCGACCGTTGAAGATGCACTGAGCGCAAATGAACTGATTGTTCTGAGCCTGACC
208.	D Y D A V Y A I L E P V T G S L S G K V I A N
	GATTATGATGCAGTTTATGCAATTCTGGAACCGGTTACCGGTAGCCTGAGCGGTAAAGTTATTGCAAAAT
277.	L S S D T P D K A R E A A K W A A K H G A K H
	CTGAGCAGCGATACACCGGATAAAGCACGTGAAGCAGCAAAATGGGCAGCAAAACATGGTGCAAAACAT
346.	L T G G V Q V P P P L I G K P E S S T Y Y S G
	CTGACCGGTGGTGTTCAGGTTCCGCCTCCGCTGATTGGTAAACCGGAAAAGCAGCACCTATTATAGCGGT
415.	P K D V F D A H E D T L K V L T N A D Y R G E
	CCGAAAAGATGTTTTTGATGCCCATGAAGATACCCCTGAAAAGTTCTGACCAATGCAGATTATCGTGGTGAA
484.	D A G L A A M Y Y Q A Q M T I F W T T M L S Y
	GATGCCGGTCTGGCAGCAATGTATTATCAGGCACAGATGACCATTTTTTGGACCACCATGCTGAGCTAT
553.	Y Q T L A L G Q A N G V S A K E L L P Y A T M
	TATCAGACCTGGCACTGGGCCAGGCAAAATGGTGTAGCGCCAAAGAACTGCTGCCGTATGCAACCATG
622.	M T S M M P H F L E L Y A Q H V D S A D Y P G
	ATGACCAGCATGATGCCGCATTTTCTGGAACGTATGCACAGCATGTTGATAGTGCCGATTATCCGGGT
691.	D V D R L A M G A A S V D H V L H T H Q D A G
	GATGTTGATCGTCTGGCAATGGGTGCAGCAAGCGTTGATCATGTTCTGCATACCCATCAGGATGCCGGT
760.	V S T V L P A A V A E I F K A G M E K G F A E
	GTTAGCACCGTTCTGCCTGCAGCAGTTGCAGAAATCTTTAAAGCAGGTATGGAAAAAGGCTTTGCCGAA
829.	N S F S S L I E V L K K P A V *
	AATAGCTTTAGCAGCCTGATTGAGGTTCTGAAAAAACCGGCAGTTTAACTCGAG

S-IRED D2PR38

Protein Sequence

MPPTDRTPVTLIGLGPMQAMTRALLAAGHPVTVWNRTPARAAGVVADGAVLA-
 ASPVEAV EAGDLVILSLTDYQAMYDVLEPATGSLAGRTVVNLSSDTPDRTRAAAD-
 WATEHGATFLTG GVMIPAPMVGTEEAYVYYSGPAEVFEKHRTTLTVIGAPRYL-
 GEDTGLAQLMYQAQLDVFL TTLSSLMHATALLGTAGVSAAESMPELIGMLRTV-
 PAMLEAGGENPGADIDADKHPGDLST ITMMGATADHIVGASETAGIDLALPRA-
 VQAHYRRAIENGHGDDNWTRIIDGIRSPR

ORF	Protected sites	Protected areas	Motifs to avoid
22-909 [CCT...TAA]	<u>16-21 NdeI [CATATG]</u> <u>910-915 XhoI [CTCGAG]</u>		NdeI [CATATG] XhoI [CTCGAG]

1.	GTGCCGCGCGGGCAGC	<u>CATATG</u>	P P T D R T P V T L I G L G P M
70.	G Q A M T R A L L A A G H P V T V W N R T P A		
139.	GGTCAGGCAATGACCCGTGCACTGCTGGCAGCAGGTCATCCGGTTACCGTTTGGAAATCGCACACCCGGCA		
208.	R A A G V V A D G A V L A A S P V E A V E A G		
277.	CGTGACGCCGGTGTGTTGTCAGATGGTGCAGTTCTGGCAGCAAGTCCGGTTGAAGCAGTTGAAGCCGGT		
346.	D L V I L S L T D Y Q A M Y D V L E P A T G S		
415.	GATCTGGTTATTCTGAGCCTGACCGATTATCAGGCCATGTATGACGTTCTGGAACCCGGCAACCCGGTAGC		
484.	L A G R T V V N L S S D T P D R T R A A A D W		
553.	CTGGCAGGTCGTACCGTTGTTAATCTGAGCAGCGATACACCCGGATCGTACCCGTGCAGCAGCAGATTGG		
622.	A T E H G A T F L T G G V M I P A P M V G T E		
691.	GCAACCGAACATGGTGCAACCTTTCTGACCGGTGGTGTATGATTCCGGCACCGATGGTTGGCACCCGAA		
760.	E A Y V Y Y S G P A E V F E K H R T T L T V I		
829.	GAGGCCTATGTGTATTATAGCGGTCCGGCAGAAGTTTTTGA AAAACATCGTACCACCCTGACCGTTATT		
898.	G A P R Y L G E D T G L A Q L M Y Q A Q L D V		
	GGTGCACCCGCGTTATCTGGGTGAAGATACCGGTCTGGCACAGCTGATGTATCAGGCCCAGCTGGATGTG		
	F L T T L S S L M H A T A L L G T A G V S A A		
	TTTCTGACCACCCTGTCAAGCCTGATGCATGCAACAGCCCTGCTGGGTACAGCGGGTGTAGCGCAGCA		
	E S M P E L I G M L R T V P A M L E A G G E N		
	GAAAGCATGCCGGAACCTGATTGGTATGCTGCGTACCGTTCTGCAATGCTGGAAGCGGGTGGTGA AAAAT		
	P G A D I D A D K H P G D L S T I T M M G A T		
	CCGGGTGCAGATATTGATGCAGATAAACATCCGGGTGATCTGAGCACCATTACCATGATGGGTGCAACC		
	A D H I V G A S E T A G I D L A L P R A V Q A		
	GCAGATCATATTGTTGGTGCAAGCGAAACCGCAGGATTGATCTGGCACTGCCTCGTGCAGTTCCAGGCC		
	H Y R R A I E N G H G G D N W T R I I D G I R		
	CATTATCGTCGTGCAATTGAAAATGGTGCATGGTGGTGATAATTGGACCCGTATTATTGATGGTATTCGT		
	S P R *		
	AGTCCGCGTTAA	<u>CTCGAG</u>	CCACTGAGATCCGGC

S-IRED D2AWI4

Protein Sequence

MNTKSVTVIGLGPMPGQAMADAYLDGGYEVTVWNRTAARADRLVARGARRAPTV-
 EAALTAN DLVVLSTLDYDAMYAILEQAPSAALAGRTVANLTSDTPEKARQAAAW-
 LAERGAVQITGGV QVPPPGIGKPGATTYYSGPEDAIEAHRPALEVLTEIDLGED-
 PGLAALFYQIGMDMFWTG ILSYVHAQAVAEANGISAERFLPNAVKTMDFRYFLE-
 FYAPRIAAGNHEGDVDRLAMGVAS MEHVLHTVEASGVDGSLPAAVLDVFRRG-
 VAAGHGQDSLTSLIKVLKR

ORF	Protected sites	Protected areas	Motifs to avoid
22-882 [AAT...TAA]	16-21 NdeI [CATATG] 883-888 XhoI [CTCGAG]		NdeI [CATATG] XhoI [CTCGAG]

1.	GTGCCGCGCGGCAGCCATATG	N T K S V T V I G L G P M G Q A
70.	M A D A Y L D G G Y E V T V W N R T A A R A D	
139.	ATGGCAGATGCATATCTGGATGGTGGTTATGAAGTTACCGTTTGGGAATCGTACCGCAGCAGCAGTGCAGAT	
208.	R L V A R G A R R A P T V E A A L T A N D L V	
277.	CGTCTGGTTGCACGTGGTGCCCGTCGTGCACCGACCGTTGAAGCAGCACTGACCGCAAATGATCTGGTT	
346.	V L S L T D Y D A M Y A I L E Q A P S A A L A	
415.	GTTCTGAGCCTGACCGATTATGATGCAATGTATGCAATCTGGAACAGGCACCGAGCGCAGCACTGGCA	
484.	G R T V A N L T S D T P E K A R Q A A A W L A	
553.	GGTCGTACCGTTGCAAATCTGACCAGCGATACACCGGAAAAAGCACGTCAGGCAGCAGCATGGCTGGCA	
622.	E R G A V Q I T G G V Q V P P P G I G K P G A	
691.	GAACGTGGTGCAGTTTCAGATTACCGTGGTGGTTCAGGTTCCGCTCCGGGATTGGTAAACCGGGTGA	
760.	T T Y Y S G P E D A I E A H R P A L E V L T E	
829.	ACCACCTATTATAGCGGTCCGGAAGATGCAATTGAAGCACATCGTCCGGCACTGGAAGTTCTGACCGAA	
898.	I D H L G E D P G L A A L F Y Q I G M D M F W	
	ATTGATCATCTGGGTGAAGATCCGGGTCTGGCAGCACTGTTTTATCAGATTGGTATGGATATGTTTTGG	
	T G I L S Y V H A Q A V A E A N G I S A E R F	
	ACCGGCATTCTGAGCTATGTTTCATGCACAGGCAGTTGCCGAAGCAAATGGTATTAGCGCAGAACGTTTT	
	L P N A V K T M D F R Y F L E F Y A P R I A A	
	CTGCCGAATGCAGTTAAAACCATGGATTTCCGTTACTTTCTGGAATTTTATGCACCGCGTATTGCAGCA	
	G N H E G D V D R L A M G G V A S M E H V L H T	
	GGCAATCATGAAGGTGATGTTGATCGCCTGGCAATGGGTGTTGCAAGCATGGAACATGTGCTGCATACC	
	V E A S G V D G S L P A A V L D V F R R G V A	
	GTGGAAGCAAGCGGTGTTGATGGTAGCCTGCCTGCAGCAGTTCTGGATGTTTTCTGTCGTGGTGGTGGCA	
	A G H G Q D S L T S L I K V L K R *	
	GCCGGTCATGGTTCAGGATTCAGTACCAGCCTGATTAAGTTCTGAAACGCTAACTCGAGCCACTGAGA	
	TCCGGC	

S-IRED J7YM26

Protein Sequence

MKSNSQNEKNGSETTNAVGNRKSVTVIGLGPMGQAMADVFLYGYSVTVWNRT-
 SSKADQL VAKGAIRVSTVNEALAANELVILSLTDYINVMYSILEPVSENLFQKV-
 LVNLSSDTPEKARK AAKWLEDGRGARHITGGVQVPPSGIGKSESYTYYSGDRVV-
 FEHRETLEVLTSDDYRGEDP GLAMLYYQIQMDIFWTAMLSYLHALAIANAN-
 GITAEQFLPYASAMMSSLPKFVEFYTPRL DEGEHPGDVDRLAMGLASVEHV-
 HTTQEAGIDIALPATVLEVFRRGMKTGHASDSFTSLI EIFKNSDIRS

ORF	Protected sites	Protected areas	Motifs to avoid
22-951 [AAA...TAA]	<u>16-21 NdeI [CATATG]</u> <u>952-957 XhoI [CTCGAG]</u>		NdeI [CATATG] XhoI [CTCGAG]

1.	GTGCCGCGCGGGCAGC	K S N S Q N E K N G S E T T N A	
70.	V G N R K S V T V I G L G P M G Q A M A D V F		
139.	GTTGGTAATCGTAAAAGCGTTACCGTTATTGGTCTGGGTCCGATGGGT		
208.	L E Y G Y S V T V W N R T S S K A D Q L V A K		
277.	CTGGAATATGGTTATAGCGTGACCGTTTGGGAATCGTACCAGCAGCAAAGCAGATCAGTCTGGTTGCAAAA		
346.	G A I R V S T V N E A L A A N E L V I L S L T		
415.	GGTGCAATTCGTGTTAGCACCGTTAATGAAGCACTGGCAGCAAATGAACTGGTTATTCTGAGCCTGACC		
484.	D Y N V M Y S I L E P V S E N L F G K V L V N		
553.	GATTACAATGTGATGTATAGCATTCTGGAACCGTTAGCGAAAACCTGTTTGGTAAAGTTCTGGTGAAT		
622.	L S S D T P E K A R K A A K W L E D R G A R H		
691.	CTGAGCAGCGATACACCGGAAAAAGCACGTAAGCAGCAAATGGCTGGAAGATCGTGGTGACACGTCAT		
760.	I T G G V Q V P P S G I G K S E S Y T Y Y S G		
829.	ATTACCGGTGGTGTTCAGGTTCCGCCTAGCGGTATTGGTAAAAGCGAAAAGCTATACCTATTATAGCGGT		
898.	D R V V F E A H R E T L E V L T S S D Y R G E		
967.	GATCGTGTGTTTTGAAGCACATCGTGAAACCTGGAAGTTCTGACCAGCAGCGATTATCGTGGTGAA		
	D P G L A M L Y Y Q I Q M D I F W T A M L S Y		
	GATCCGGGTCTGGCAATGCTGTATTATCAGATTCAGATGGATATCTTTGGACCAGCAATGCTGAGCTAT		
	L H A L A I A N A N G I T A E Q F L P Y A S A		
	CTGCATGCACCTGGCAATTGCAAATGCAAATGGTATTACCGCAGAACAGTTTCTGCCGTATGCAAGCGCA		
	M M S S L P K F V E F Y T P R L D E G E H P G		
	ATGATGAGCAGCCTGCCGAAATTTGTTGAATTCTATACACCGCGTCTGGATGAAGGCGAACATCCGGGT		
	D V D R L A M G L A S V E H V V H T T Q E A G		
	GATGTTGATCGTCTGGCCATGGGTCTGGCCAGCGTTGAACATGTTGTTTCATACCACCAAGAAGCCGGT		
	I D I A L P A T V L E V F R R G M K T G H A S		
	ATTGATATTGCACTGCCTGCAACCGTTCTGGAAGTTTTTCGTGCGGGTATGAAAACCGGTTCATGCAAGC		
	D S F T S L I E I F K N S D I R S *		
	GATAGCTTTACCAGCCTGATTGAGATTTTCAAAAATAGCGATATCCGCAGCTAA		
	CTCGAGCCACTGAGA		
	TCCGGC		

S-IRED K0F8R0

Protein Sequence

MSEQHTPRSVSVVGLGPMGQSMVRALLDAGVEVTVWNRSTDKVDAMVELGAV-
 RAETVAAA LAANDVTVLSLTHYAAMYSVLEQAADQLAGKVIVNLSSDSPEKARK-
 GAEWVRSHGAEFLS GGVMSAGDNIAHPASYIFYSGPREVFDHAHAELLRPLSPQEYL-
 GTDDGLSQVYYQALLTIF HPWLLAFDQATAMIERSGNSIAQFIPFAVRSAAAY-
 PYFMEEFSVANQNGGWATLASLMMM DAGAQHIIDASEEVGV DATFSHTAQAY-
 WRKAVAASEEKGEAVSTYALMRGADA

ORF	Protected sites	Protected areas	Motifs to avoid
22-900 [AGC...TAA]	<u>16-21 NdeI [CATATG]</u> <u>901-906 XhoI [CTCGAG]</u>		NdeI [CATATG] XhoI [CTCGAG]

1.	GTGCCGCGCGGGCAGCCATATGAGCGAACAGCATAACCCGCGTAGCGTTAGCGTTGTTGGTCTGGGTCCG
	M G Q S M V R A L L D A G V E V T V W N R S T
70.	ATGGGTCAGAGCATGGTTCGTGCACTGCTGGATGCCGGTGTGAAAGTTACCGTTTGGAAATCGTAGCACC
	D K V D A M V E L G A V R A E T V A A A L A A
139.	GATAAAGTTGATGCAATGGTTGAACTGGGTGCAGTTCGTGCAGAAACCGTTGCAGCAGCACTGGCAGCA
	N D V T V L S L T H Y A A M Y S V L E Q A A D
208.	AATGATGTTACCGTTCGTGAGCCTGACCCATTATGCAGCAATGTATAGCGTTCTGGAACAGGCAGCAGAT
	Q L A G K V I V N L S S D S P E K A R K G A E
277.	CAGCTGGCAGGTAAGTTATTGTTAATCTGAGCAGCGATAGTCCGGAAAAAGCACGTAAGGTGCAGAA
	W V R S H G A E F L S G G V M S A G D N I A H
346.	TGGGTTTCGTAGCCATGGTGGCAATTTCTGAGCGGTGGTGTATGAGTGCCGGTGATAATATTGCACAT
	P A S Y I F Y S G P R E V F D A H A E L L R P
415.	CCGGCAAGCTATATCTTTTATAGCGGTCCGCGTGAAGTTTTTGTATGCACATGCAGAACTGCTGCGTCCG
	L S P Q E Y L G T D D G L S Q V Y Y Q A L L T
484.	CTGAGTCCGCAAGAATATCTGGGCAACCGATGATGGTCTGAGCCAGGTTTATTATCAGGCACTGCTGACC
	I F H P W L L A F D Q A T A M I E R S G N S I
553.	ATTTTTTCATCCGTGGCTGCTGGCATTGATCAGGCAACCGCAATGATTGAACGTAGCGGTAATAGCATT
	A Q F I P F A V R S A A A Y P Y F M E E F S V
622.	GCACAGTTTATTCCGTTTGGCGTTCGTAGCGCAGCAGCATATCCGTATTTTATGGAAGAATTTAGCGTG
	A N Q N G G W A T L A S L K M M D A G G A Q H I
691.	GCCAATCAGAATGGTGGTGGGCAACCCTGGCAAGCCTGAAAATGATGGATGCGGGTGCACAGCATATT
	I D A S E E V G V D A T F S H T A Q A Y W R K
760.	ATTGATGCAAGCGAAGAGGTTGGTGTGATGCCACCTTTAGCCATACCGCACAGGCATATTGGCGTAAA
	A V A A S E E K G E A V S T Y A L M R G A D A
829.	GCAGTTGCAGCCAGCGAAGAAAAAGGTGAAGCAGTTAGCACCTATGCACTGATGCGTGGTGCAGATGCA
	*
898.	TAACTCGAGCCACTGAGATCCGGC

S-IRED K0K4C6

Protein Sequence

MSTPLTLIGLGPMSGQAMVAKYLEHGHPVTVWNRTASRADDLVARGAVRADTPRD-
 AVAANR LVVLSLTDYQAMYDVLGDAELAGKTVVNLSSDTPDKTLKAAAWLAER-
 GAELVGGVMVPA PLVGEEAAYVFYSGPKAVFEQHAEVLAVIGRTEYLGEDHA-
 LAQLFYQAQLDFLTTLAAT LHSVALVRTAGVTAAQFAPYLKDNAESIWMYLEE-
 TITAVDRGEHPGDLANIVMMGATADH VVGASEATGVDAGLPRAVQDMYRRAI-
 EAGHGQESWTALYEVKPAK

ORF	Protected sites	Protected areas	Motifs to avoid
22-879 [AGC...TAA]	16-21 NdeI [CATATG] 880-885 XhoI [CTCGAG]		NdeI [CATATG] XhoI [CTCGAG]

1.	GTGCCGCGCGGGCAGCCATATGAGCACACCCGCTGACCCTGATTGGTCTGGGTCCGATGGGTGAGGCAATG	S T P L T L I G L G P M G Q A M
70.	V A K Y L E H G H P V T V W N R T A S R A D D GTTGCAAAATATCTGGAACATGGTCATCCGGTTACCGTTTGGAAATCGTACCGCAAGCCGTGCAGATGAT	
139.	L V A R G A V R A D T P R D A V A A N R L V V CTGGTTGCACGTGGTGCAGTTCGTGCAGATACACCCGCGTGATGCAGTTGCAGCAAATCGTCTGGTTGTT	
208.	L S L T D Y Q A M Y D V L G D A E L A G K T V CTGAGCCTGACCGATTATCAGGCCATGTATGACGTTCTGGGTGATGCAGAACTGGCAGGTAAAACCGTT	
277.	V N L S S D T P D K T L K A A A W L A E R G A GTTAATCTGAGCAGCGATACACCCGGATAAAACCCCTGAAAGCAGCAGCATGGCTGGCAGAACGTGGTGCC	
346.	E L V V G G V M V P A P L V G E E A A Y V F Y GAACTGGTTGTTGGTGGTGTATGGTTCCGGCACCCGCTGGTTGGTGAAGAGGCAGCCTATGTGTTTTAT	
415.	S G P K A V F E Q H A E V L A V I G R T E Y L AGCGGTCCGAAAAGCAGTTTTTGAACAGCATGCAGAAAGTTCTGGCAGTTATTGGTCGTACCGAATATCTG	
484.	G E D H A L A Q L F Y Q A Q L D F F L T T L A GGTGAAGATCATGCACTGGCACAGCTGTTTTATCAGGCCGAGCTGGATTTTTTCTGACCACCCTGGCA	
553.	A T L H S V A L V R T A G V T A A Q F A P Y L GCAACCCTGCATAGCGTTGCACTGGTTTCGTACAGCCGGTGTACCAGCAGCACAGTTTGCACCGTATCTG	
622.	K D N A E S I W M Y L E E T I T A V D R G E H AAAGATAATGCAGAAAAGCATTGGATGTACCTGGAAGAAAACCATTACCGCAGTTGATCGTGGTGAACAT	
691.	P G D L A N I V M M G A T A D H V V G A S E A CCGGGTGATCTGGCAAATATTGTTATGATGGGTGCAACCGCAGATCATGTTGTGGGTGCAAGCGAAGCA	
760.	T G V D A G L P R A V Q D M Y R R A I E A G H ACCGGTGTTGATGCAGGTCTGCCTCGTGCAGTTCAGGATATGTATCGTTCGTGCAATTGAAGCAGGTCAT	
829.	G Q E S W T A L Y E V I K P A K * GGTCAAGAAAGCTGGACCGCACTGTATGAAGTTATTAACCGGCAAAATAACTCGAGCCCACTGAGATCC	
898.	G G C	

4.2 GC & HPLC Chromatograms

On the following pages chiral example chromatograms (left hand- and right hand columns, respectively) of the performed biotransformations are shown. The retention times are given for each compound involved.

The following table summarizes the retention times of achiral conversion measurements.

Compound	t_R [min]	Method
72a	4.33	2-MP_HP-5
73a	4.14	2-MP_HP-5
74a	5.49	2-MPI_HP-5
78a	4.63	2-MPI_HP-5
62	16.02	1M-DHIQ_DB-1701
59	15.95	1M-DHIQ_DB-1701
110	15.98	DM-DHIQ_DB-1701
112	15.85	DM-DHIQ_DB-1701
56	16.28	1M-DM-DHIQ_DB-1701
57	15.84	1M-DM-DHIQ_DB-1701
111	9.25	TMI_HP-5
113	9.78	TMI_HP-5

Biotransformation of 2-methyl-1-pyrroline (72a)

Method: TBDAc_2-MP-Ac

Column: Hydrodex- β -TBDAc: Macherey-Nagel, 723 384.50, 50 m, 0.25 mm

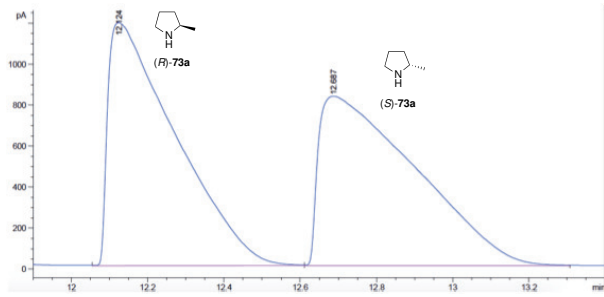
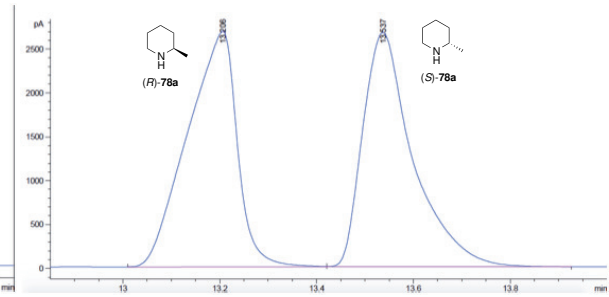
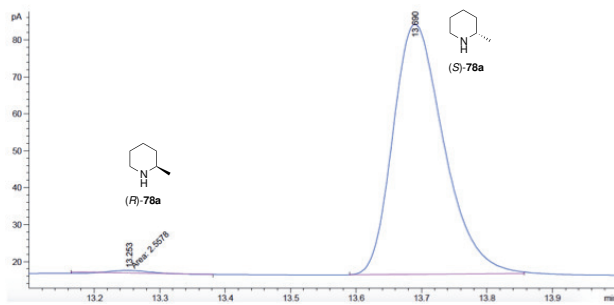
Temperature Program: 70 °C (1 min) –[20 °C/min]–> 150 °C (10 min) –[20 °C/min]–> 210 °C (2 min)

Carrier Gas Flow: (H₂) 1 mL/min

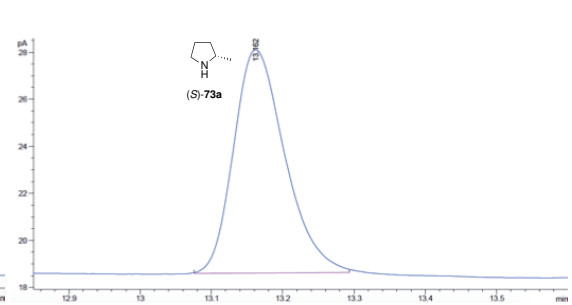
Split Ratio: 20:1

Injector Temperature: 230 °C

	Compound			
	(R)-73a	(S)-73a	(R)-78a	(S)-78a
Method	TBDAc_2-MP-Ac			
t_R [min]	12.12	12.69	13.21	13.54

*rac.* 73a*rac.* 78a

Biotransformation of 78a (S-IRE D M4ZS15)



Biotransformation of 73a (S-IRE D2PR38)

Biotransformation of 1-methyl-3,4-dihydroisoquinoline (62) & 1-methyl-6,7-dimethoxy-3,4-dihydroisoquinoline (56)

Method: A

Column: Daicel Chiracel OD-H, 0.46 cm Øx 25 cm

Solvent ratio [%]: 99 heptane/1 *i*-propanol, 0.1 diethylamine

Solvent Flow: 0.5 mL/min

Oven Temperature: 30 °C

Method: B

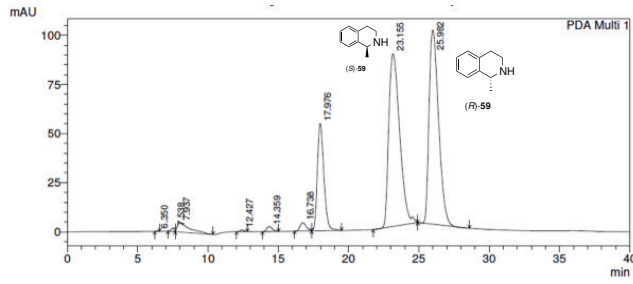
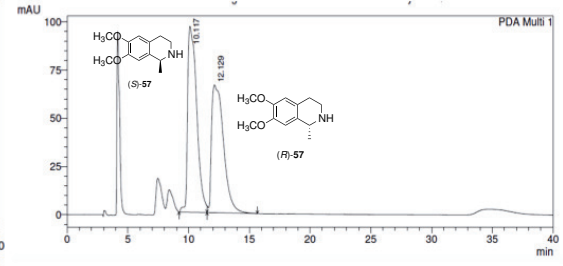
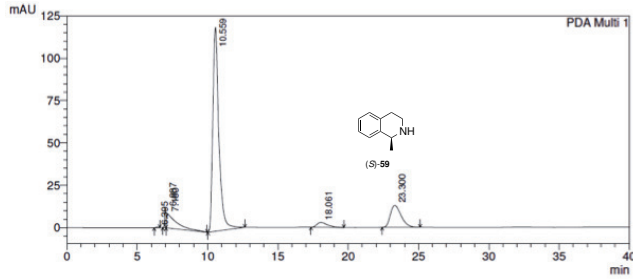
Column: Daicel Chiracel OD-H, 0.46 cm Øx 25 cm

Solvent ratio [%]: 90 heptane/10 *i*-propanol, 0.1 diethylamine

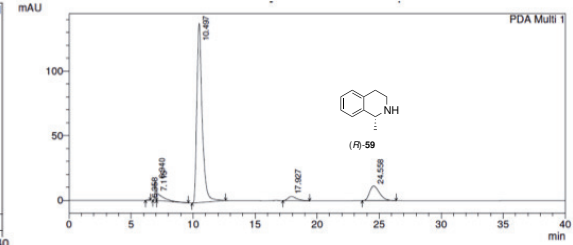
Solvent Flow: 1 mL/min

Oven Temperature: 30 °C

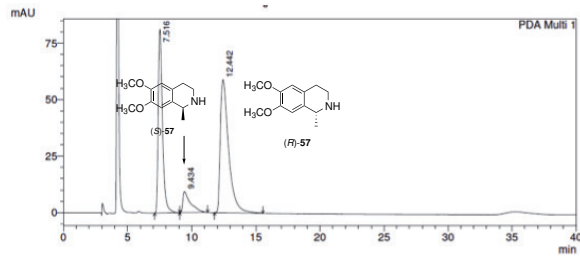
	Compound			
	(R)-59	(S)-59	(R)-57	(S)-57
Method	A		B	
t_R [min]	25.98	23.16	12.13	10.12

*rac.* 59*rac.* 57

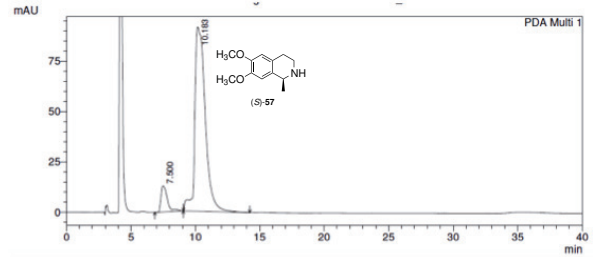
Biotransformation of 62 (S-IRED K0F8R0)



Biotransformation of 62 (R-IRED W7VJL8)



Biotransformation of 56 (R-IRED V6KA13)



Biotransformation of 56 (S-IRED M4ZS15)

Biotransformation of 2,3,3-trimethyl-3H-indole (111)

Method: C

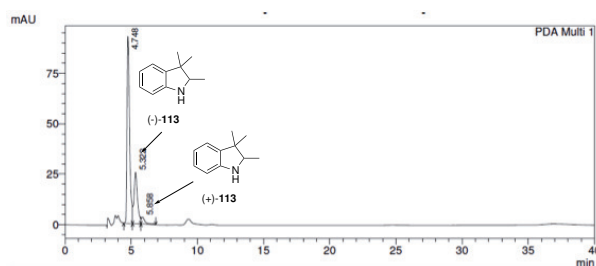
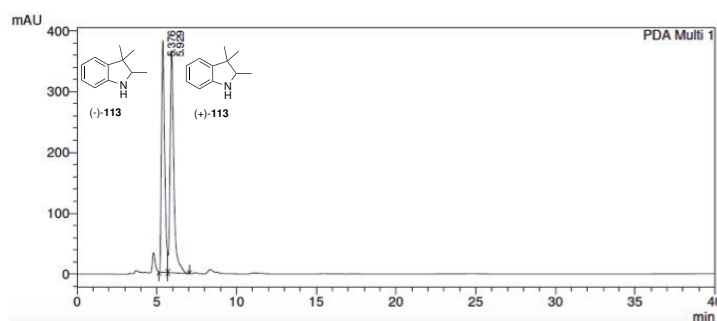
Column: Daicel Chiracel OD-H, 0.46 cm Øx 25 cm

Solvent ratio [%]: 97 heptane/3 *i*-propanol, 0.1 diethylamine

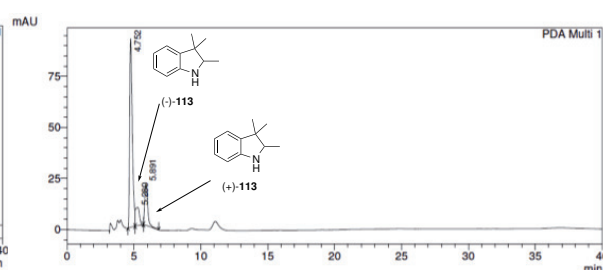
Solvent Flow: 1 mL/min

Oven Temperature: 30 °C

	Compound	
	(+)-113	(-)-113
Method	C	
t_R [min]	5.93	5.38



Biotransformation of 111 (R-IRE D V7GV82)



Biotransformation of 111 (S-IRE D2PR38)

References

- [1] D. Ghislieri, N. Turner, *Top. Catal.* **2014**, *57*, 284–300.
- [2] *Topics in Current Chemistry, Vol. 343: Stereoselective Formation of Amines*, (Hrsg.: W. Li, X. Zhang), Springer, Berlin/Heidelberg, **2014**.
- [3] *Chiral Amine Synthesis*, (Hrsg.: T. C. Nugent), Wiley-VCH, Weinheim, **2010**.
- [4] T. C. Nugent, M. El-Shazly, *Adv. Synth. Catal.* **2010**, *352*, 753–819.
- [5] M. Breuer, K. Ditrich, T. Habicher, B. Bauer, M. Kessler, R. Stuermer, T. Zelinski, *Angew. Chem. Int. Ed.* **2004**, *43*, 788–824.
- [6] K. H. Hopmann, A. Bayer, *Coord. Chem. Rev.* **2014**, *268*, 59–82.
- [7] S. Rossi, M. Benaglia, E. Massolo, L. Raimondi, *Catal. Sci. Technol.* **2014**, *4*, 2708–2723.
- [8] A. Bartoszewicz, N. Ahlsten, B. Martin-Matute, *Chem. Eur. J.* **2013**, *19*, 7274–7302.
- [9] Q.-A. Chen, Z.-S. Ye, Y. Duan, Y.-G. Zhou, *Chem. Soc. Rev.* **2013**, *42*, 497–511.
- [10] D. W. Stephan, *Org. Biomol. Chem.* **2012**, *10*, 5740–5746.
- [11] J. G. de Vries, N. Mrcsic, *Catal. Sci. Technol.* **2011**, *1*, 727–735.
- [12] U. T. Bornscheuer, G. W. Huisman, R. J. Kazlauskas, S. Lutz, J. C. Moore, K. Robins, *Nature* **2012**, *485*, 185–194.
- [13] C. M. Cloutier, J. N. Pelletier, *Chem. Soc. Rev.* **2012**, *41*, 1585–1605.
- [14] M. T. Reetz, *J. Am. Chem. Soc.* **2013**, *135*, 12480–12496.
- [15] A. Wells, H.-P. Meyer, *ChemCatChem* **2014**, *6*, 918–920.
- [16] G. W. Huisman, S. J. Collier, *Curr. Opin. Chem. Biol.* **2013**, *17*, 284–292.
- [17] R. C. Simon, F. G. Mutti, W. Kroutil, *Drug Discov. Today Technol.* **2013**, *10*, e37–e44.
- [18] R. N. Patel, *ACS Catal.* **2011**, *1*, 1056–1074.
- [19] J. Tao, J. H. Xu, *Curr. Opin. Chem. Biol.* **2009**, *13*, 43–50.
- [20] *Industrial Biotransformations*, (Hrsg.: A. Liese, K. Seelbach, C. Wandrey), Wiley-VCH, Weinheim, 2nd ed., **2006**.
- [21] M. Ikeda, *Advances in Biochemical Engineering/Biotechnology, Vol. 79: Microbial Production of L-Amino Acids*, (Hrsg.: T. Scheper, R. Faurie, J. Thommel), Springer, Berlin/Heidelberg, **2003**, S. 1–35.
- [22] W. Leuchtenberger, K. Huthmacher, K. Drautz, *Appl. Microbial. Biotechnol.* **2005**, *69*, 1–8.
- [23] N. J. Turner, *Curr. Opin. Chem. Biol.* **2011**, *15*, 234–240.
- [24] B. Weiner, G. J. Poelarends, D. B. Janssen, B. L. Feringa, *Chem. Eur. J.* **2008**, *14*, 10094–10100.
- [25] H. Raj, W. Szymanski, J. de Villiers, H. J. Rozeboom, V. P. Veetil, C. R. Reis, M. de Villiers, F. J. Dekker, S. de Wildeman, W. J. Quax, A.-M. Thunnissen, B. L. Feringa, D. B. Janssen, G. J. Poelarends, *Nat. Chem.* **2012**, *4*, 478–484.

- [26] V. P. Veetil, H. Raj, M. de Villiers, P. G. Tepper, F. J. Dekker, W. J. Quax, G. J. Poelarends, *ChemCatChem* **2013**, *5*, 1325–1327.
- [27] B. de Lange, D. J. Hyett, P. J. D. Maas, D. Mink, F. B. J. van Assema, N. Sereinig, A. H. M. de Vries, J. G. de Vries, *ChemCatChem* **2011**, *3*, 289–292.
- [28] F. Parmeggiani, S. L. Lovelock, N. J. Weise, S. T. Ahmed, N. J. Turner, *Angew. Chem. Int. Ed.* **2015**, *54*, DOI : 10.1002/anie.201410670.
- [29] E. Busto, V. Gotor-Fernandez, V. Gotor, *Chem. Rev.* **2011**, *111*, 3998–4035.
- [30] F. van Rantwijk, R. A. Sheldon, *Tetrahedron* **2004**, *60*, 501–519.
- [31] F. Balkenhohl, B. Hauer, W. Landner, U. Pressler, *Pat.*, DE4332738 (BASF AG), **1995**.
- [32] H. Kohls, F. Steffen.Munsberg, M. Hoehne, *Curr. Opin. Chem. Biol.* **2014**, *19*, 180–192.
- [33] M. Hoehne, U. T. Bornscheuer, *ChemCatChem* **2009**, *1*, 42–51.
- [34] R. S. Heath, M. Pontini, B. Bechi, N. J. Turner, *ChemCatChem* **2014**, *6*, 996–1002.
- [35] J. H. Schrittwieser, B. Groenedaal, S. C. Willies, D. Ghislieri, I. Rowles, V. Resch, J. H. Sattler, E.-M. Fischereeder, B. Grischek, W.-D. Lienhart, N. J. Turner, W. Kroutil, *Catal. Sci. Technol.* **2014**.
- [36] J. H. Schrittwieser, B. Groenedaal, V. Resch, D. Ghislieri, S. Wallner, E.-M. Fischereeder, E. Fuchs, B. Grischek, J. H. Sattler, P. Macheroux, N. J. Turner, W. Kroutil, *Angew. Chem. Int. Ed.* **2014**, *53*, 3731–3734.
- [37] D. Ghislieri, A. P. Green, M. Pontini, S. C. Willies, I. Rowles, A. Frank, G. Grogan, N. J. Turner, *J. Am. Chem. Soc.* **2013**, *135*, 10863–10869.
- [38] D. Ghislieri, D. Houghton, A. P. Green, S. C. Willies, N. J. Turner, *ACS Catal.* **2013**, *3*, 2869–2872.
- [39] D. Koszelewski, K. Tauber, K. Faber, W. Kroutil, *Trends Biotechnol.* **2010**, *28*, 324–332.
- [40] S. Mathew, H. Yun, *ACS Catal.* **2012**, *2*, 993–1001.
- [41] R. C. Simon, N. Richter, E. Busto, W. Kroutil, *ACS Catal.* **2014**, *4*, 129–143.
- [42] C. K. Savile, J. M. Janey, E. C. Mundorff, J. C. Moore, S. Tam, W. R. Jarvis, J. C. Colbeck, A. Krebber, F. J. Fleitz, J. Brands, P. N. Devine, G. W. Huisman, G. J. Hughes, *Science* **2010**, *329*, 305–309.
- [43] D. Gamnara, P. D. de Maria, *Org. Biomol. Chem.* **2014**, *12*, 2989–2992.
- [44] N. J. Turner, *Comprehensive Organic Synthesis II, Second Edition*, (Hrsg.: P. Knochel), Elsevier, Amsterdam, **2014**, S. 328–338.
- [45] F. Leipold, S. Hussain, S. P. France, N. J. Turner, *Science of Synthesis: Biocatalysis in Organic Synthesis 2*, (Hrsg.: K. Faber, W.-D. Fessner, N. J. Turner), Thieme, Stuttgart, **2015**, S. 359–382.
- [46] J. Crugerias, A. Rios, E. Riveiros, J. P. Richard, *J. Am. Chem. Soc.* **2009**, *131*, 15815–15824.
- [47] J. R. Schnell, H. J. Dyson, P. E. Wright, *Annu. Rev. Biophys. Biomol. Struct.* **2004**, *33*, 119–140.

- [48] B. Thoeny, G. Auerbach, N. Blau, *Biochem. J.* **2000**, *347*, 1–16.
- [49] R. L. Blakley, *Advances in Enzymology and Related Areas of Molecular Biology*, Vol. 70, (Hrsg.: A. Meister), **1995**, S. 23–102.
- [50] E. R. Werner, N. B. B. Thoeny, *Biochem. J.* **2011**, *438*, 397–414.
- [51] W. L. F. Armarego, D. Randles, P. Waring, *Med. Res. Rev.* **1984**, *4*, 267–321.
- [52] E. E. Howell, *ChemBioChem* **2005**, *6*, 590–600.
- [53] F. A. Firgaira, R. G. Cotton, D. M. Danks, *Biochem. J.* **1981**, 197.
- [54] R. C. Hider, X. Kong, *Nat. Prod. Rep.* **2010**, *27*, 637–657.
- [55] D. A. Miller, L. Luo, N. Hillson, T. A. Keating, C. T. Walsh, *Chem. Biol.* **2002**, *9*, 333–344.
- [56] H. M. Patel, C. T. Walsh, *Biochemistry* **2001**, *40*, 9023–9031.
- [57] C. Reimann, H. M. H. M. P. Serino, M. Barone, C. T. Walsh, D. Haas, *J. Bacteriol.* **2001**, *183*, 813–820.
- [58] M. F. Roberts, *Phytochemistry* **1975**, *14*, 2393–2397.
- [59] S. T. Lee, B. T. Green, K. D. Welch, J. A. P. K. E. Panter, *Chem. Res. Toxicol.* **2008**, *21*, 2061–2064.
- [60] J. N. Tawara, A. Blokhin, T. A. Foderaro, F. R. Stermitz, H. Hope, *J. Org. Chem.* **1993**, *58*, 4813–4818.
- [61] F. R. Stermitz, J. N. Tawara, M. Boekl, M. Pomeroy, T. A. Foderaro, F. G. Todd, *Phytochemistry* **1994**, *35*, 951–953.
- [62] J. M. Finefield, D. H. Sherman, M. Kreitman, R. M. Williams, *Angew. Chem. Int. Ed.* **2012**, *51*, 4802–4836.
- [63] W. De-Eknamkul, M. H. Zenk, *Tetrahedron Lett.* **1990**, *31*, 4855–4858.
- [64] W. De-Eknamkul, M. H. Zenk, *Phytochemistry* **1992**, *31*, 813–821.
- [65] C. Wallwey, M. Matuschek, X.-L. Xie, S.-M. Li, *Org. Biomol. Chem.* **2010**, *8*, 3500–3508.
- [66] M. Matuschek, C. Wallwey, B. Wollinsky, X. Xie, S.-M. Li, *RSC Adv.* **2012**, *2*, 3662–3669.
- [67] E. Adams, L. Frank, *Annu. Rev. Biochem.* **1980**, *49*, 1005–1061.
- [68] T. Yura, H. J. Vogel, *J. Biol. Chem.* **1959**, *234*, 335–338.
- [69] M. E. Smith, D. M. Greenberg, *Nature* **1956**, *177*, 1130–1130.
- [70] Y. Yang, S. Xu, M. Zhang, R. Jin, L-Zhang, J. Bao, H. Wang, *Protein Expres. Purif.* **2006**, *45*, 241–248.
- [71] R. V. Krishna, P. Beilstein, T. Leisinger, *Biochem. J.* **1979**, *181*, 223–230.
- [72] R. Kruegger, H.-J. Jaeger, M. Hintz, E. Pahlich, *Plant Physiology* **1986**, *80*, 142–144.
- [73] Z. Meng, Z. Liu, Z. Lou, X. Gong, Y. Cao, M. Bartlam, K. Zhang, Z. Rao, *Protein Expres. Purif.* **2009**, *64*, 125–130.
- [74] B. Gerratana, *Med. Res. Rev.* **2012**, *32*, 254–293.

- [75] U. Peschke, H. Schmidt, H.-Z. Zhang, W. Piepersberg, *Mol. Microbiol.* **1995**, *16*, 1137–1156.
- [76] W. Li, S. Chou, A. Khullar, B. Gerratana, *Appl. Environ. Microbiol.* **2009**, *75*, 2958–2963.
- [77] W. Li, A. Khullar, S. Chou, A. Sacramo, B. Gerratana, *Appl. Environ. Microbiol.* **2009**, *75*, 2869–2878.
- [78] I. Hoefler, M. Cruesemann, M. Radzom, B. Geers, D. Flachshaar, X. Cai, A. Zeeck, J. Piel, *Chem. Biol.* **2011**, *18*, 381–391.
- [79] T. D. H. Bugg, *Introduction to Enzyme and Coenzyme Chemistry*, Blackwell, Oxford, 2nd ed., **2004**.
- [80] M. Taylor, C. Scott, G. Grogan, *Trends Biotechnol.* **2013**, *45*, 63–64.
- [81] A. Hallen, J. F. Jamie, A. J. L. Cooper, *Amino Acids* **2013**, *45*, 1249–1272.
- [82] H. Muramatsu, H. Mihara, R. Kakutami, M. Yasuda, M. Ueda, T. Kurihara, N. Esaki, *J. Biol. Chem.* **2005**, *280*, 5329–5335.
- [83] A. Meister, S. D. Buckley, *Biochim. Biophys. Acta* **1957**, *23*, 202–203.
- [84] A. Hallen, A. J. L. Cooper, J. F. Jamie, P. A. Haynes, R. D. Willows, *J. Neurochem.* **2011**, *118*, 379–387.
- [85] M. Goto, H. Muramatsu, H. Mihara, T. Kurihara, N. Esaki, R. Omi, I. Miyahara, K. Hirotsu, *J. Biol. Chem.* **2005**, *280*, 40875–40884.
- [86] M. Nardini, G. Ricci, A. M. Caccuri, S. P. Solinas, L. Vesci, D. Cavallini, *Eur. J. Biochem.* **1988**, *173*, 689–694.
- [87] M. Nardini, G. Ricci, L. Vesci, L. Pecci, D. Cavallini, *Biochim. Biophys. Acta* **1988**, *957*, 286–292.
- [88] H. Mihara, H. Muramatsu, R. Kakutami, M. Yasuda, M. Ueda, T. Kurihara, N. Esaki, *FEBS* **2005**, *272*, 1117–1123.
- [89] H. Muramatsu, H. Mihara, R. Kakutami, M. Yasuda, M. Ueda, T. Kurihara, N. Esaki, *Tetrahedron: Asymmetry* **2004**, *15*, 2841–2843.
- [90] L. S. Frost, M. Carpenter, W. Paranchych, *Nature* **1978**, *271*, 87–89.
- [91] S. A. Survase, L. D. Kagliwal, U. S. Annapure, R. S. Singhal, *Biotechnol. Adv.* **2011**, *29*, 418–435.
- [92] A. A. Sy-Cordero, C. J. Pearce, N. H. Oberlies, *J. Antibiot.* **2012**, *65*, 541–549.
- [93] D. P. Levine, *Clin. Infect. Dis.* **2006**, *42*, S5–S12.
- [94] R. Finking, M. A. Marahiel, *Annu. Rev. Microbiol.* **2004**, *58*, 453–488.
- [95] A. O. Subtelny, M. C. T. Hartman, J. W. Szostak, *J. Am. Chem. Soc.* **2008**, *130*, 6131–6136.
- [96] L. Aurelio, A. B. Hughes, *Amino Acids, Peptides and Proteins in Organic Chemistry*, (Hrsg.: A. B. Hughes), Wiley-VCH, Weinheim, **2009**, S. 245–289.
- [97] A. S. Bommarius, S. K. Au, *Science of Synthesis: Biocatalysis in Organic Synthesis 2*, (Hrsg.: K. Faber, N. J. Turner, W.-D. Fessner), Thieme, Stuttgart, **2015**, S. 335–358.

- [98] W. Hummel, H. Groeger, *Enzyme Catalysis in Organic Synthesis*, (Hrsg.: K. Drauz, H. Groeger, O. May), Wiley-VCH, Weinheim, **2012**, S. 1165–1203.
- [99] J. C. Moore, C. K. Savile, S. Pannuri, B. Kosjek, J. M. Janey, *Comprehensive Chirality*, (Hrsg.: E. M. Carreira, H. Yamamoto), Elsevier, Amsterdam, **2012**, S. 318–341.
- [100] R. L. Hanson, *ACS Symposium Series, Vol. 1009: Asymmetric Synthesis and Application of α -Amino Acids*, (Hrsg.: V. A. Soloshonok, K. Izawa), American Chemical Society, Washington DC, **2009**, S. 306–321.
- [101] T. Sonke, B. Kaptein, H. E. Schoemaker, *Amino Acids, Peptides and Proteins in Organic Chemistry*, Wiley-VCH Verlag GmbH & Co. KGaA, **2009**, S. 77–117.
- [102] S. Y. K. Seah, *Industrial Enzymes*, (Hrsg.: J. Polaina, A. P. MacCabe), Springer, Dordrecht, **2007**, S. 489–504.
- [103] N. M. W. Brunhuber, J. S. Blanchard, *Crit. Rev. Biochem. Mol. Biol.* **1994**, *29*, 415–467.
- [104] T. Ohshima, K. Soda, *Advances in Biochemical Engineering/Biotechnology, Vol. 42: Bioprocesses and Applied Enzymology*, Springer, Berlin/Heidelberg, **1990**, S. 187–209.
- [105] A. DeLuna, A. Avendano, L. Riego, A. Gonzalez, *J. Biol. Chem.* **2001**, *276*, 43775–43783.
- [106] K. Tsukada, *J. Biol. Chem.* **1966**, *241*, 4522–4528.
- [107] G. Kaczorowski, L. Shaw, M. Fuentes, C. Walsh, *J. Biol. Chem.* **1975**, *250*, 2855–2865.
- [108] P. J. Olsiewski, G. J. Kaczorowski, C. Walsh, *J. Biol. Chem.* **1980**, *255*, 4487–4494.
- [109] J. Thompson, J. A. Donkersloot, *Annu. Rev. Biochem.* **1992**, *61*, 517–554.
- [110] F. Regnouf, N. van Thoai, *Comp. Biochem. Physiol.* **1970**, *32*, 411–416.
- [111] M. Grieshaber, G. Gaede, *J. Comp. Physiol. B* **1976**, *108*, 225–232.
- [112] M. Grieshaber, G. Gaede, *Comp. Biochem. Physiol. B: Comp. Biochem.* **1977**, *58*, 249–252.
- [113] P. Hockachka, P. Hartline, J. Fields, *Science* **1977**, *195*, 72–74.
- [114] M. Harcet, D. Perina, B. Plese, *Biochem. Genet.* **2013**, *51*, 666–676.
- [115] J. A. Lippincott, B. B. Lippincott, *Science* **1970**, *170*, 176–177.
- [116] M.-D. Chilton, M. H. Drummond, D. J. Merlo, D. Sciaky, A. L. Montoya, M. P. Gordon, E. W. Nester, *Cell* **1977**, *11*, 263–271.
- [117] A. Pitzschke, H. Hirt, *EMBO Journal* **2010**, *29*, 1021–1032.
- [118] A. Mueller, F. Janssen, M. K. Grieshaber, *FEBS J.* **2007**, *274*, 6329–6339.
- [119] H. J. Smits, A. M. M. Schmitt, M. K. Grieshaber, *J. Mol. Biol.* **2008**, *381*, 200–211.
- [120] Y. Kato, H. Yamada, Y. Asano, *J. Mol. Catal. B: Enzym.* **1996**, *1*, 151–160.
- [121] Y. Asano, K. Yamaguchi, K. Kondo, *J. Bacteriol.* **1989**, *171*, 4466–4471.

- [122] S. H. J. Smits, T. Meyer, A. Mueller, N. van Os, M. Stoldt, D. Willibold, L. Schmitt, M. K. Grieshaber, *PLoS ONE* **2010**, *5*, e12312.
- [123] S. S. Chimni, R. J. Singh, *World J. Microbiol. Biotechnol.* **1997**, *14*, 247–250.
- [124] H. Li, P. Williams, J. Micklefield, J. M. Gardiner, G. Stephens, *Tetrahedron* **2004**, *60*, 753–758.
- [125] T. Vaijyanthi, A. Chadha, *Tetrahedron: Asymmetry* **2008**, *19*, 93–96.
- [126] T. Huber, Diss., University of Freiburg, **2014**.
- [127] A. L. Rothman, B.Sc. thesis, University of Florida (Gainesville, USA), **2010**.
- [128] F Sibilla, Diss., RWTH Aachen (Germany), **2008**.
- [129] M. Espinoza-Moraga, T. Petta, M. Vasquez-Vasquez, V. F. Laurie, L. A. B. Moraes, L. S. Santos, *Tetrahedron: Asymmetry* **2010**, *21*, 1988–1992.
- [130] Y. Mirabal-Gallardo, M. d. P. C. Soriano, L. S. Santos, *Tetrahedron: Asymmetry* **2013**, *24*, 440–443.
- [131] J. B. G. Roelfes, *Curr. Opin. Chem. Biol.* **2014**, *19*, 135–143.
- [132] J. C. Lewis, *ACS Catal.* **2013**, *3*, 2954–2975.
- [133] M. R. Ringenberg, T. R. Ward, *Chem. Commun.* **2011**, *47*, 8470–8476.
- [134] M. Duerrenberger, T. Heinisch, Y. M. Wilson, T. Rossel, E. Nogueira, L. Knoerr, A. Mutschler, K. Kersten, M. J. Zimbron, J. Pierron, T. Schirmer, T. R. Ward, *Angew. Chem. Int. Ed.* **2011**, *50*, 3026–3029.
- [135] F. Schwizer, V. Koehler, M. Duerrenberger, L. Knoerr, T. R. Ward, *ACS Catal.* **2013**, *3*, 1752–1755.
- [136] V. Koehler, Y. M. Wilson, M. Duerrenberger, D. Ghislieri, E. Churakova, T. Quinto, L. Knoerr, D. Haeussinger, F. Hollmann, N. J. Turner, T. R. Ward, *Nat. Chem.* **2013**, *5*, 93–99.
- [137] J. M. Zimbron, T. Heinisch, M. Schmid, D. Hamels, E. S. Nogueira, T. Schirmer, T. R. Ward, *J. Am. Chem. Soc.* **2013**, *135*, 5384–5388.
- [138] T. Quinto, F. Schwizer, J. M. Zimbron, A. Morina, V. Koehler, T. R. Ward, *ChemCatChem* **2014**, *6*, 1010–1014.
- [139] M. Genz, V. Koehler, M. Krauss, D. Singer, R. Hoffmann, T. R. Ward, N. Straeter, *ChemCatChem* **2014**, *6*, 736–740.
- [140] T. Fujii, M. Mukaihara, H. Agematu, H. Tsunekawa, *Biosci. Biotechnol. Biochem.* **2002**, *66*, 736–740.
- [141] H. Muramatsu, H. Mihara, M. Yasuda, M. Ueda, T. Kurihara, N. Esaki, *Biosci. Biotechnol. Biochem.* **2006**, *70*, 2296–2298.
- [142] M. Yasuda, M. Ueda, H. Muramatsu, H. Mihara, N. Esaki, *Biosci. Biotechnol. Biochem.* **2006**, *17*, 1775–1779.
- [143] K. Mitsukura, M. Suzuki, K. Tada, Y. Yoshida, T. Nagasawa, *Org. Biomol. Chem.* **2010**, *8*, 4533–4535.
- [144] K. Mitsukura, M. Suzuki, S. Shinoda, T. Kuramoto, T. Yoshida, T. Nagasawa, *Biosci. Biotechnol. Biochem.* **2011**, *75*, 1778–1782.

- [145] K. Mitsukura, T. Kuramoto, T. Yoshida, N. Kimoto, H. Yamamoto, T. Nagasawa, *Appl. Microbiol. Biotechnol.* **2013**, *97*, 8079–8086.
- [146] F. Leipold, S. Hussain, D. Ghislieri, N. J. Turner, *ChemCatChem* **2013**, *5*, 3505–3508.
- [147] S. Hussain, F. Leipold, H. Man, E. Wells, S. P. France, K. R. Mullholland, G. Grogan, N. J. Turner, *ChemCatChem* **2015**, *7*, 579–583.
- [148] T. Nagasawa, T. Yoshida, K. Ishida, H. Yamamoto, N. Kimoto, *Pat.*, 2011/0287494 (Daicel Chemical Industries, Ltd.) **2011**.
- [149] M. Rodriguez-Mata, A. Frank, E. Wells, F. Leipold, N. J. T. S. Hart, J. P. Turkenburg, G. Grogan, *ChemBioChem* **2013**, *14*, 1372–1379.
- [150] M. Hamasaki, K. Kimoto, H. Yamamoto, *Pat.*, 2011/177029 (Daicel Chemical Industries, Ltd.) **2011**.
- [151] P. N. Scheller, S. Fademrecht, S. Hofelzer, J. Pleiss, F. Leipold, N. J. Turner, B. M. Nestl, B. Hauer, *ChemBioChem* **2014**, *15*, 2201–2204.
- [152] M. Gand, H. Mueller, R. Wardenga, M. Hoehne, *J. Mol. Catal. B: Enzym.* **2014**, *110*, 126–132.
- [153] T. Huber, L. Schneider, A. Praeg, S. Gerhardt, O. Einsle, M. Mueller, *ChemCatChem* **2014**, *6*, 2248–2252.
- [154] K. Vedha-Peters, M. Gunawardana, J. D. Rozzell, S. J. Novick, *J. Am. Chem. Soc.* **2006**, *128*, 10923–10929.
- [155] H. Akita, K. Doi, Y. Kawarabayasi, T. Oshima, *Biotechnol Lett* **2012**, *34*, 1693–1699.
- [156] R. L. Hanson, R. M. Johnston, S. L. Goldberg, W. L. Parker, A. Goswami, *Org. Process Res. Dev.* **2013**, *17*, 693–700.
- [157] H. Akita, H. Suzuki, K. Doi, T. Ohshima, *Appl. Microbiol. Biotechnol.* **2014**, *98*, 1135–1143.
- [158] H. Akita, Y. Imaizumi, H. Suzuki, K. Doi, T. Ohshima, *Biotechnol Lett* **2014**, *36*, 2245–2248.
- [159] N. Itoh, C. Yachi, T. Kudome, *J. Mol. Catal. B: Enzym.* **2000**, *10*, 281–290.
- [160] R. A. Sheldon, *Multi-Step Enzyme Catalysis*, (Hrsg.: E. Garcia-Junceda), Wiley-VCH, Weinheim, **2008**.
- [161] M. J. Abrahamson, E. Vazquez-Figueroa, N. B. Woodall, J. C. Moore, A. S. Bommarius, *Angew. Chem. Int. Ed.* **2012**, *51*, 3969–3972.
- [162] M. J. Abrahamson, J. W. Wong, A. S. Bommarius, *Adv. Synth. Catal.* **2013**, *355*, 1780–1786.
- [163] S. K. Au, B. R. Bommarius, A. S. Bommarius, *ACS Catal.* **2014**, *4*, 4021–4026.
- [164] B. R. Bommarius, M. Schurmann, A. S. Bommarius, *Chem. Commun.* **2014**, *50*, 14953–14955.
- [165] T. Dairi, Y. Asano, *Appl. Environ. Microbiol.* **1995**, *61*, 3169–3171.
- [166] C. Haibin, S. J. Collier, J. Nazor, J. Sukumaran, D. Smith, J. C. Moore, G. Hughes, J. Janey, G. Huisman, S. Novick, *Pat.*, 2013/0302859 (Codexis, Inc.) **2013**.

- [167] O. Alvizo, M. Mayo, N. Agard, S. Collier, J. Sukumaran, S. Jenne, A. Bautista, S. Novick, W. Yeo, D. Smith, J. Riggings, S. Ng, D. Entwistle, A. Krebber, G. Huisman, J. Nazar, H. Chen, G. Hughes, J. Jacob, G. Cope, P. Orth, N. Elsen, „Imine Reductases: Extending the Synthesis of Chiral Amines, poster presentation at biocat2014: 7th International Congress on Biocatalysis, Hamburg (Germany), 31.08.-04.09.2014“, **2014**.
- [168] G. W. Huisman, „Innovations in Biocatalysis for Pharmaceutical Applications oral presentation at biocat2014: 7th International Congress on Biocatalysis, 31.08.-04.09.2014, Hamburg (Germany)“.
- [169] Z. Meng, Z. Lou, Z. Liu, M. Li, X. Zhao, M. Bartlam, Z. Rao, *J. Mol. Biol.* **2006**, *359*, 1364–1377.
- [170] G. Bhabha, D. C. Ekiert, M. Jennewein, C. M. Zmasek, L. M. Tuttle, G. Kroon, H. J. Dyson, A. Godzik, I. A. Wilson, P. E. Wright, *Nat. Struct. Mol. Biol.* **2013**, *20*, 1243–1249.
- [171] K. I. Varughese, M. M. Skinner, J. M. Whiteley, D. A. Matthews, N. H. Xuong, *Proc. Natl. Acad. Sci. U. S. A.* **1992**, *89*, 6080–6084.
- [172] K. M. Meneely, A. L. Lamb, *Biochemistry* **2012**, *51*, 9002–9013.
- [173] P. J. Baker, A. P. Turnbull, S. E. Sedelikova, T. J. Stillman, D. W. Rice, *Structure* **1995**, *3*, 693–705.
- [174] Y. Zhao, T. Wakamatsu, K. Doi, H. Sakuraba, T. Ohshima, *J. Mol. Catal. B: Enzym.* **2012**, *83*, 65–72.
- [175] J. L. Vanhooke, J. B. Thoden, N. M. W. Brunhuber, J. S. Blanchard, H. M. Holden, *Biochemistry* **1999**, *38*, 2326–2339.
- [176] N. M. W. Brunhuber, J. B. Thoden, J. S. Blanchard, J. L. Vanhooke, *Biochemistry* **2000**, *39*, 9174–9187.
- [177] K. L. Britton, Y. Asano, D. W. Rice, *Nat. Struct. Biol.* **1998**, *5*, 593–601.
- [178] J. F. Morrison, S. R. Stone, *Biochemistry* **1988**, *27*, 5499–5506.
- [179] C. M. Czekster, A. Vandemeulebroucke, J. S. Blanchard, *Biochemistry* **2011**, *50*, 7045–7056.
- [180] P. Shrimpton, R. K. Allemann, *Protein Sci.* **2002**, *11*, 1442–1451.
- [181] B. Nocek, C. Chang, H. Li, L. Lezondra, D. Holzle, F. Collart, A. Joachimiak, *J. Mol. Biol.* **2005**, *354*, 91–106.
- [182] D. G. Gourley, A. W. Schuettelkopf, G. A. Leonard, J. Juba, L. W. Hardy, S. M. Beverley, W. N. Hunter, *Nat. Struct. Biol.* **2001**, *8*, 521–525.
- [183] G. Grogan, „Structure, mechanism and application of NADPH-dependent Imine Reductases (IREDs) oral presentation at biocat2014: 7th International Congress on Biocatalysis, 31.08.-04.09.2014 Hamburg (Germany)“.
- [184] C. Filling, K. D. Berndt, J. Benach, S. Knapp, T. Prozorovski, E. Nordling, R. Ladenstein, H. Joernvall, U. Oppermann, *J. Biol. Chem.* **2002**, *277*, 25677–25684.
- [185] N. H. Schlieben, K. Niefind, J. Mueller, B. Riebel, W. Hummel, D. Schonburg, *J. Mol. Biol.* **2005**, *349*, 801–813.

- [186] W. Hummel, *Advances in Biochemical Engineering/Biotechnology* **1997**, *58*, 145–184.
- [187] S. Leuchs, L. Greiner, *Chemical & Biochemical Engineering Quarterly* **2011**, *25*, 267–281.
- [188] M. Cowart, J. K. Pratt, A. O. Stewart, Y. L. Bennani, T. A. Esbenschade, A. A. Hancock, *Bioorg. Med. Chem. Lett.* **2004**, *14*, 689–693.
- [189] M. Sun, C. Zhao, G. A. Gfesser, C. Thiffault, T. R. Miller, K. Marsh, J. Wetter, M. Curtis, R. Faghieh, T. A. Esbenschade, A. A. Hancock, M. Cowart, *J. Med. Chem.* **2005**, *48*, 6482–6490.
- [190] H. Man, E. Wells, S. Hussain, F. Leipold, S. Hart, J. P. Turkenburg, N. J. Turner, G. Grogan, *ChemBioChem* **2015**, *16*, 1052–1059.
- [191] H.-U. Blaser, H.-P. Buser, R. Haeusel, H.-P. Jalett, F. Spindler, *Journal of Organometallic Chemistry* **2001**, *621*, 34–38.
- [192] R. Cao, W. Peng, Z. Wang, A. Xu, *Current Medicinal Chemistry* **2007**, *14*, 479–500.
- [193] R. Carr, M. Alexeeva, A. Enright, T. S. C. Eve, M. J. Dawson, N. J. Turner, *Angew. Chem. Int. Ed.* **2013**, *42*, 4807–4810.